# Stony Brook University

# Ultrafast vibrational studies of biological chromophores: Light-driven structural changes in yellow fluorescent protein and the bacterial blue light sensing protein, AppA

A Dissertation Presented

by

Allison Lynn Stelling

to

The Graduate School

in Partial Fulfillment of the Requirements

for the Degree of

Doctor of Philosophy

in

Chemistry

Stony Brook University

December 2008

Stony Brook University

The Graduate School

Allison Lynn Stelling

We, the dissertation committee for the above candidate for the Doctor of Philosophy degree, hereby recommend acceptance of the dissertation.

Dr. Peter Tonge
Advisor
Professor of Chemistry

Dr. Erwin London
Professor of Biochemistry and Cell Biology

Dr. Nancy Goroff
Professor of Chemistry

Dr. Steven Smith
Professor of Biochemistry and Cell Biology

This dissertation is accepted by the Graduate School.

Lawrence Martin
Dean of the Graduate School

# Abstract of the Dissertation

# Ultrafast vibrational studies of biological chromophores: Light-driven structural changes in yellow fluorescent protein and the bacterial blue light sensing protein, AppA

by

Allison Lynn Stelling

Doctor of Philosophy

in

Chemistry

Stony Brook University

2008

Professor Peter J. Tonge

Light driven reactions are fundamental to life on earth and include biological processes such as photosynthesis as well as the photophobic and phototaxic responses of organisms to sunlight. Biological systems interact with photons via chromophores that are bound within a protein matrix, and this work focuses on two light-activated systems that differ fundamentally in their response to light. In fluorescent proteins, protein chromophore interactions have evolved to maximize the fluorescent quantum yield from the chromophore while in the bacterial anti-repressor AppA photoexcitation causes structural changes in the protein that result in dissociation of a transcription factor and an inhibition of photosystem biosynthesis. Fluorescent proteins, such as the well-known green

fluorescent protein (GFP), are used very extensively in biology as genetically encoded imaging agents in live cells. Many mutants of GFP have been created to tailor absorption and emission maxima, including yellow fluorescent protein (YFP) a GFP variant that emits at 527 nm. In addition to fluorescence emission, irradiation of YFP leads to the formation of non-fluorescent states which can potentially complicate imaging applications. Steady-state vibrational spectroscopy has been used to determine that formation of the non-fluorescent state in YFP involves *cis* to *trans* isomerization of the 4-hydroxybenzylidene imidazolinone chromophore, a structural change that is normally inhibited by the protein matrix. In the blue-light-utilizing FAD (BLUF) protein AppA, the signaling state is formed within a nanosecond of excitation, and picosecond infrared absorption spectroscopy (TRIR) has been used to elucidate early structural events in the AppA photocycle. The flavin chromophore in AppA is rigid, raising questions concerning how excitation is coupled to changes in protein structure. In the TRIR data, a mode is observed at 1666 $cm^{-1}$ in the dark and light states of AppA whose origin is under debate. Using site-directed mutagenesis and isotope-labeling, the 1666 $cm^{-1}$ mode is assigned to the side chain of Q63, a residue that is hydrogen-bonded to the flavin. Photoexcitation of AppA is proposed to result in rotation or keto-enol tautomerism of the Q63 amide side chain, resulting in alterations in hydrogen-bonding that lead to formation of the signaling state of the protein.

Dedicated to Dr. Andrew Jaye

# Contents

# List of Figures

# List of Tables

## Publications

- Minako Kondo, Jerome Nappa, Kate L. Ronayne, **Allison L. Stelling**, Peter J. Tonge, and Stephen R. Meech. *Ultrafast Vibrational Spectroscopy of the Flavin Chromophore*. Journal of Physical Chemistry B. 110(41): 20107 -20110. September 23, 2006. Abstract PDF

- **Allison L. Stelling**, Kate L. Ronayne, Jerome Nappa, Peter J. Tonge, and Stephen R. Meech. *Ultrafast Structural Dynamics in BLUF Domains: Transient Infrared Spectroscopy of AppA and its Mutants*. Journal of the American Chemical Society. 129(50):15556-64. November 22, 2007. Abstract PDF

- Gabrielle D. Maloa, Meitian Wang, Di Wua, **Allison L. Stelling**, Peter J. Tonge, and Rebekka M. Wachter. *Crystal structure and Raman studies of dsFP483, a cyan fluorescent protein from Discosoma striata*. Journal of Molecular Biology. 378(4): 869-884. May 9, 2008. Abstract PDF

- **Allison L. Stelling**, Minako Kondo, Ian P. Clark, Allison L. Haigney, Adelbert Bacher, Boris Illarionov, Steve Meech and Peter J. Tonge. *Ultrafast Infrared Studies of Isotopically Labeled Flavins Bound to the BLUF Domain of AppA*. In preparation.

# Chapter 1

# Introduction

## 1.1 The Photochemistry of Life

Life has evolved a myriad of responses to and interactions with radiation. The incoming photon interacts with the molecular machines known as photoproteins via an embedded chromophore that transmits the ultrafast light signal into a biological response. These chromophores are typically sensitive to particular wavelengths of radiation. Light may be employed in the energy harvesting reactions of photosynthesis, or used for bioluminescence, like the green fluorescent proteins (GFPs). Light sensor proteins such as cryptochromes, the blue light sensing using flavin (BLUF) domain, and rhodopsins function to instigate a variety of behaviorial processes including photoavoidance, phototaxis and phototropism [75]. Conformational changes

of the protein upon absorption of a photon by the chromophore transduce the environmental signal into a cellular response.

Typically upon excitation a dramatic structural change of the embedded chromophore occurs, which then is transmitted to the protein environment [75, 28]. Such is the case in photoproteins such as the rhodopsins and phytochromes, which feature *cis-trans* photoisomerization of their chromophores upon absorption of a photon [75] (see Figure 1.1). Other proteins employ electrochemistry to form transient bonds between the chromophore and the surrounding protein, as in the case of the light oxygen voltage (LOV) domain where a transient flavin-cysteine bond is formed during the photocycle [75]. In the case of wild type GFP, an ultrafast deprotonation of the chromophore occurs through a hydrogen bond network to a nearby glutamine [77].

Rhodopsins are typically membrane bound G-protein coupled receptors. In the Eukarya and the Archaea, activation leads to behavioral swimming responses. In the Chlamydomonas rhodopsin initiates phototaxis while bacteriorhodopsin from *Halobacterium salinarium* functions as a light driven proton pump [75]. During its photocycle, the retinal chromophore in rhodopsin (Figure 1.1) changes conformation from all-*trans* to 11-*cis* on a picosecond timescale (see Figures 1.1, 1.2 and 1.4) [75, 3]. The retinal chromophore in bacteriorhodopsin undergoes isomerization in a different bond, changing from

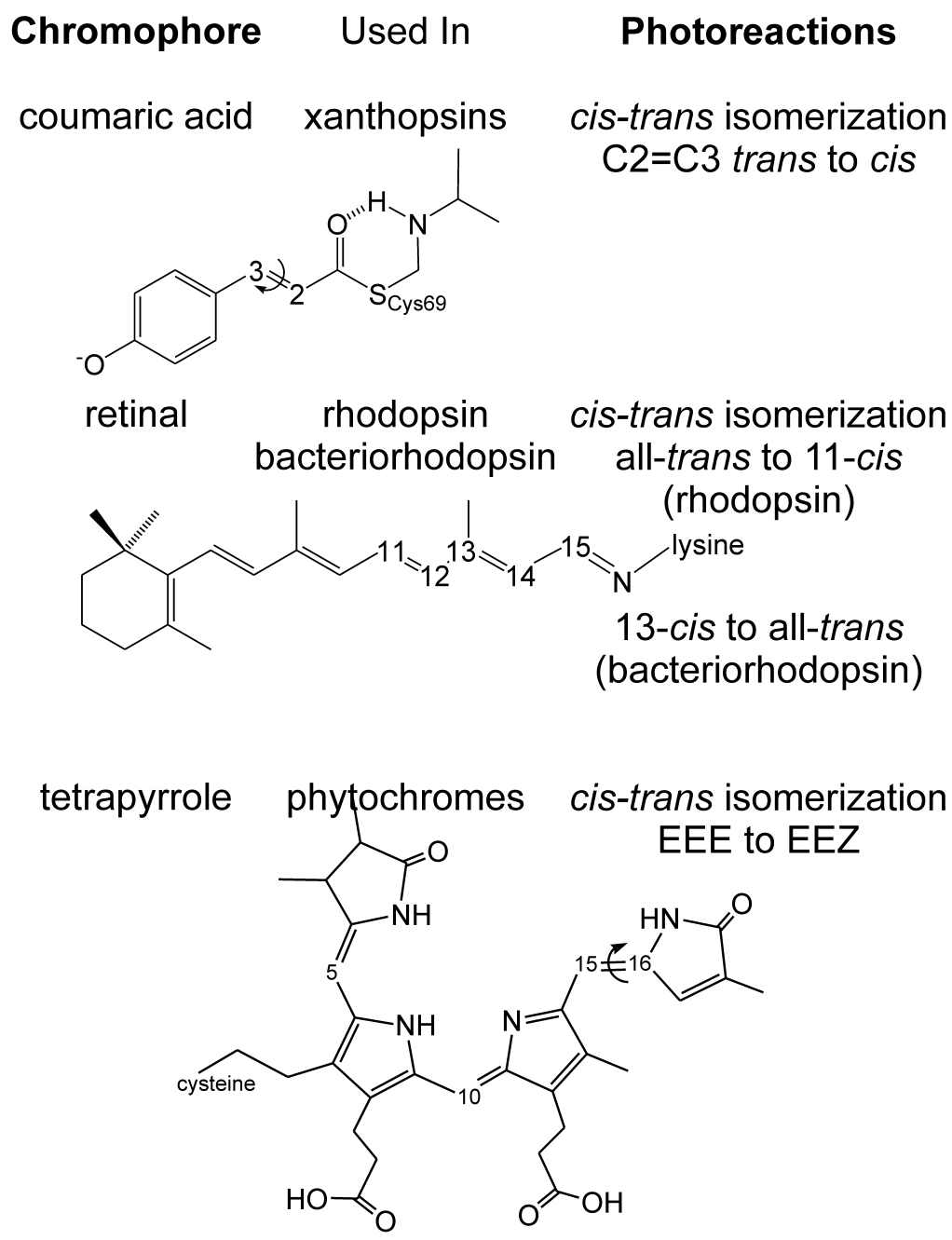


Figure 1.1: Structures of several biological chromophores that undgero *cis-trans* photoisomerization reactions.

11-*cis* to all-*trans* upon excitation [3]. The photocycle is complete within 10 to 1000 ms, depending on the specific protein.

The xanthopsins use an anionic *trans*-p-coumaric acid chromophore (see Figure 1.1 and 1.4), linked to the protein via a thio-ester bond [75]. The 125-amino acid photoactive yellow protein (PYP), the best studied of this family, governs photoavoidance behavior in *Ectothiorhodospira halophila* [83]. PYP is a prototype for the PAS (Per-Arndt-Sims) domain, a ubiquitous module involved in many signaling and regulatory proteins. These domains have 2 $\alpha$-helices at the N-terminus, and in the center a six stranded $\beta$-sheet, as shown in Figure 1.2. Absorption of blue light causes isomerization of the chromophore to the *cis* conformation, a process that requires less than a picosecond. Proton transfer to the nearby glutamate (E46) then occurs on the microsecond timescale [75], followed by partial unfolding of the protein in the signaling state. The protein recovers to its resting state within hundreds of milliseconds [21].

The phytochromes employ a tetrapyrrole (see Figure 1.1 and 1.4) as a chromophore, covalently linked to the protein with a thioester bond. The photosensing domains of these proteins are generally about 300 amino acids long and may be found in fungi, plants, and bacteria [79]. Crystal structures of *Deinococcus radiodurans* bacteriophytochrome photoreceptor (DrBphP) reveal

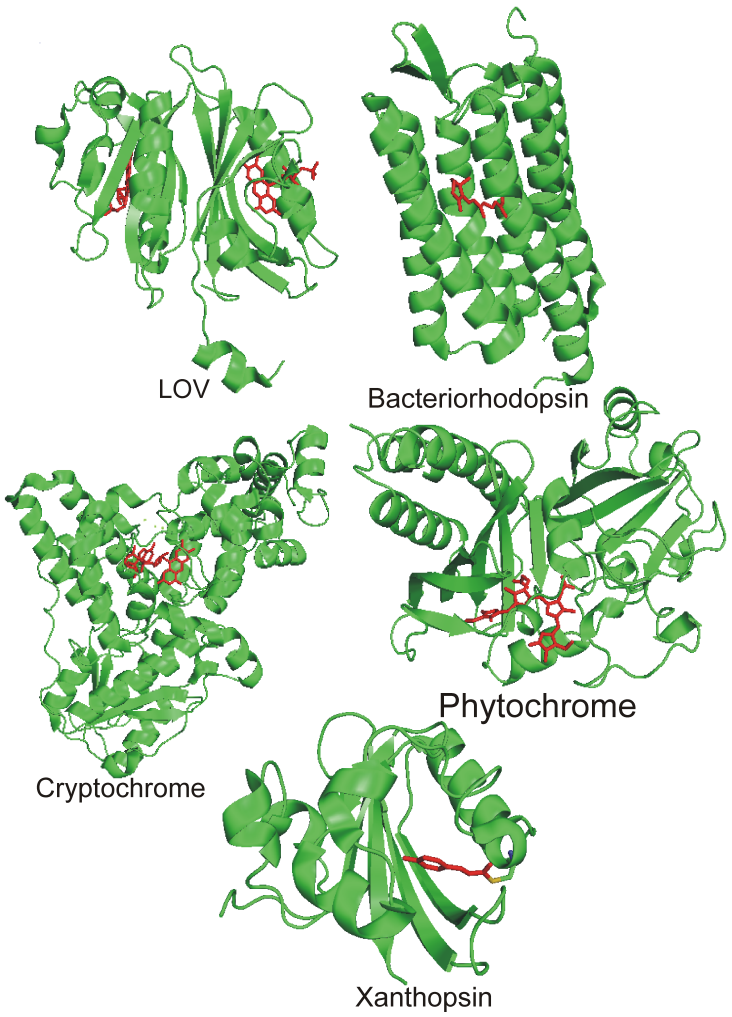


Figure 1.2: Crystal structures of several photoreceptor proteins. Cryptochrome from *Arabidopsis thaliana*, Brautigam et al. 2004 [8]; PDBID: 1U3C. Bacteriorhodopsin from *Halobacterium salinarium*, Luecke et al. 2000 [39]; PDBID: 1F4Z. Phytochrome from *Deinococcus radiodurans*, Wagner el al. 2005 [79]; PDBID: 1ZTU. The xanthopsin from *Ectothiorhodospira halophila*, Getzoff et al. 2003 [13], PDBID: 1NWZ. LOV from *Arabidopsis thaliana*, Nakasako et al. 2008 [53], PDBID: 2Z6C.

a PAS domain that binds the chromophore through a cysteine. The PAS domain is linked by ten residues to a GAF (cGMP phosphodiesterase/adenyl cyclase/FhlA) domain [79]. Phytochromes govern a range of physiologic processes, including seed germination, phototaxis [82] and circadian clock regulation [75]. As shown in Figure 1.1 red light absorption induces a 15Zanti to 15Eanti isomerization of the C15=C16 double bond of the chromophore [79, 58]. Relaxation back to the resting state can take hours if left in the dark, while absorption of another red photon will cause immediate recovery [75]. A histidine kinase domain at the C-terminus ultimately transforms the light signal into a chemical signal by the autophosphorylation of a histidine [82].

The cryptochromes comprise another family of blue light photoreceptors that are found in both plants and animals and generally serve to regulate 24-hour circadian cycles [56]. The *Arabidopsis* CRY1 protein was among the first of these photoreptors discovered. Mutants in the *Arabidopsis cry1* gene lead to deficiencies in anthocyanin production, chalcone synthase gene expression, and flowering time, while overexpression results in hypersensitivity of the plants to UV light [37].

These "clock genes" were found to be essential for circadian timekeeping in mammals, interacting with several proteins that form positive/negitive feedback loops to regulate gene expression [35]. Several sleep disorders have

| Chromophore | Used In | Photoreactions |
|---|---|---|
| isoalloxazine ring | cryotochromes | proton transfer |
| 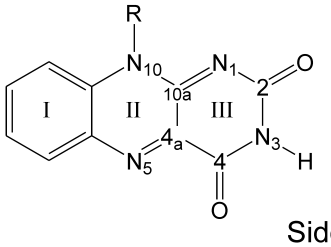 | blue light using flavin (BLUF) | electron transfer |
| | light/oxygen/voltage (LOV) | cysteinyl adduct formation |

Side chains of flavin isoalloxazine ring

lumiflavin, R = -$CH_3$

riboflavin (Rf), R =

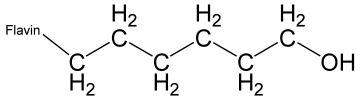

flavin mononucleotide (FMN), R =

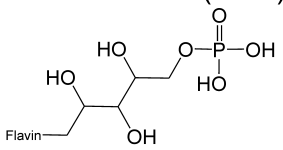

flavin adenine dinucleotide (FAD), R =

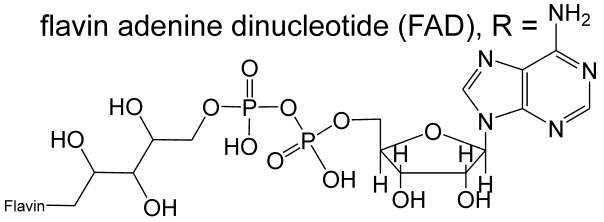

Figure 1.3: Structure of the flavin isoalloxazine ring and several side chains.

been associated with mutations in the clock genes, although other pathologies seem to be linked to their expression [35]. Experiments that monitored *cry1* gene expression (and other clock genes) in humans found they were expressed rhythmically in control pineal glands, however, expression was arrhythmic in preclinical and clinical Alzheimers disease patients [35]. As cell cycle division is under circadian control, cancer has been implicated as a circadian-related disorder as well. Higher levels of the clock protein PER1, which has been shown to physically interact with CRY, have been associated with reduction in cancer cell growth rate, and tumor cell samples from cancer patients have a lowered concentration of *PER1* RNA [35].

The cryptochromes use flavin and pterin chromophores, which are non-covalently bound to a 50 to 70-kDa protein [56] (see Figures 1.1 and 1.2). These proteins show high homology to photolyases in their N-terminal domain, where the chromophore binds, but have no DNA repair activity [75] and lack a positively charged DNA binding groove [38]. The C-termini of the cryptochromes show a high degree of diversity [37] and ranges from 30 to 350 amino acids in length. In *Arabidopsis* CRY1 the C-terminal domain has been shown to directly associate with COP1 (a negative regulator for photomorphogenesis), suggesting that this terminus functions as a modular domain for signal propagation [37, 56].

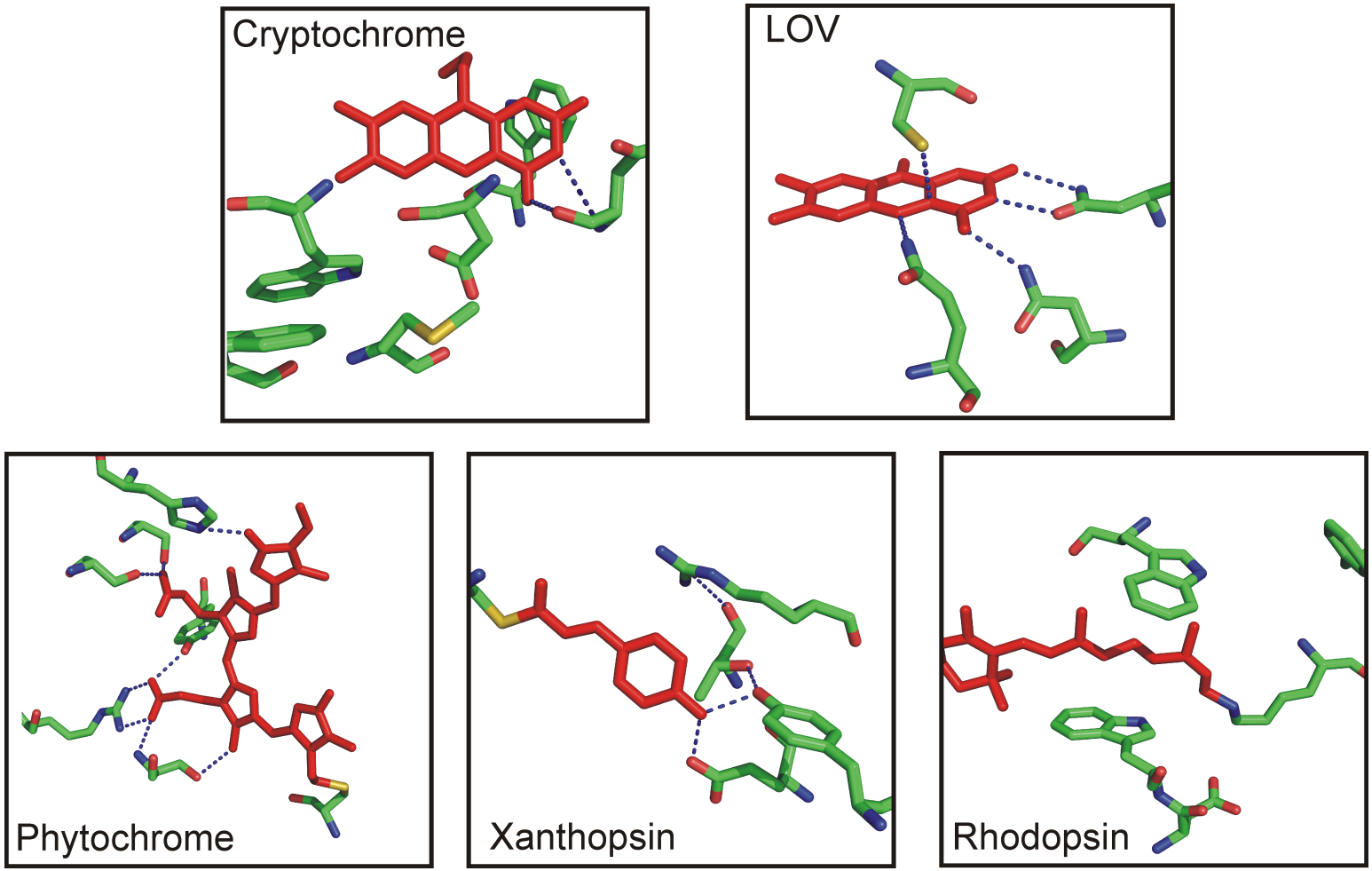


Figure 1.4: Chromophore binding sites of several photoreceptor proteins. Cryptochrome from *Arabidopsis thaliana*, Brautigam et al. 2004 [8]; PDBID: 1U3C. Bacteriorhodopsin from *Halobacterium salinarium*, Luecke et al. 2000 [39]; PDBID: 1F4Z. Phytochrome from *Deinococcus radiodurans*, Wagner el al. 2005 [79]; PDBID: 1ZTU. The xanthopsin from *Ectothiorhodospira halophila*, Getzoff et al. 2003 [13], PDBID: 1NWZ. LOV from *Arabidopsis thaliana*, Nakasako et al. 2008 [53], PDBID: 2Z6C.

Flavins cannot undergo *cis-trans* isomerization reactions, and so flavin based photoreceptors such as cryptochromes must use a different mechanism than phytochromes, xanthopsins, or rhodopsins for signal transmission from the chromophore to the protein. Current hypotheses for signal transmission involve the initial absorption of a photon by the pterin, which then activates the flavin chromophore [38]. In the animal cryptochromes, photoreduction of the flavin to a neutral radical has been observed in living cells [20]. Insect cryptochromes have been better studied, and when purified their flavins can be easily reduced to the FAD radical anion with a quantum efficiency of about 0.2 [27]. Electrons for the reduction are provided by a tryptophan triad, and a trapped, highly acidic water molecule is proposed to be the proton donor [27]. While the electron transfer to the tryptophans (see Figure 1.4) occurs on a picosecond timescale, the proton transfer is much slower (seconds) and several flavin intermediates have been identified. Recovery back to the resting state is slow.

Other flavin photoreceptors exist. The phototropins are found in higher plants, fungi, and bacteria and in the green algae *Chlamydomonas reinhardtii* [9]. These proteins regulate phototropic plant movement and other biological processes related to plant growth and pigment production. The phot protein family contains two light, oxygen, and voltage (LOV) sensing domains that

bind a flavin mononucleotide (see Figure 1.3) and a C-terminal kinase domain [32]. The size of the LOV proteins is highly variable and ranges from small, single domain proteins (see Figure 1.2) to multidomain proteins containing upwards of 2,000 amino acids. The PAS-like LOV domain is nearly always found in the N-terminal [9].

Illumination of LOV results in nanosecond formation of the red-absorbing triplet FMN, which then decays on a millisecond timescale. From the triplet state a second intermediate is formed that absorbs at 390 nm, and consists of an FMN covalently attached to a conserved cysteine through the C4a of the flavin ring (see Figure 1.4). FTIR studies in the S-H stretching region revealed that the cysteine is neutral in the dark and is deprotonated upon illumination [32]. The resting state, which absorbs at 447 nm, is regenerated within a few hundred seconds [32].

The work presented here focuses on two photoproteins that each respond quite differently to light absorption: the bioluminescent GFPs and the blue light using flavin domain (BLUF) domain, a photoreceptor found in many bacteria. The GFP mutant yellow fluorescent protein (YFP) has been shown to convert to non-fluorescent states upon irradiation, which causes problems in imaging studies. The GFP-like protein dsFP483 has a blue shifted emission wavelength (483 nm) with an abnormally high quantum yield (0.78). High

quantum yields are more typical for anions of the GFP chromophore, as the neutral state is more prone to nonradiative decay pathways. However, the blue shifted emission suggests a neutral chromophore in dsFP483. The BLUF domains have a different reaction to light absorption than that of the GFPs. Instead of being enhanced, fluorescence from their flavin chromophores is rapidly quenched, and flavins cannot undergo dramatic structural changes such as photoisomerization that are seen in the other photoreceptors. A slight rearrangement of hydrogen bonds around the BLUF chromophore induces a conformational change in the protein that transmits the signal into a photophobic behavioral response that regulates DNA expression [75, 28]. The goal of the research presented in this thesis is to use vibrational spectroscopy to understand how the protein matrix in the BLUF domain of AppA and the fluorescent GFPs control the response of the chromophore to light absorption.

## 1.2 The Green Fluorescent Proteins

GFP was first discovered in the bioluminescent jellyfish *Aequorea victoria* in 1961 [64]. Many GFP-like proteins from corals and other marine organisms have been described since. Common to these is the 11-stranded $\beta$-barrel tertiary structure (see Figure 1.5) that surrounds a chromophore formed posttranslationally from three protein residues (S65/Y66/G67) [55] (see Figure

1.7). The electronic absorption spectrum of wild type GFP contains a maximum at 400 nm that is the major peak and another minor peak at 480 nm. The 400 nm absorption is due to the neutral form of the GFP chromophore, while the 480 nm absorption has been assigned to the anionic form. Excitation at either 400 nm or 475 nm results in a single emission band at around 500 nm. While both neutral and anionic forms of the GFP chromophore exist within the protein $\beta$-barrel, these forms are not solvent-exposed in the wild type protein, and are thus cannot be interconverted by changing the pH.

Wild-type GFP has two maxima in its electronic absorption spectrum, one at 400 nm and the other at 475 nm. Excitation at either wavelength produces emission at 508 nm, with a quantum efficiency of 0.80 [55]. The high quantum yield in wild type GFP is the result of suppression by the protein environment of photoreactions that do not result in fluorescence. The single emission band produced in wild type GFP is the result an excited state proton transfer reaction that occurs within a few picoseconds of excitation. While the wild type GFP does not interconvert between neutral and anionic forms of its chromophore by altering the pH, this excited-state photoreaction transfers the proton off the phenolic oxygen, though a hydrogen-bond wire to a nearby glutamate (E222). Thus, the florescence from the neutral form of the chromophore in the wild type protein is due to an anion that is formed within

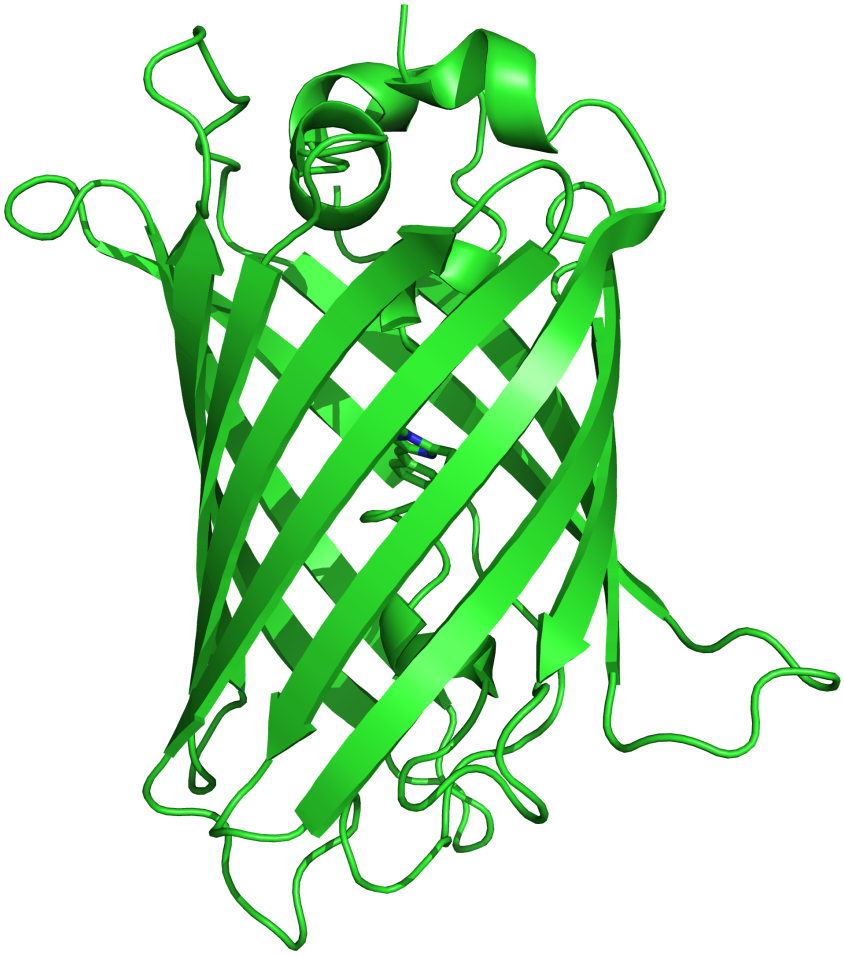

Figure 1.5: Crystal structure of the 11 stranded $\beta$-barrel common to the GFPs (PDB ID: 1YFP). From Wachter et al., 1998 [78].

the lifetime of the excited state.

Mutants of GFP that are pH sensitive show only small amounts of fluorescence (at around 460 nm) from their neutral forms, while the anionic forms are highly fluorescent. This high yield for fluorescence from the anionic chromophore is thought to be due to the suppression of alternate photoreactions that would normally deplete the excited state of the chromophore. One such photoreaction in wild type GFP is the transfer of energy to the proximal glutamate, which decarboxylates and results in nonfluorescent protein. Another photoreaction is the *cis-trans* isomerization about the exocyclic double bond of the chromophore. The *cis-trans* photoreaction is suppressed in the wild type GFP environment, however some mutants of GFP as well as several GFP-like fluorescent proteins do exhibit photoisomerization reactions.

Formation and fluorescence of the chromophore requires the presence of molecular oxygen and fully folded protein (see Figure 1.7). A model organic chromophore, 4-hydroxybenzilydene-imidazolinone (HBDI), has been synthesized. At room temperature this model chromophore has a very low yield for fluorescence, highlighting the important role the protein environment plays in tuning the photophysical properties of the embedded chromophore. Many variants of GFP have been developed to tailor the absorption and emission properties of the chromophore.

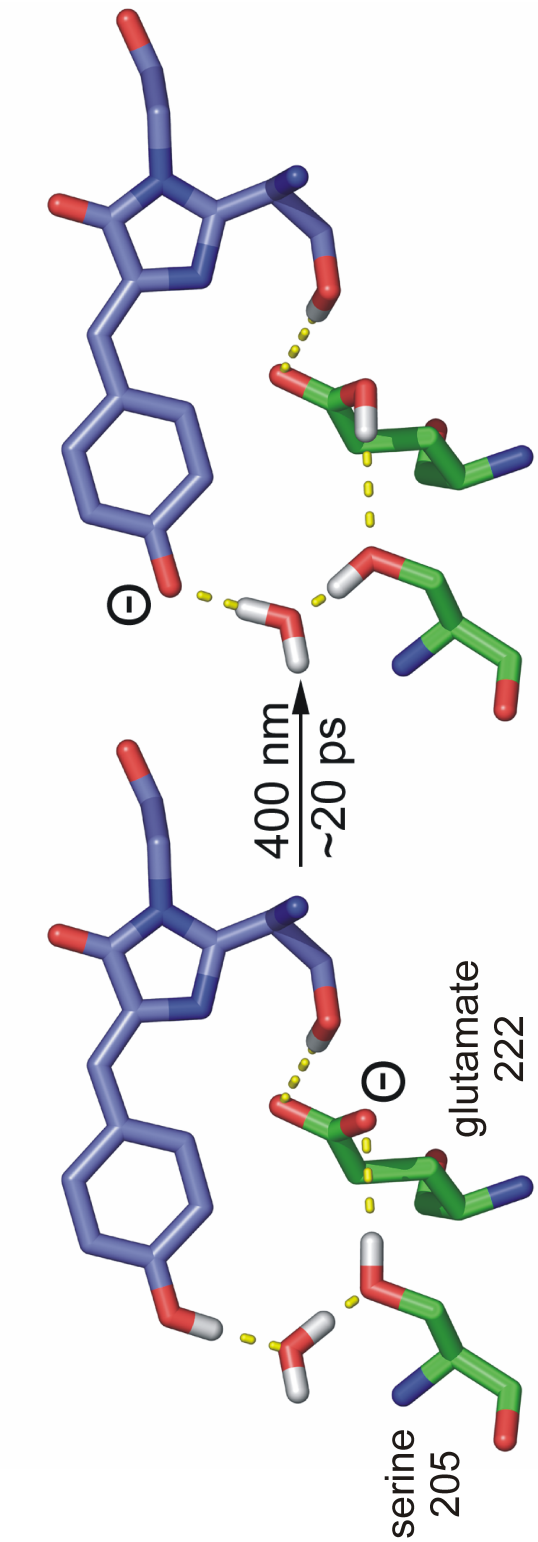


Figure 1.6: Crystal structure of the wild type GFP chromophore and immediate protein environment. Shown is the excited-state proton transfer reaction that occurs immediately upon excitation at 400 nm.

The GFPs have found a wide range of uses in biology. The fluorescent protein may be covalently attached to another protein by inserting the GFP sequence into the gene of the protein under study, generally at its N- or C-terminal domain. Expression of the gene in question then results in expression of the fluorescent protein as well, thus generating a protein with a fluorescent label attached. Fluorimetry may be used to locate the subcellular position of the GFP-tagged target protein in real time. The importance of multicolored, genetically encodable, and relatively non-invasive tags in biomedicine, developmental biology, cancer research, and basic molecular biology cannot be overstated. Indeed, the 2008 Nobel prize in chemistry was awarded to Shimomura for his discovery of the wild type protein in *Aequorea victoria*. Others (Tsien) shared the prize for developing the GFP mutants that give the wide range of colors, from blue to the far-red, and for the development of fusion proteins (Chalfie). Such a range is useful as multiple proteins may be labeled and their locations and interactions followed.

Another use for multiple colors of GFPs is fluorescence resonance energy transfer (FRET). These experiments gain information on distances from one to ten nanometers. FRET may occur when the $\lambda_{max}$ of absorption for the chromophore of one GFP (the acceptor) and the $\lambda_{max}$ of emission for the chromophore of another GFP (the donor) overlap. This overlap allows energy

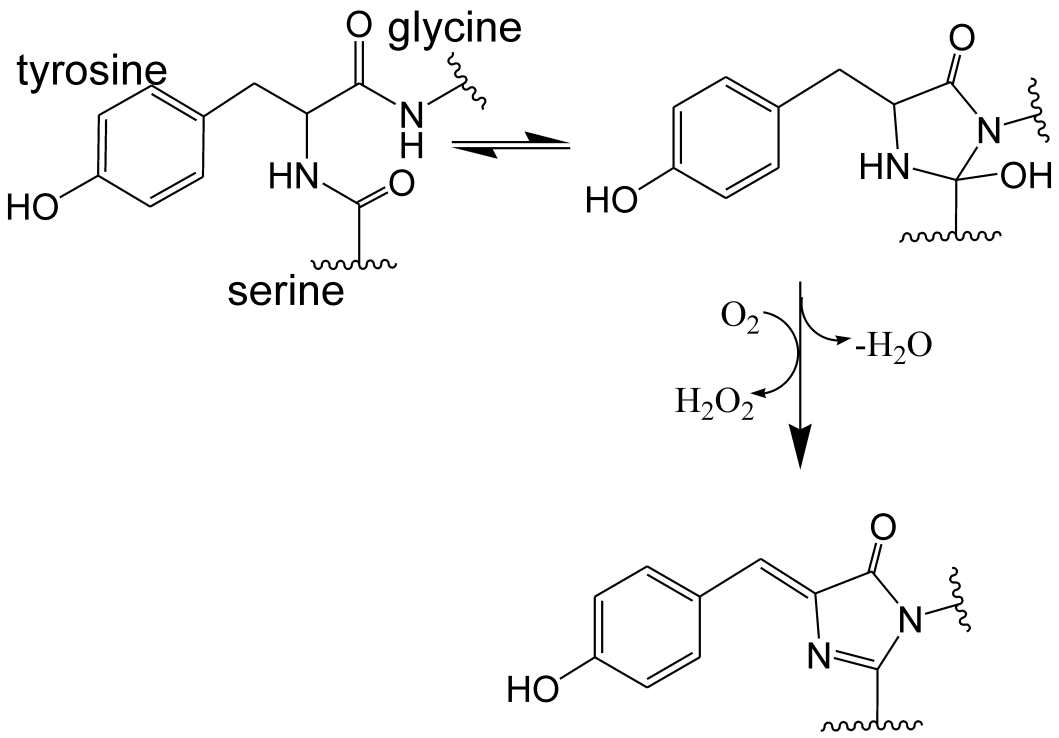


Figure 1.7: Shown is the posttranslational reaction of three protein residues (S65/Y66/G67 in wild type GFP) that creates the GFP chromophore [57, 85]. Chromophore formation occurs after the protein is folded.

to be transferred from the donor chromophore to the acceptor chromophore, thus quenching the fluorescence of the donor and resulting in emission from the acceptor upon irradiation into the $\lambda_{max}$ of the donor. The quenching is strongly dependant on the distance between the the two chromophores. Two proteins suspected of interacting *in vivo* may be labeled with a donor and an acceptor. Quenching occurs when the two are in proximity [70], resulting in a spectroscopic ruler. Yellow fluorescent protein (YFP, a yellow emitting mutant of GFP) and a fluorescent protein with cyan emission (around 475 nm) are frequently used in many studies. The blue cyan emission overlaps with the absorption band of YFP, whose fluorescent form absorps at 514 nm. The shoulders of the cyan emission and the YFP absorption bands overlap, allowing energy transfer when the two proteins are in proximity. In a particular study, the cAMP-dependent protein kinase A (PKA) and the catalytic subunit of PKA were fused to cyan fluorescent protein and yellow fluorescent protein, respectively. Binding of cAMP to PKA induced dissociation of the two subunits, resulting in a disruption of quenching via FRET and a fluorescent signal from the cyan [51].

FRAP (florescence recovery after photobleaching) is another useful technique that uses GFPs. Usually photobeaching is an undesirable quality in a fluorophore, however FRAP experiments exploit this phenomenon. Fluores-

cence from tagged proteins is deliberately and irreversibly photobleached in a narrow area within a cell by a focused laser beam [23]. After photobleaching, lower intensities of light can be used to monitor the diffusion of new, labeled proteins into the small intracellular area. This gives valuable information about the diffusion rates of proteins *in vivo* [23].

The proteins in the GFP family also undergo other useful photoreactions, such as photoswitching behavior. Photoswitching proteins are fluorescent molecules that may be interconverted between two configurations with different wavelengths of light. One configuration is the fluorescent, or bright state, and the other configuration is nonfluorescent. Such proteins have an "on/off switch" that may be exploited in biotechnology. While wild type GFP does not undergo photoswitching itself, homologous proteins as well as a few GFP mutants show this behavior of their chromophores. For example, the GFP-like protein asFP595 from *Anemonia sulcata* (see Figure 1.8) shows photoconversion of its chromophore between an emissive state and a dark state [60, 2]. The chromophore of asFP595 may be interconverted between two states, one of them fluorescent and the other dark, via different wavelengths of light [2]. Crystal structures have shown that the nonfluorescent state of the asFP595 chromophore, which is identical to the GFP chromophore, is in the *trans* configuration [2], while the fluorescent form of the chromophore is *cis*.

In wild type GFP, only the *cis* conformation is observed.

Modeling studies have shown that there is enough room in the protein environment for a volume-conserving hula-twist about the exocyclic double bond of the chromophore [40]. This twisting in the excited state of the chromophore is thought to be responsible for deactivation of the asFP595 fluorescent state and photoconversion to the nonfluorescent *trans* configuration, see Figure 1.8 [40]. The protein environment of wild type GFP has evolved to suppress this photoisomerization, as the reaction would deplete the emitting, excited neutral state and reduce the quantum yield for fluorescence. Such photobehavior may lead to the development of erasable three-dimensional data storage devices [22]. Other interesting applications for the photoswitching behavior include the breaking of the diffraction barrier in microscopy with a technique called stimulated emission depletion (STED). High resolutions (20 to 50 nms) may be achieved in imaging experiments with such techniques [22].

While a wide range of colors is very useful, GFPs can also be made sensitive to environmental factors like oxygen concentration, the concentration of ions such as chloride or $Ca^{+2}$, or pH [62]. The wild type GFP is not pH sensitive, however, point mutations such as serine 65 to threonine render the phenolic hydrogen of the modified tyrosine in GFP susceptible to protonation. Thus, the S65T GFP mutant is pH sensitive, and the neutral and anionic

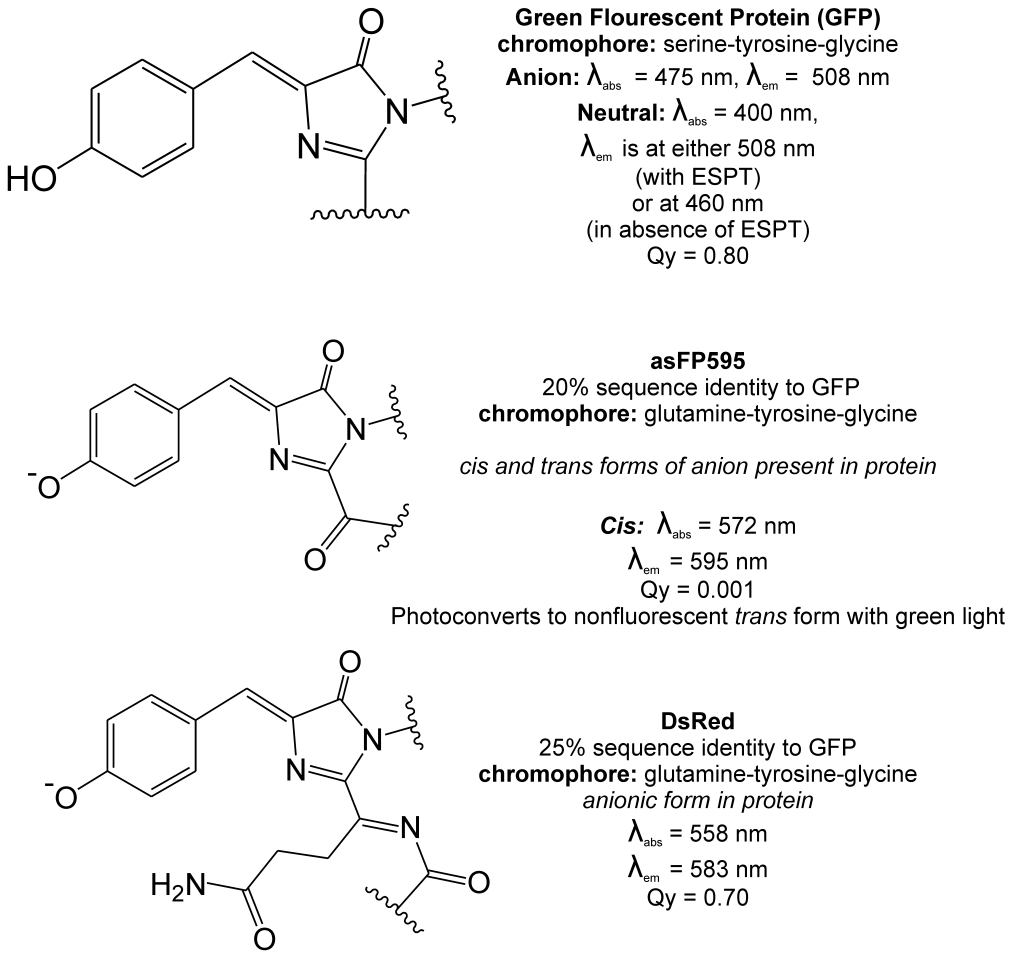


Figure 1.8: Structure of the wild type GFP chromophore and several GFP-like chromophores [19, 77]. Abbreviations: ESPT, excited state proton transfer.

chromophore forms may be observed by raising or lowering the pH of the solution. These genetically encodable sensors can report on the intercellular conditions experienced by a target protein fused to the GFP *in vivo*. For example, a fluorescent protein sensitive to chloride was recently used to non-invasively follow fluctuations within rat hippocampal cells [42].

Understanding how protein scaffolding manipulates the electronic properties of chromophores aids in the design of useful photoproteins. Single point mutations of GFP proximal to its chromophore, in addition to rendering GFP pH sensitive, can alter the color of emission. Such is the case in yellow fluorescent protein (YFP), where the mutation of a threonine (T203) to a tyrosine positioned directly beneath the chromophore delocalizes the $\pi$ electrons and shifts the wavelength of emission from green to yellow. YFP is pH sensitive as well, with a pKa of 6.3. Such diversely colored, genetically expressible imaging agents are invaluable for research in multiple areas including protein protein interactions (FRET), cell dynamics, and highly resolved localization studies of proteins within the cell.

A key factor to investigate in the GFPs is what affects their quantum yield for emission. While the GFPs have evolved to maximize their quantum yields for fluorescence, irradiation can result in the photochemical formation of nonfluorescent states. Several important mutants of GFP used in imaging

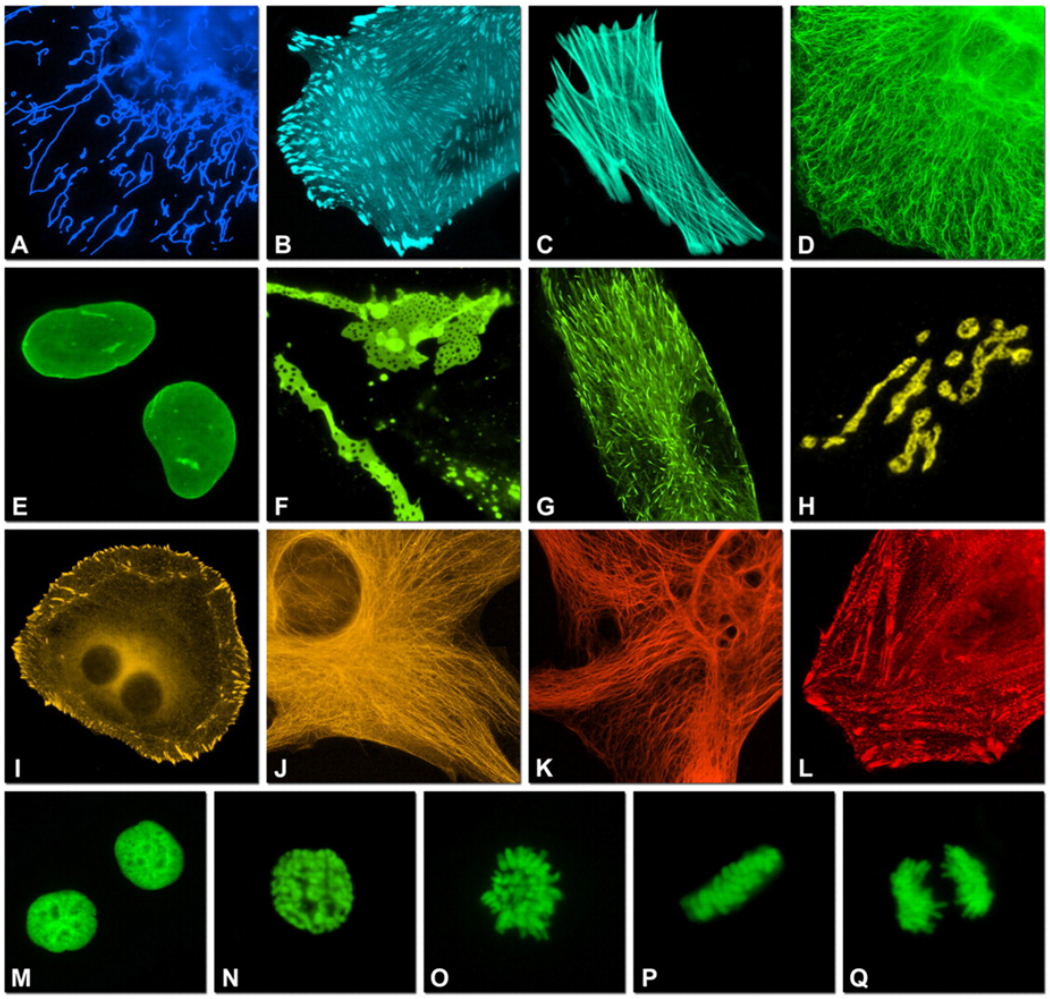


Figure 1.9: Organelles imaged with targeted fluorescent proteins. (A) Mitochondria; (B) Focal adhesions; (C) Filamentous actin; (D) Intermediate filaments; (E) Nuclear envelope; (F) Gap junctions; (G) Human microtubule-associated protein; (H) Golgi complex; (I) Focal adhesions; (J) Microtubules; (K) Human vimentin, intermediate filaments; (L) Cytoskeleton; (M) Interphase; (N) Prophase; (O) Prometaphase; (P) Metaphase; (Q) Anaphase. Figure from Shaner et al., 2007 [62].

experiments show these photoconversions to fluorescently dark states under commonly used wavelengths and intensities. These "dark" states can severely interfere with data collection in imaging experiments. To properly analyze the data from such experiments, photobleaching must be accounted for. Other photoreactions have been noted in such experiments, such as the "blinking" of mutant GFPs and GFP-like fluorescent proteins. Such blinking behavior is thought to be due to conversion between fluorescent and dark conformations of the chromophore, similar to the *cis-trans* interconversion seen in the photoswitching asFP595. These dark conformations have uses as well, and may be used in FRAP experiments or, in the case of reversible photobleaching, may be used to significantly improve resolution in microscopy experiments [22].

To design fluorescent proteins for further use in biotechnology an intimate knowledge of how the protein environment affects the photophysical properties of the chromophore is required. The present work investigates the photoconversion of YFP, an important GFP mutant that is used in many molecular biology experiments. YFP has been shown photoconvert, in small amounts, to a nonfluorescent state that is not itself irreversibly photobleached. Irradiation in the ultraviolet of this dark YFP state results in recovery of fluorescence. Steady state Raman spectroscopy was used to investigate the molecular nature of this nonemissive state.

This work also examines the cyan emitting GFP-like dsFP483. Though dsFP483 shows the 11-stranded $\beta$-barrel structure that is highly conserved in marine fluorescent proteins, it has only about 25% sequence identity with GFP and has a higher degree of similarity (55%) to the red emitting protein DsRed from the reef coral *Discosoma sp* (see Figure 1.8). [41]. The DsRed protein shows only 25% sequence identity with wild type GFP, but retains the $\beta$-barrel structure and a chromophore that while chemically quite similar to wtGFP has a red shifted emission maximum. This is due to an additional covalent modification that extends the conjugation by the addition of a acylimine moiety (see Figure 1.8) [80].

Point mutations of GFP, such as tyrosine 66 to tryptophan, result in similar, blue shifted emission peaks. However, the chromophore of dsFP483 is identical to wild type GFP, thus raising the question of how the blue shifted emission is produced. Raman spectroscopy was employed to elucidate the effect of the dsFP483 protein environment on the GFP chromophore and to reveal the structural origin for the cyan fluorescence.

## 1.3 BLUF: A Sensor for Blue Light

Unlike the *cis-trans* isomerization seen in GFPs and other photosensitive proteins, the flavin chromophore in BLUF domains cannot undergo significant

structural changes when illuminated. Fluorescence from the bound flavin is rapidly quenched, as opposed to enhanced in GFPs, by the protein environment. The BLUF domain exhibits a photocycle in which a biologically active signaling state (light AppA, or lAppA) is formed within a nanosecond of excitation. The signaling state slowly relaxes back to its dark form (dark AppA, or dAppA) over about a half hour, see Figure 1.11.

The BLUF domain arises in a variety of bacteria. The first and best characterized is the BLUF-containing AppA protein from the purple heterotroph *Rhodobacter sphaeroides*. All flavins found within the cell may bind to BLUF domains [33], although the proteins are usually reconstituted with FAD, FMN or riboflavin (Figure 1.3) to ensure a homogenous sample for spectroscopic studies. The side chain of the flavin has been shown to not participate in the photochemistry of the BLUF domain [46]. The full-length AppA protein is 400 amino acids long and integrates both light and voltage information from the environment to regulate the transcription of photosynthetic genes, see Figure 1.10. The N-terminus of AppA contains the BLUF domain which noncovalently binds a flavin chromophore. The C-terminal domain of AppA is cysteine rich and is thought to transmit information about environmental oxygen levels through a bound heme.

AppA is known to associate with the transcriptional repressor PpsR in

its dark, resting state (see Figures 1.10 and 1.11), under dim light conditions and low concentrations of environmental oxygen. Upon intense ultraviolet light exposure, or an increase in environmental oxygen concentrations, the PpsR protein is released to regulate the transcription of photosynthetic genes [44]. The photosynthetic proteins encoded by these genes are highly sensitive to photodegradation. Thus, this photophobic response to irradiation at blue or ultraviolet wavelengths downregulates photosynthetic gene transcription. When oxygen levels are high, the bacterium may engage in the more efficient process of aerobic respiration to meet its energy requirements. The photosyntheic genes are once again downregulated under high oxygen conditions so the bacterium does not waste energy in the synthesis of the less efficient light harvesting proteins.

The light, signaling state of AppA is formed on a nanosecond timescale directly from the singlet excited state of the flavin (see Figure 1.11) [12]. A conformational change of the protein is thought to transform the ultrafast blue light environmental information into the biologic response of DNA transcription. The quantum yield for red state formation in AppA is 0.24, similar to other flavin-based photoreceptors [12]. A small red shift of about 10 nm is observed in the electronic absorption spectrum of the flavin upon entry into the signaling state, indicated that no major structural changes occur to

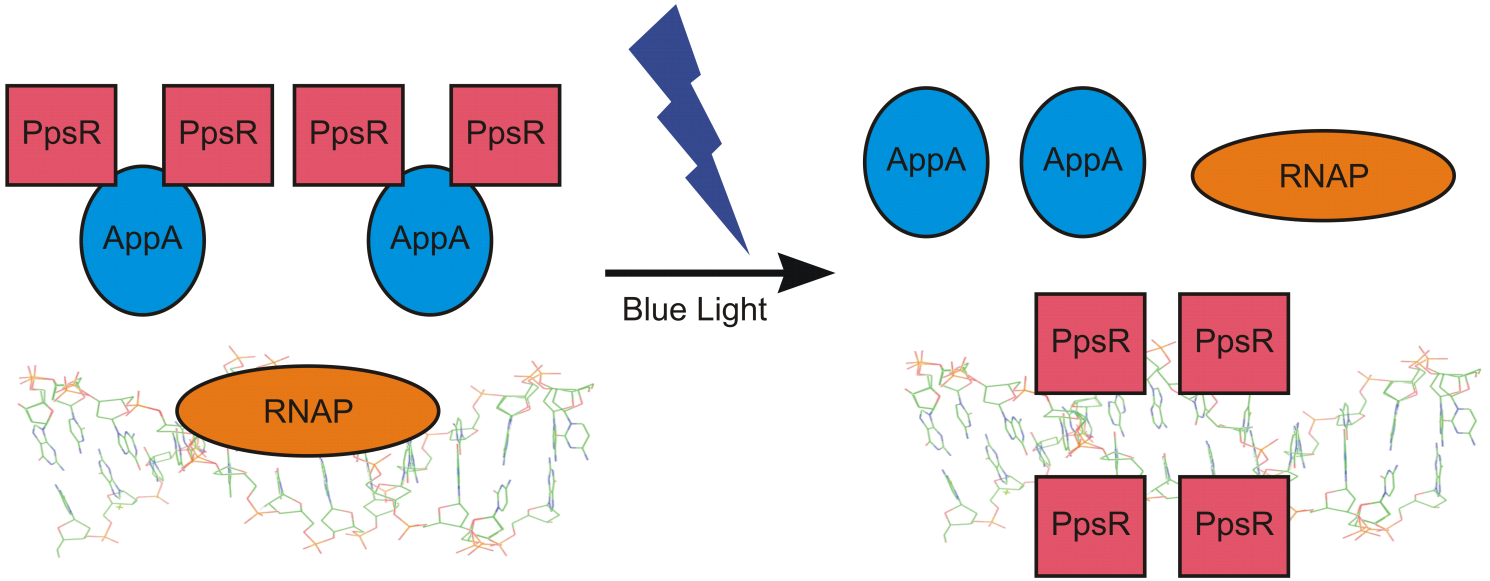


Figure 1.10: Biological response of AppA to blue light input. From Masuda et al., 2002. Abbreviations: RNAP, RNA polymerase.

the flavin chromophore upon entry into the AppA signaling state [44]. The recovery back to the dark, resting state for AppA is slow ($t_{1/2}$ = 0.5 hours) and occurs via a monoexponential process [12].

Important interactions between the flavin chromophore and the protein environment that regulate the photophysics of the AppA BLUF domain have been discovered through site directed mutagenesis. A conserved glutamine (Q63) and tyrosine (Y21) in the AppA BLUF domain have been implicated by such studies in responding to flavin excitation on an ultrafast timescale (see Figure 1.13). The Q63L and Y21F mutants of AppA are photoinactive, showing no changes in their spectra when illuminated. This demonstrates the importance of both the glutamine and the tyrosine in the BLUF photocycle. However, mutation of the tryptophan (W104) to a phenylalanine or an alanine results in photoactive protein with a slightly higher quantum yield for the light state formation and an increased rate of recovery back to the dark state by at least half [48, 49]. This indicates that the amino acids immediately surrounding the flavin chromophore play an extremely important role in determining the photophysical prosperities of the AppA BLUF domain. Interestingly, mutation of a leucine approximately 3 Å from the chromophore to a cysteine results in cysteinyl adduct formation to the flavin such as that seen in the LOV domains [68].

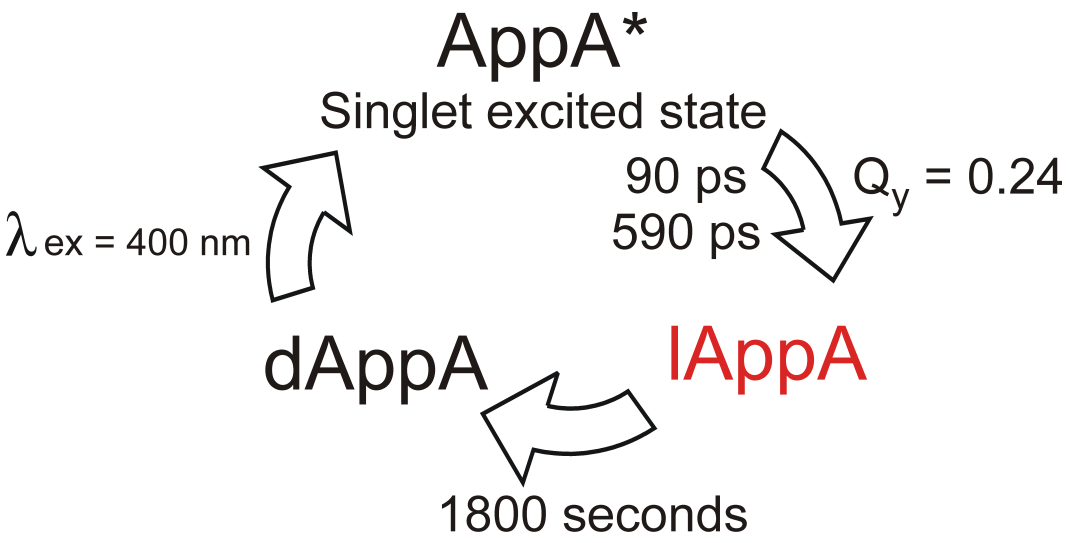


Figure 1.11: Photocycle of the AppA BLUF domain. Notation: dAppA refers to the dark AppA state, lAppA refers to the light AppA (signaling) state. From Gauden et al., 2005 [34].

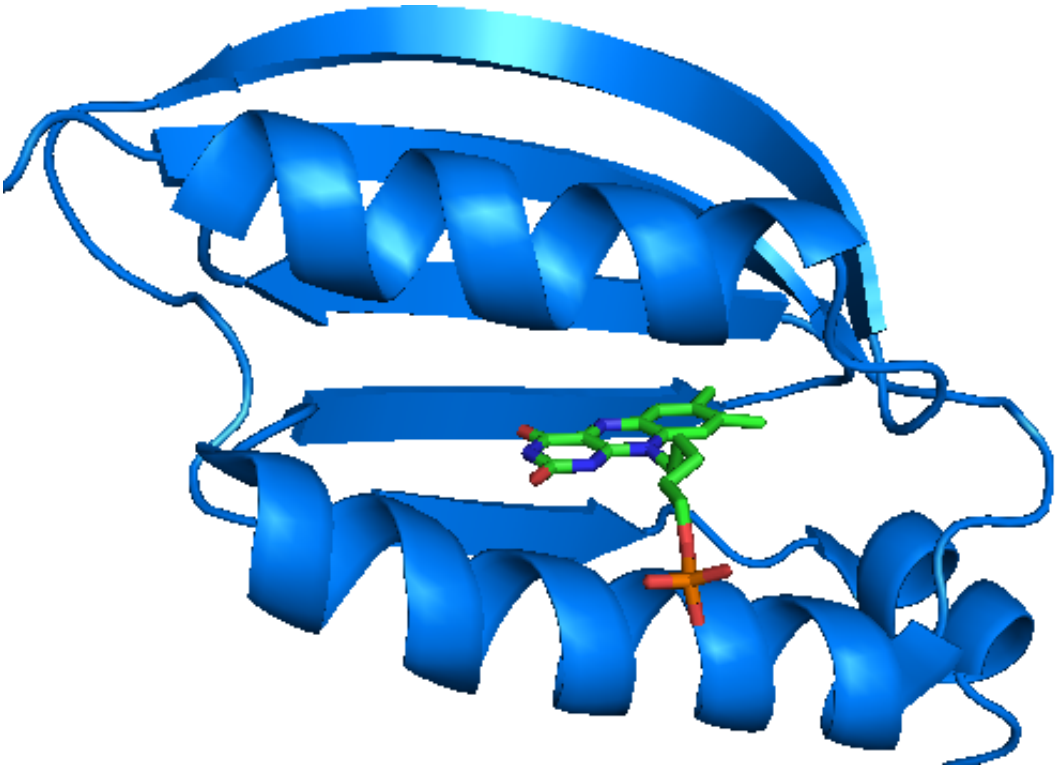

Figure 1.12: Crystal structure of the AppA BLUF domain. From Anderson et al., 2005 [1]. (PDBID: 1YRX)

While all BLUF domains show a high degree of homology, the photophysical properties such as the yield for formation of the light state of the protein as well as the recovery time back to the dark state varies greatly between the BLUF domains of different species. The full length AppA protein is 400 amino acids long, and its BLUF domain is just the first hundred residues. The full length BLUF photosensing proteins from other bacteria are much smaller, generally less than 200 amino acids long (see Table 1.1).

While showing a high degree of homology to the BLUF domain of AppA, the shorter BLUF domains of other bacteria have different photocycle characteristics than shown for the AppA BLUF. Specifically, these short BLUFs have higher quantum yields for formation of their light states than the BLUF domain of AppA, ranging from 0.3 to 0.4. Another difference between the short BLUF domains and the AppA BLUF domain is the recovery time back to the dark state (see Figure 1.11). In AppA, which must regulate transcriptional machinery to propagate its biological response, this time is about 15 minutes. Compared to AppA, the short BLUF domains have a dramatically reduced recovery time, with each of them requiring less than 20 seconds to return to their dark states. Interestingly, the biological responses of these short BLUF proteins (where known) generally involve the regulation of cellular processes that occur on shorter timescales that DNA transcription.

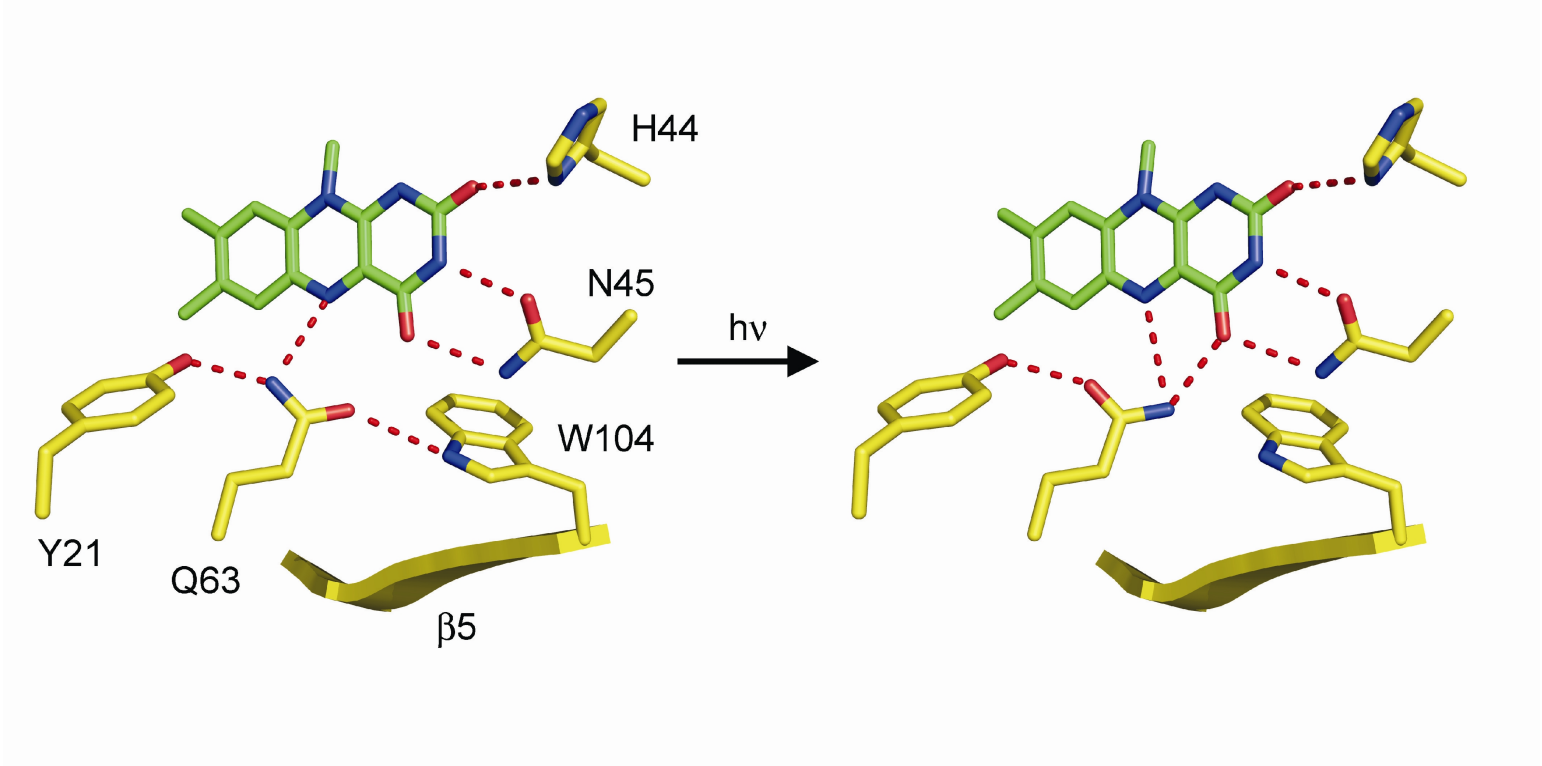


Figure 1.13: The flavin binding site and its protein environment of the AppA BLUF domain. Shown is a possible configuration of the light state of AppA where the glutamine 63 has been rotated 180 °. From Anderson et al., 2005 [1]. (PDBID: 1YRX)

These processes include controlling intracellular cyclic AMP concentrations, as well as regulating phototaxis, in response to a blue light input signal. These proteins also have a methionine the place of the tryptophan 104 seen in AppA (see Figure 1.13). Since mutation at the 104 position in AppA results in proteins with shortened recovery times and higher quantum yields, this position may serve tune the biological lifetime of the light BLUF state in all BLUF domains.

Many structural studies, ranging from NMR and X-ray crystallography to vibrational techniques such as Raman and FTIR spectroscopy, have been performed on BLUF domains to determine the molecular configuration of the protein environment around the flavin chromophore in the signaling state (or light state) of the protein. The dark state of the BLUF domain from AppA is readily crystalized, but irradiation of the AppA crystals damages them. This is not the case for all BLUF domains, however, and crystallography studies of short BLUF domains have been able to obtain data from the light state of the protein.

The X-ray crystallography and NMR studies that have been performed on the AppA BLUF domain [1, 15, 26, 16] and on BLUF domains from other bacteria [25, 29, 84] reveal a domain with a ferredoxin like fold consisting of five $\beta$-sheets and two $\alpha$ helices that sandwich the flavin chromophore (see Figure

Table 1.1: Photophysical properties of BLUF domains from several bacteria. Recovery times are in $H_2O$. Quantum yields refer to the yield of light state formation.

| | Number amino acids | Biological function | Recovery time | Quantum yield |
|---|---|---|---|---|
| **AppA** | 400 | DNA regulation | 15 minutes | 0.24 |
| **Slr1694** | 151 | phototaxis | 20 seconds | 0.63 |
| **BlrB** | 140 | unknown | 2 seconds | 0.40 |
| **T110078** | 143 | unknown | 1.5 seconds | 0.30 |

1.12). The flavin is noncovalently bound to the protein though a hydrogen bond network.

Slight structural differences exist between these BLUF proteins, both compared to AppA and to other, short BLUF domains. Specifically, crystal structures of the dark states of BlrB from *R. sphaeroides* and Tll0078 *Thermosynechococcus elongatus* (also referred to as TePixD) show a flipped orientation of the essential glutamine amide side chain to that seen in the AppA structure from Anderson el al., 2005 (see Figure 1.13).

The Slr1694 BLUF protein (also called PixD) from *Synechocystis sp.* PCC 6803 has a glutamine orientation similar to that of AppA and opposite that of BlrB and T110078 [29]. The 20 second recovery time for this BLUF domain is slightly longer than seen in the proteins with a flipped glutamine side chain orientation, and its quantum yield is about three times that of AppA. In the Slr1694 crystal structure, two orientations of the glutamine can be seen [84]. One is called the pseudo-dark state by the authors as their protein crystals had been exposed to (dim) irradiation. This pseudo-dark state has the same glutamine orientation as seen in the Anderson 2005 crystal structure of AppA, which was also grown under low-light condition. Upon irradiation of Slr1694 crystals, the glutamine side chain flipped by 180°. Interestingly, the pseudo-dark state of Slr1694 does not show a hydrogen bond between the glutamine

and tryptophan. However, the light state shows an interaction between the glutamine and a methionine that is solvent exposed in the dark, similar to those seen in the BlrB and T110078 BLUFs. Therefore, the Slr1694 BLUF protein seems to combine the dark glutamine orientation of AppA and the methionine hydrogen bond seen in BlrB and T110078. This configuration of the glutamine side chain combined with the methionine hydrogen bond may be responsible for the longer recovery time observed in Slr1694, which at 20 seconds is much less than that of AppA, and 20 times that of BlrB and T110078.

The BLUF domians function as "blue light input domains" and can regulate a range of cellular processes. A recently discovered BLUF from *Euglena gracilis* was found to have photoactivated adenylyl cyclase (PAC) activity. This BLUF PAC was expressed in *Xenopus laevis* oocytes, HEK293 cells, and in *Drosophila melanogaster* [61]. The authors found they were able to manipulate intracellular cAMP levels in the oocytes and HEK293 cells with high spatiotemporal resolution, and that behavioral changes could be induced with light in *Drosophila*. Studies such as these that seek to obtain fine tuned control over cellular processes typically must employ much slower methods and invasive labels [61].

Steady-state difference IR and Raman studies have shown changes in a carbonyl mode that indicate a stronger hydrogen bonding environment around

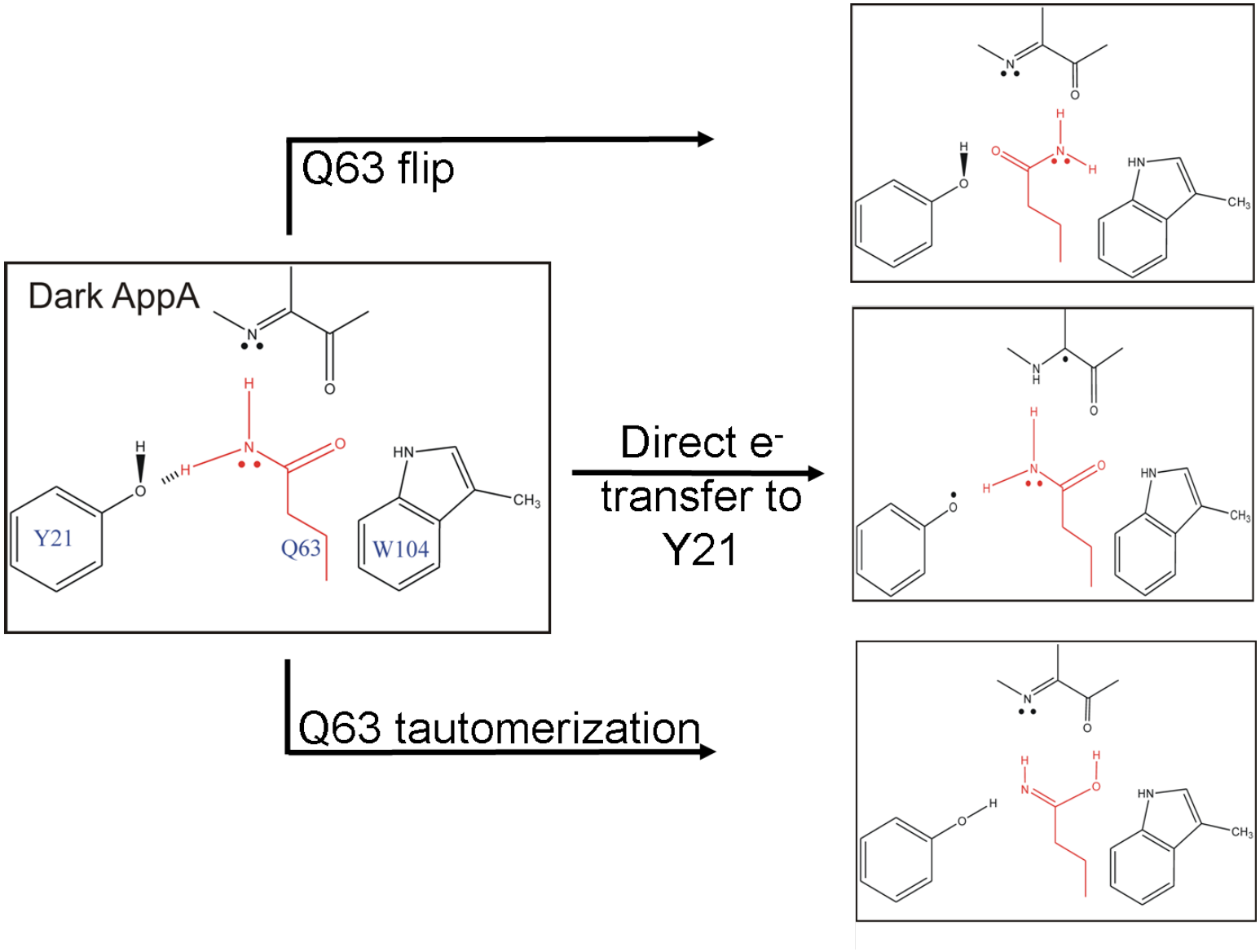


Figure 1.14: Models for light state formation in AppA. From Anderson et al., 2005; Laan et al., 2006; and Stelling et al.; 2007 [1, 65, 34].

the flavin C4=O group in the light state. Labeling studies have been performed with AppA grown on either $^{15}$N or $^{13}$C media, thus labeling every carbon or nitrogen within the protein [47]. Studies that use flavin labeled with $^{13}$C at every carbon within the isoalloxazine ring have been performed as well [47]. The light minus dark FTIR and Raman difference spectra show changes to a flavin carbonyl mode at around 1700 cm$^{-1}$, this mode is assigned to the C4=O group of the flavin and the chnges to this flavin mode are consistant with strangthing of the hydrogen boding environemnt about this caronyl in the light state of AppA. When the protein is labeled with $^{15}$N or $^{13}$C difference modes in the FTIR at (+)1630 and (-)1620 cm$^{-1}$ shift [47], indicating that there are changes to the protein residues when entering the light state.

Current models for formation of the light state of AppA include a simple 180° flip of the proximal glutamine side chain, tautomerization of the glutamine side chain, and direct proton transfer from the tyrosine (Y21) to the flavin N5 (see Figure 1.14). NMR data shows that the tyrosine phenolic hydrogen is exchangeable in the dark state, but is protected from exchange upon entering the signaling state [15]. Analysis of crystal structure data leaves the orientation of the glutamine side chain ambiguous, and several computational studies at the QM/MM level have been undertaken on BLUF domains to elucidate the initial events of the photocycle [10, 59]. These studies

predict a light induced tautomerization of the Q side chain. A recent EPR study readily observed the formation of a tyrosine/neutral flavin radical pair in T110078 [52]. Interestingly, the photoinactive Y21F mutant still produced a radical flavosemiquinone species, suggesting that the initial proton transfer must come from a residue other than the tyrosine [52].

To investigate the method by which the ultrafast light signal is translated into changes on a biological timescale, picosecond infrared absorption and transient emission (PIRATE) studies describe in this work were performed on the light and dark state of both the wild type and mutants of the AppA BLUF domain. To discriminate between protein and flavin vibrational modes, isotopically labeled flavins were bound to the wild type domain and examined with the PIRATE technique.

## 1.4 Probing Photoreactions with Vibrational Spectroscopy

Vibrational spectroscopy, such as infrared and Raman spectroscopy, is sensitive to changes in molecular structure and environment. Biological chromophores have large, delocalized $\pi$ electron systems that have a large Raman cross section. These strong Raman intensities allow the analysis of subtle

changes to the chromophore caused by immersion in the protein environment. Recent advances in detection and light filtering technology allow for efficient removal of the Rayleigh scattered light, which can overwhelm the weak Raman effect. Excitation at an off-resonance wavelength (752 nm) avoids the common problem of sample fluorescence that can overwhelm the weak Raman scattering effect of biological samples.

Steady-state infrared spectroscopy is another useful technique that can access chemical bond information. Difference spectra can be generated to analyze the changes between two different states of a protein. Infrared spectroscopy requires higher concentrations of protein (1 to 3 mM) than Raman spectroscopy and must be performed in $D_2O$ to avoid the intense OH absorption from water.

Photoproteins respond to light on an ultrafast timescale (pico to nanosecond), and to monitor these photoreactions a pump-probe setup is employed. The PIRATE (picosecond infrared absorption and transient emission) technique uses a tunable pump beam in the visible region to excite chromophores into their electronically excited states. An infrared probe beam is then used to examine these states at different time delays. The ground state IR (-50 ps prior to excitation) is subtracted from the IR of the excited state to give time resolved difference spectra that show the picosecond resolved evolution of the

photoreaction.

In the present work, steady state Raman spectroscopy was employed to investigate the photoconversion of the dimly fluorescent neutral YFP chromophore to a completely dark, nonfluorescent form of the chromophore. Steady state Raman and IR spectroscopy were also performed on the BLUF domain of AppA bound to flavin containing isotopes in specific position around the isoalloxazine ring to aid in the assignment of protein and chromophore modes. Time-resolved infrared spectroscopy was then employed to probe the early structural events of the AppA BLUF domain photoreaction to its light state with proteins containing both isotopically labeled and unlabeled flavins, and to examine several important point mutants of the domain that affect the photocycle.

# Chapter 2

# Light Driven Formation of Nonfluorescent States in Yellow Fluorescent Protein

## 2.1 Abstract

Yellow fluorescent protein (YFP) is a mutant of green fluorescent protein that has a wide range of applications in biotechnology. The YFP mutations render the protein pH sensitive, as well as red shifting shifting the emission maximum of its anion to 527 nm. Recent studies show that the YFP fluorescence exhibits photobleaching behavior, wherein the YFP chromophore is photoconverted to nonfluorescent states. Some of this photoconversion is due to a decarboxylation reaction that results in irreversibly bleached YFP. However, McAnaney et al. (2005) discovered that a small percentage of the yellow fluorescence could be recovered by either leaving the protein in the dark,

or by irradiation at ultraviolet wavelengths. The recovery of florescence was slow (hours) in the dark and fast (minutes) with the UV light, and involved a transition to the neutral form of the YFP chromophore. To isolate this reversibly bleachable state of YFP, the neutral form of the chromophore was populated by lowering the pH. Photoconversion of the neutral form of YFP resulted in a new absorbance at 330 nm. Raman spectroscopy was then employed to examine the photoconversion of the neutral YFP chromophore to this reversibly bleached state. The results were consistent with *cis-trans* photoisomerization of the neutral YFP chromophore.

## 2.2 Introduction

The GFP mutant yellow fluorescent protein (YFP), has a red-shifted emission maxima compared to the wild type protein. YFP is an important mutant that is widely used in molecular and cell biology. YFP differs from GFP by the introduction of four mutations (S65G, V68L, S72A and T203Y). Unlike GFP, the chromophore in YFP is sensitive to pH (see Figure 2.2), ionizing with a pKa value of 6.3. The anion absorbs at 513 nm while the neutral lies at 400 nm. Excitation of the neutral form at 400 nm results in low yields (0.002) of yellow fluorescence at 527 nm. This is thought to be due to an excited state proton transfer reaction similar to that seen in the wild type

protein, but much less efficient (see Figure 2.3). Excitation of the anion at 513 nm, however, results in high yields of 527 nm fluorescence. YFP therefore fluoresces from the anionic from of its chromophore, as is the case in wild type GFP.

Recent work by McAnaney et al., 2005 found that the YFP anion could be both irreversibly and reversibly photoconverted using wavelengths and intensities common in fluorescence studies [50]. The authors found that the irreversible bleaching was due to conversion to a decarboxylated, irreversibly photobleached state of the protein (XFP in Figure 2.3), similar to what is seen in wild type GFP. The side chain of glutamate 222 acts as a proton acceptor for the excited state deprotonation reaction, however, this residue eventually decarboxylates. Decarboxylation of the glutamate side chain in wild type GFP results in protein that does not give green florescence when excited at 400 nm, as the neutral form of the GFP chromophore can no longer be deprotonated in its excited state to create the emitting anion. Since the decarboxylation of the glutamate side chain is irreversible, wild type GFP is irreversibly photoconverted to a nonfluorescent state.

As mentioned above, YFP undergoes a similar irreversible decarboxylation reaction like that seen in wild type GFP. However, another photoreaction can be observed in YFP. When McAnaney et al. performed their bleaching

experiments, it was found that small amounts of fluorescence could be regained by keeping the YFP molecules in the dark. After a few hours in the dark, it was found that a small percentage of fluorescence was recovered. Interestingly, it was also possible to convert a small fraction of this reversibly bleached YFP population back to the bright, emissive state by exposing the proteins to just a few minutes of UV light. This photorecovery of fluorescence seen in YFP, then, occurs via a process that is slow in the ground state but fast in the excited state.

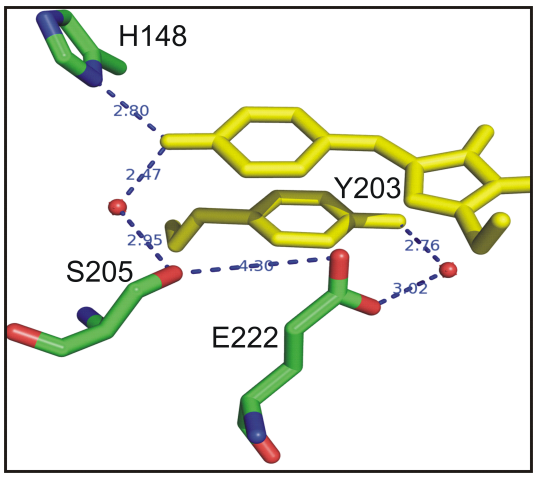


Figure 2.1: Crystal structure of the YFP chromophore and protein environment (PDB ID: 1YFP). From Wachter et al., 1998 [78].

YFP is commonly used for imaging studies using light microscopy as well as FRET experiments. Under the conditions employed for these experiments, the intensity of YFP fluorescence has been shown to decrease leading to the possi-

bility that data obtained in the imaging experiments could be misinterpreted. There is thus significant interest in understanding the molecular basis for this bleaching in fluorescence. A common concern in such studies is the reversible "blinking" behavior, where the chromophore switches between bright and dark states over periods ranging from seconds to hours [50]. The GFP-like asFP595 has a chromophore that resembles that of wild type GFP save for the addition of another double bond that extends the $\pi$ conjugation. Blinking in asFP595 has been shown to be due to photoisomerization to a nonflorescent *trans* state of the chromophore. In YFP, the nature of the reversibly bleached state is unknown.

A photokinetic scheme is described in McAnaney et al., 2005 for YFP whereby the excited state of the emitting anion is depleted by an excited state protonation reaction to form a neutral chromophore (see Figure 2.3). This is the opposite of the wild type GFP, which undergoes an excited state deprotonation reaction to convert to the anionic, florescent from. The excited, neutral YFP may be deprotonated and revert back to the fluorescent anion in the reverse reaction. Alternately, as discovered by McAnaney et al., the YFP excited neutral state may be even further converted to a reversibly bleached, dark neutral state ("YFP reversibly bleached" form of YFP in Figure 2.3). It was found that the excited state of this neutral, bleached form decayed

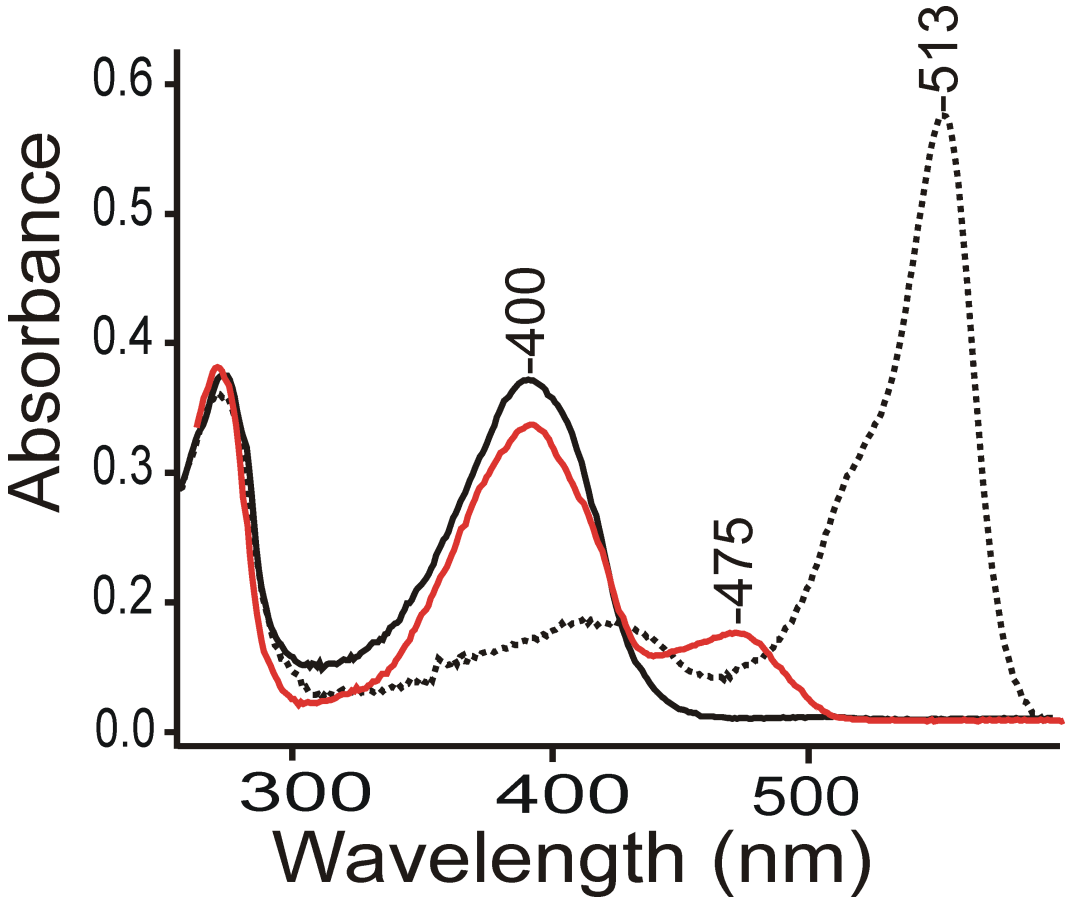


Figure 2.2: Electronic absorption spectra of YFP in pH 8 (dashed) or pH 6 (solid) buffer. The spectrum of wild type GFP, which is pH-independent, is shown in red.

very rapidly into its ground state, thus kinetically trapping the chromophore once it was in the nonfluorescent, neutral configuration. Thus, it is though the excited state of the neutral chromophore that photoconversion to the reversibly dark state occurs (see Figure 2.3). The excited state of the anionic form is slowly depleted by conversion to first the neutral, and then on to the reversibly bleached neutral state. This results in a gradual loss of the yellow fluorescence as the YFP anion is slowly converted to the unknown bleached state.

Interestingly, irradiation in the UV results in recovery of YFP fluorescence within a matter of minutes. The blue light permits the reversibly bleached, neutral YFP to go back into its excited state (see Figure 2.3). While the ground state conversion back to neutral YFP is slow, the excited state pathway is fast. The reversibly bleached neutral YFP may therefore convert to the unbleached neutral YFP quickly in its excited state. The excited, neutral chromophore may then undergo an excited state protonation and revert back to the emitting anionic form, which regains the yellow fluorescence.

The chemical nature of the YFP reversibly bleached neutral form, as mentioned, is not known. Hampering investigation of this form is the fact that the yield for formation of the unknown state at is quite small. Additional considerations further limit the methods by which this dark form may be examined, as the reversible photobeaching does not occur with high concen-

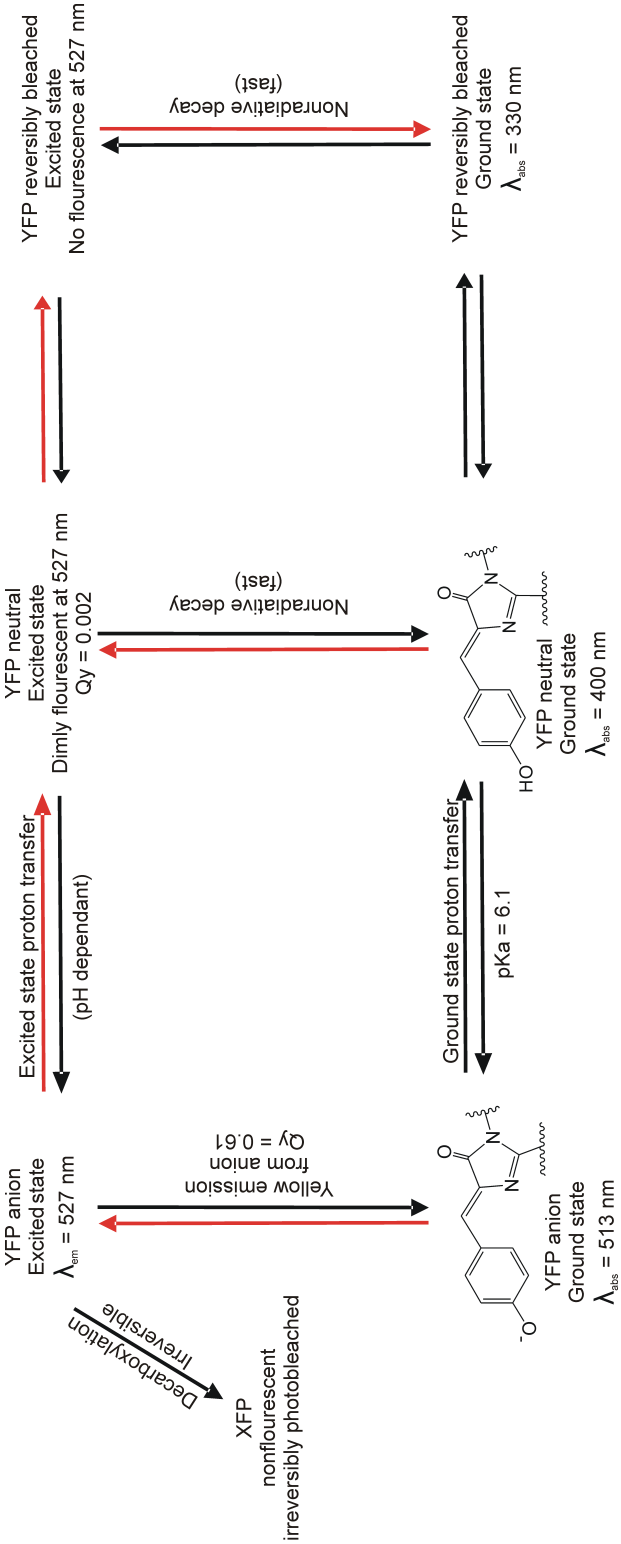


Figure 2.3: Routes for decay of the fluorescent YFP anion. The anion may be converted to the neutral in the excited state, and the neutral may further convert to the reversible bleached form of YFP [50]. Red lines indicate routes for conversion to reversibly bleached YFP. From McAnaney et al., 2005 [50]

trations (mM) of YFP [63]. Thus a technique is required that will not use overly high concentrations of YFP (50 to 70 $\mu$M). Such low concentration requirements means that techniques such as NMR and infrared spectroscopy, that require mM concentrations of anylate, cannot be used to monitor the YFP photobleaching behavior.

However, Raman spectroscopy may be used to observe proteins in the 50 to 70 $\mu$M concentration range. Raman spectroscopy is sensitive to chemical bonds and their environment, and so this vibrational technique may be employed to examine the YFP neutral, reversibly bleached state to determine its chemical nature. The Raman spectra of both wild type and mutants of GFP, including the S64T point mutant that renders GFP pH sensitive, have been characterized [5]. In particular, there are several pH-sensitive modes in the GFP chromophore that are observed in the Raman spectrum. Among these modes is the exocyclic C=C stretch, whose frequency ranges from 1640 $cm^{-1}$ in the neutral to 1618 $cm^{-1}$ in the anion. Thus, Raman spectroscopy is sensitive enough to determine the protonation state of the GFP chromophore. The protonation state directly affects photophysical properties in the GFP chromophore, such as the color of emission and its quantum yield for florescence. It is therefore vital to determine the chromophore protonation state as this aids in the design of, among other things, new colors for use in molecular biology experiments.

Only small yields of photoconversion to the reversibly bleached neutral YFP were observed by McAnaney et al. in YFP at pH 8, as the anion is the emissive state of the YFP chomophore. This is because the chromophore must be neutral before it may further photoconvert to the reversibly bleached form. At pH 8, which is well above the pKa for YFP, only small amounts of the neutral form are observed (see Figure 2.4) [50]. The studies performed by McAnaney et al. were performed at a pH of about 8, and were thus examining only the anionic form of YFP. Another reason for the low photoconversion yields in the study by McAnaney was the excitation wavelength [50]. The authors only exited the anion of YFP, which means the protein must undergo a protonation reaction before further converting to the reversibly bleached from [50]. Excitation of the neutral YFP, which absorbs at 400 nm, allows a more direct route to the reversibly bleached from.

Charged molecules tend to have a larger Raman cross section, and thus the presence of an anion would overwhelm any signal from the neutral form. Therefore, both to increase the yield for the YFP photoreaction to the reversibly bleached, neutral state and to decrease the population of the YFP anion, the pH was lowered to 5.8, and wavelengths that excited only the neutral form (400 nm) were employed. Raman spectroscopy was then performed to determine the molecular nature of the reversibly bleached, neutral state of YFP.

## 2.3 Materials and Methods

*Sample Preparations:* YFP was expressed and purified according to standard procedures. BL21DE3 plyS E. coli cells transformed with a plasmid containing the YFP sequence and a C-terminal His6-tag were grown in 1 L of LB medium (4 L flask) containing 0.5 mM ampicillin at 37 °C for 4 h until an OD600 was reached. Protein expression was then induced by addition of 0.8 mM of isopropyl $\beta$-D-1-thiogalactopyranoside (IPTG) followed by incubation at 25 °C overnight in the dark. Cells were harvested by centrifugation and resuspended in 30 mL of lysis buffer (50 mM sodium phosphate, 150 mM NaCl, pH 8.0) to which 15 $\mu$L of the protease inhibitor PMSF (50 mM stock solution in ethanol) had been added. After lysing the cells by sonication, cell debris was removed by centrifugation (33 K, 1.5 h). Subsequently, YFP was purified by Ni-NTA chromatography (Qiagen), using 10 to 20 mM imidazole buffer (50 mM sodium phosphate, 200 mM NaCl, pH 8) as the wash buffer and 250 mM imidazole in the same buffer to elute the protein from the column. Column fractions containing protein were combined and dialyzed overnight in the dark against 150 mM sodium phosphate, 300 mM NaCl, pH 8 buffer. Protein purity was assessed by SDS-PAGE electrophoresis and UV-vis spectroscopy (protein, $\epsilon_{514}$ = 30,800 $M^{-1}cm^{-1}$; $\epsilon_{400}$ = 18,000 $M^{-1}cm^{-1}$). Typical yields for YFP production were 8 to 12 mg/L of LB broth.

*Photoconversion:* Photoconversion experiments were performed with a 500 W Oriel XeHg lamp using a 405 nm band-pass filter. Typically, 40 uM YFP in 300 mM NaCl, 50 mM sodium phosphate pH 5.8 buffer was exposed to up to 50 mW of 400 nm light in a 1 cm cuvette for 1 hour. Steady-state absorption spectra were recorded at 25 °C on a Varian Cary 300 UV-vis spectrometer. Typical photoconversion yields were around 80%, typical concentrations were at 10 to 20 $\mu$M YFP.

*Steady-State Raman Spectroscopy:* Steady-state Raman spectroscopy was performed on using an off resonance instrument that has been described previously [5]. Data for the neutral YFP were collected with 752 nm excitation employing a 90° collection geometry. Power at the 2 mm by 2 mm fluorimeter cell that held 60 $\mu$L of sample was 700 mW. YFP concentrations were at about 60 $\mu$M to avoid protein aggregation problems [63] and a 20 mM sodium phosphate, 150 mM NaCl, pH 5.8 buffer was used. Use of buffers with lower pHs denatured the protein. Spectra were acquired using 2 second accumulation times and 300 scans. After the protein spectrum had been acquired, a buffer spectrum containing no protein was obtained. The buffer spectrum was then subtracted from the protein + buffer spectrum to give the Raman spectrum of the protein. Spectra were wavenumber calibrated using the Raman spectrum of cyclohexanone.

## 2.4 Results and Discussion

*Electronic absorption spectroscopy of the reversibly photobleached YFP:* To isolate and investigate the reversibly bleached, neutral from of YFP, the pH was lowered to 5.8 to ensure a large population of the protonated species that is key for obtaining high yields of the reversibly photoconverted neutral YFP form (see Figure 2.8). Irradiation with 400 nm light of the neutral form of YFP resulted in a new absorption at 330 nm in the electronic absorption spectrum (see Figure 2.4 and 2.8), quite similar to though much more intense than that reported by McAnaney et al. This new species, assumed to be reversibly bleached, neutral YFP in McAnaney's photokinetic scheme (see Figures 2.3 and 2.8), fully converts back to the neutral form of YFP slowly in the dark (hours) or rapidly with 330 nm irradiation (minutes).

The Stokes shift of 70 nm observed in YFP photoconversion is typical for dramatic structural changes to GFP chromophores. One such structural change is *cis-trans* isomerization of the GFP chromophore. While wild type GFP does not undergo this reaction, several related florescent proteins such as asFP595 and eqFL611 do. These protein have anionic, GFP-like chromophores and are able to undergo a photoinduced *cis-trans* isomerization, switching between fluorescent and nonfluorescent states. A Stokes shift of about 30 nm is observed between the two configurations of the chromophore [14]. This

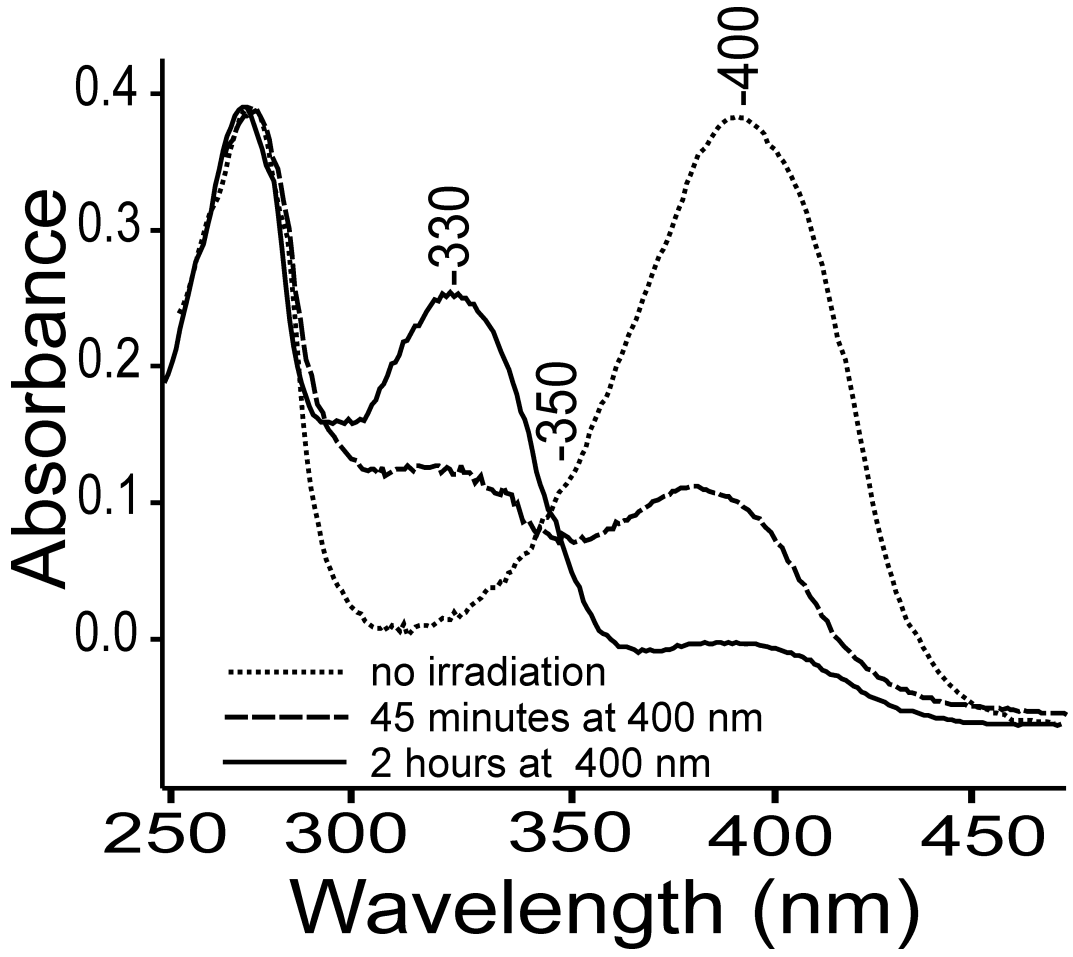


Figure 2.4: The electronic absorption spectrum of the photoconversion of YFP neutral (pH 5.8) at 400 nm.

behavior is known as photoswitching, and has potential applications in both high resolution imaging experiments as well as use as a non-volatile all-optical memory device, with the off and on states of the chromophore serving as either a "1" or "0" [54].

NMR and Raman spectroscopic studies have been performed on the small organic model chromophore of GFP, HBDI (see Figure 2.5), which undergos a photoisomerization reaction when irradiated at 365 nm [18]. The energy barrier for isomerization of HBDI varies with its protonation state, with the anionic form lying at 2.3 kcal/mol. The energy barrier for isomerization of the neutral form is slightly less, at 2.1 kcal/mol [18]. The Raman spectra of the HBDI with and without irradiation contain several modes that change upon isomerization, making Raman spectroscopy an ideal tool to elucidate the configuration of the neutral, reversibly bleached YFP chromophore.

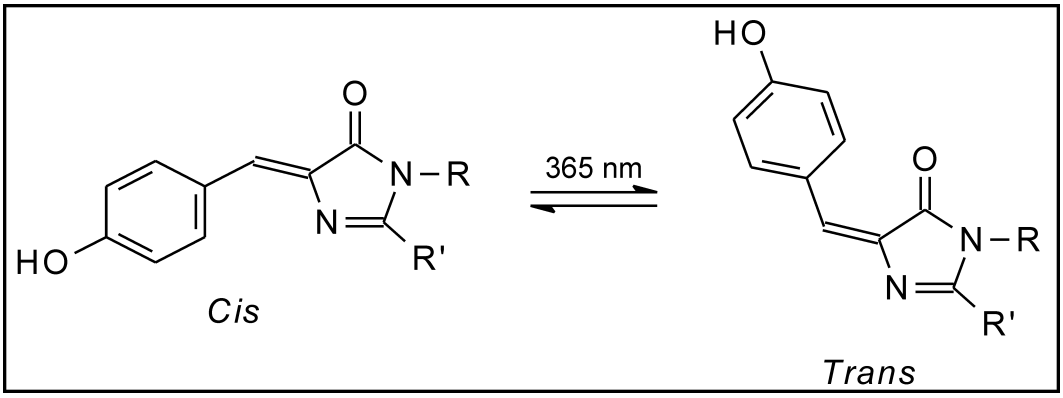


Figure 2.5: Photoisomerization between *cis* and *trans* states of the neutral HBDI model chromophore [18].

*Raman spectroscpy of photoconverted YFP:* Raman spectroscopy was used to probe the structure of the reversibly bleached, photoconverted state of neutral YFP. Shown in Figure 2.6 is the low-pH Raman spectrum of YFP with and without irradiation at 400 nm, and the Raman spectrum of neutral HBDI with and without irradiation at 365 nm. The 1666 $cm^{-1}$ mode observed in the YFP neutral spectrum aries from the amide I band of the protein [5], and is thus not present in the HBDI spectrum. Irradiation shifts the 1640 $cm^{-1}$ exocyclic C=C stretch in HBDI to 1635 $cm^{-1}$. The amide mode in YFP hides the 1640 $cm^{-1}$ mode in YFP, which is present as a shoulder in the dark protein spectrum, and disappears in the light spectrum. Subtraction of the YFP light spectrum from that of the dark protein, however, reveals a bleach of the 1640 $cm^{-1}$ mode due to the *cis* chromophore, and a new mode at 1620 $cm^{-1}$. Based on the HBDI Raman spectrum, which shows identical modes in its difference spectrum at 1640 $cm^{-1}$ and 1620 $cm^{-1}$, the new 1620 $cm^{-1}$ mode in YFP may be assigned to exocyclic C=C stretch of the *cis* conformation in the neutral chromophore.

The 1565 $cm^{-1}$ mode is assigned to the C=N stretch in HBDI. This mode decreases in intensity and undergoes a blue shift to 1575 $cm^{-1}$ upon irradiation of the model HBDI chromophore. This change is observed in the neutral YFP Raman spectrum as well, as the 1560 $cm^{-1}$ mode decreases in intensity with

irradiation, and a new mode appears at 1580 $cm^{-1}$. The 1580 $cm^{-1}$ mode observed in the protein is present as a shoulder in the unsubtracted spectrum. Subtraction of the reversibly bleached, neutral YFP Raman spectrum from the unbleached neutral YFP reveals an intense, positive absorption at 1580 $cm^{-1}$, as well as loss of the 1560 $cm^{-1}$. The mode at 1600 $cm^{-1}$ does not appear to change with irradiation.

## 2.5 Summary

The light driven photoconversion of the neutral YFP chromophore was investigated with electronic absorption and Raman spectroscopy. Several photoconversion reactions deplete the excited state of the the YFP anion, including the formation of an irreversibly bleached, decarboxylated from of the protein (XFP, see Figure 2.3). The reversible blinking behavior of the anionic chromophore may be explained by conversion in the excited state to the neutral form. The excited state of the neutral YFP chromophore has several pathways open to it, including the reverse protonation reaction back to the excited state anion to give fluorescence at 527 nm (see Figure 2.3). One of these pathways for decay traps the neutral chromophore in a nonfluorescent state. Only a small amount of the emitting anion may be photoconverted at pH 8, however, since the excited-state proton transfer reaction is pH dependant

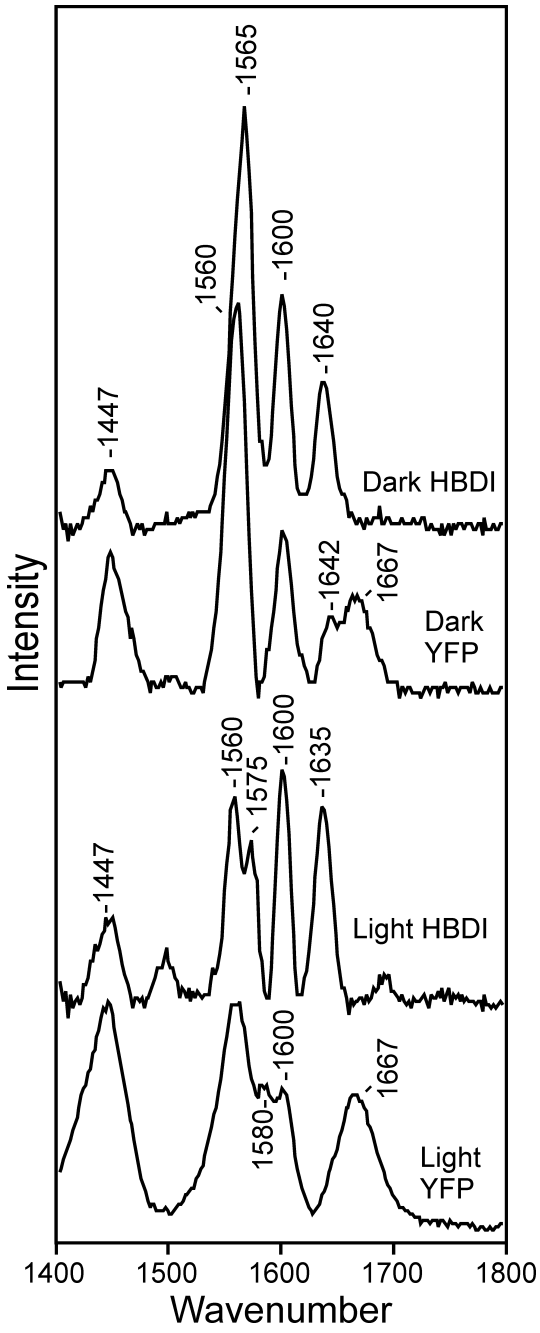


Figure 2.6: Off resonance Raman spectra of neutral YFP (60 $\mu$M, pH = 5.8) and neutral HBDI with and without irradiation.

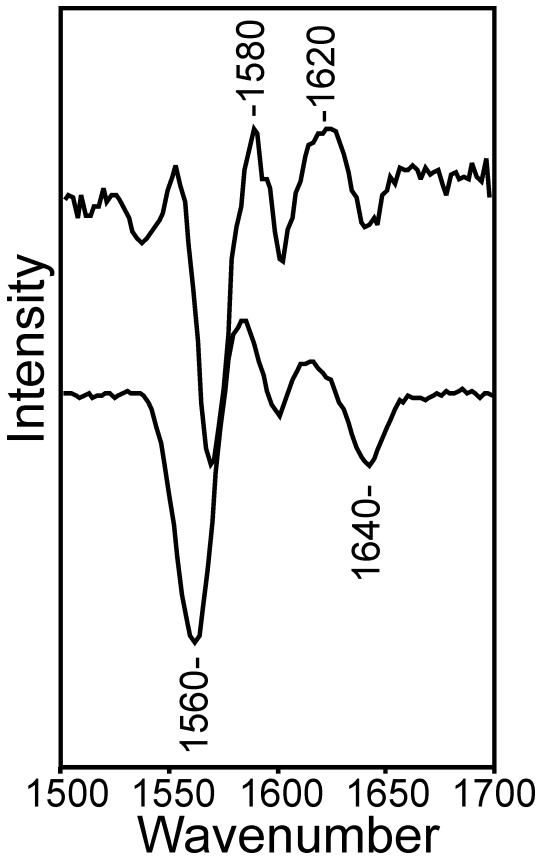


Figure 2.7: Off resonance Raman difference spectrum of neutral YFP (60 $\mu$M, pH = 5.8). The dark protein spectrum was subtracted from the spectrum of the protein acquired after two hours of irradiation at 400 nm.

in YFP (though not in wild type GFP).

YFP is pH sensitive, so to investigate the nonfluorescent neutral state of its chromophore, the pH was lowered so that the neutral form of the chromophore could be examined without interference from the anionic form (see Figure 2.8). The YFP neutral from could be readily converted with 400 nm light to a form with an electronic absorbance at 330 nm with an isobestic point at 350 nm. Raman spectroscopy was performed on both the neutral unbleached and neutral reversibly bleached forms of YFP. The YFP photoconversion was compared to the Raman spectrum of HBDI upon photoisomerization at 365 nm. Photoisomerization of HBDI can be monitored with Raman spectroscopy, as several HBDI modes are sensitive to molecular configuration. One such mode is the exocyclic C=C bond which lies at 1640 $cm^{-1}$ in *cis* HBDI and at 1620 $cm^{-1}$ in the *trans* form of HBDI. These changes are seen in the YFP Raman spectrum when its neutral from is irradiated, thus confirming that irradiation of YFP results in photoisomerization to the *trans* configuration of its chromophore, and that this *trans* state is responsible for the reversible photobleaching behavior of YFP.

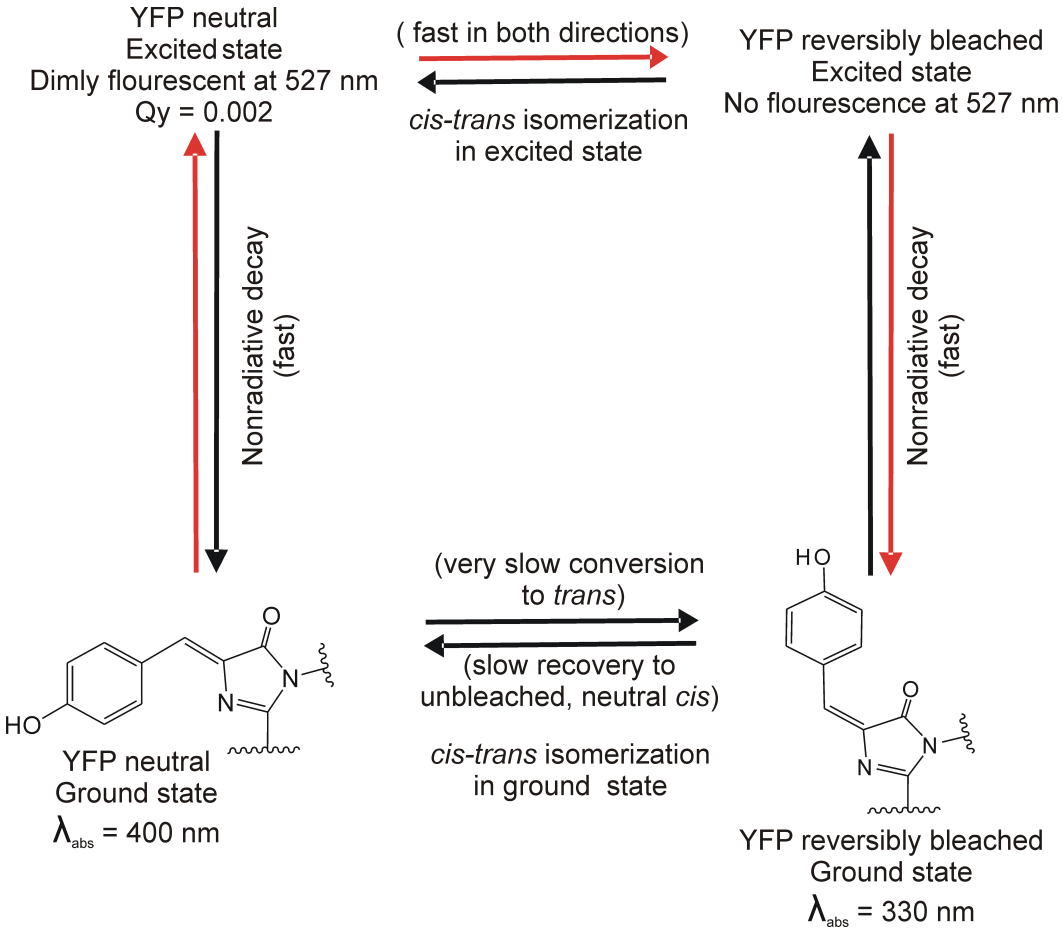


Figure 2.8: Photokinetic scheme for YFP at pH 5.8 [50]. Red arrows show the route from the neutral, unbleached *cis* state of YFP to the neutral, reversibly bleached *trans* state of YFP.

# Chapter 3

# Structural Origin of Cyan Emission in dsFP483

Part of this work has been published in Malo et al., 2008 [41].

## 3.1 Abstract

The fluorescent protein dsFP483 from the reef-building coral *Discosoma striata* exhibits cyan fluorescence from a GFP-like chromophore, with an emission $\lambda_{max(1)}$ = 483 nm. The absorption maximum of dsFP483 (450 nm) is in between that of neutral and anionic GFP chromophores (400 nm and 475 nm, respectively). This raises the question of whether the cyan fluorescence is due to an anionic or neutral chromophore, and how the protein efficiently promotes fluorescence with a quantum yield of 0.78. Raman spectra

of both wild type dsFP483 and a red-shifted mutant, K70M, are presented and are compared to spectra of a pH-sensitive GFP mutant, S65T. The wild type dsFP483 has several marker bands in its Raman spectrum that indicate a neutral chromophore. The Raman spectrum of the red shifted dsFP483 K70M mutant, meanwhile, exhibits frequencies more in line with an anionic chromophore, highlighting the role this position plays in tuning the cyan fluorescence.

## 3.2 Introduction

The cyan fluorescent protein dsFP483 from the reef-building coral *Discosoma striata* emits at 483 nm. The cyan light is the result of a unique protein environment surrounding the GFP-like chromophore formed from the post-translational modification of residues Q66/Y67/G68. This cyan fluorescent protein has only about 20% homology to wild type GPF, and is more similar to the DsRed protein (55%), however, its chromophore does not contain the extra conjugation observed in the DsRed chromophores. Therefore the electronic properties of the wild type dsFP483 chromophore more closely resemble that of the less conjugated, green emitting GFP chromophore (see Figure 3.1). The protein environment surrounding the wild type dsFP483 chromophore, however, is more similar to DsRed than to wild type GFP. Thus, the dsFP483

protein has an unconjugated, GFP-like chromophore embedded in a DsRed-like environment, see Figure 3.1.

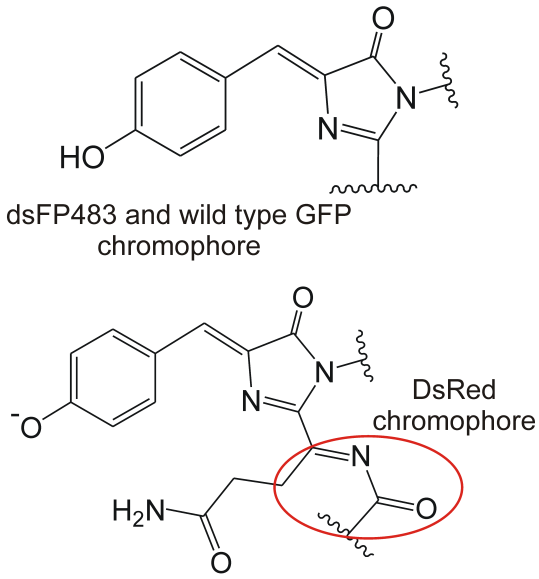


Figure 3.1: Chromophore structure of wild type GFP and dsFP483, shown in the neutral state. The DsRed chromophore in its anionic state is shown for comparison. The DsRed chromophore has extra $\pi$ conjugation (red circle). The two extra $\pi$ bonds red shift the $\lambda_{abs}$ and $\lambda_{em}$ the DsRed chromophore compared to the less conjugated GFP chromophore.

The exact molecular nature of the emitting chromophore and the protein environment that tunes its spectral properties remains elusive in dsFP483. The dsFP483 protein has a high quantum yield (0.78), close to that of wild type GFP. Like wild type GFP, dsFP483 also shows no pH dependance to its absorption or emission spectra [41]. In wild type GFP, it has been shown that the emitting state of the chromophore is anionic. Both neutral and anionic forms of the chromophore may be observed in the electronic absorption

spectrum of wild type GFP, which shows a fixed ratio of each form and no pH dependance. However, a single point mutation close to the chromophore (S65T) renders GFP pH sensitive. In wild type GFP, the neutral from of the chromophore absorbs at 400 nm and is the major form in the absorbance spectrum, while the anion has a minor absorbance at 475 nm. Excitation with either wavelength results in green fluorescence at 508 nm.

The large Stokes shift for neutral fluorescence seen in wild type GFP is the result of a high yield ultrafast deprotonation reaction that occurs within picoseconds of excitation at 400 nm. The excited, neutral chromophore is deprotonated at its phenolic hydrogen by a nearby protein residue (E222) promptly upon entry into its excited state. This photoreaction converts the chromophore to an excited anionic state, which then fluoresces at 508 nm. Therefore, wild type GFP may be excited at two different wavelengths of light to produce the single emission peak from the anion at 508 nm. Mutants of GFP that block the excited state deprotonation reaction, such as the point mutant E222Q, do not show fluorescence at 508 nm when the neutral from is excited. Instead, fluorescence from the excited state of the neutral is observed at 460 nm with very low quantum yields.

Tuning the spectral properties of the embedded chromophore, such as altering the $\lambda_{max}$s for absorption and emission, requires a knowledge of both the

Table 3.1: Optical properties of wild type dsFP483, the dsFP483 K40M mutant, wild type GFP, and DsRed.

| Protein | Excitation $\lambda_{max(1)}$ (nm) | Excitation $\lambda_{max(2)}$ (nm) | Emission $\lambda_{max}$ (nm) | Quantum yield $\Phi_F$ | Effective Stokes shift‡ (nm) |
|---|---|---|---|---|---|
| dsFP483 | 437(major) | 453(minor) | 483 | 0.78 | 46 |
| K70M | 445(minor) | 460(major) | 500 | 0.05 | 40 |
| wtGFP | 400(major) | 478(minor) | 508 | 0.80 | 108 |
| DsRed | 558 | – | 583 | 0.70 | 20 |

Data for wild type GFP and DsRed shown for comparison [19, 77, 41].
‡ Calculated utilizing the overall excitation maximum.

chromophore state (neutral or anionic, for example) as well as its configuration and the residues in the protein that it interacts with. High quantum yields for emission are generally seen for proteins whose environment immediately surrounding the chromophore suppresses excited state reactions of the chromophore, such as *cis-trans* isomerization.

Interestingly, the electronic absorbance spectrum of dsFP483 ($\lambda_{max} = 437$ nm, Table 3.1) is in between that of the neutral and anionic forms in wild type GFP. The emission maximum of dsFP483 (483 nm) is intermediate as well, as the neutral wild type GFP chromophore has low yields of 460 nm fluorescence from the neutral form while the anion's maximum lies at 508 nm. This suggests that the chromophore in dsFP483 may be a red shifted neutral species. However, high quantum yields, like that of dsFP486, are generally not seen for neutral GFP chromophores as the excited neutral species typically decays nonradiatively within the fluorescence lifetime. This is because the GFP

environment surrounding its chromophore has evolved to suppress processes other than fluorescence for its emitting anionic chromophore. Again, the chromophore prior to excitation in wild type GFP is in its neutral state, however, the excited state deprotonation reaction forms the emitting anion on an ultrafast timescale [67]. Wild type GFP, therefore, has evolved its chromophore environment to stop nonradiative decay from its anion, thus increasing the quantum yield for this form of the chromophore.

The problem of blue shifting the emission maximum away from that of anion while maintaining the high quantum yield observed in anionic GFP chromophores has been solved within the environment of dsFP483. To understand how the protein environment tunes the absorbtion and emission properties of the chromophore, knowledge of the protonation state of the chromophore is essential.

A recent crystal structure describes many hydrogen bonding interactions with the phenolic hydrogen of the cyan chromophore (see Figure 3.2). Intermediate values of the $\lambda_{max}$s for both absorption and emission leaves the protonation state of the modified tyrosine in question in wild type dsPF483 [41]. The GFP-like chromophore in dsFP483 protein environment could be described as either a red shifted neutral species or a blue shifted anionic species. Since desired photophysical properties have been shown to depend strongly on

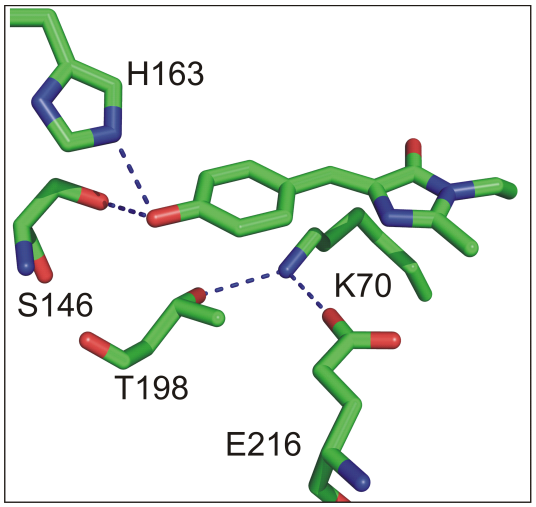


Figure 3.2: Crystal structure of the dsFP483 chromophore and protein environment (PDB ID: 3CGL). From Malo et al., 2008 [41].

protonation state, understating how the protein environment positions the phenolic hydrogen of the modified tyrosine is key to the development of novel fluorescent proteins.

Wild type GFP contains both the anionic and neutral forms of its chromophore in fixed amounts. Mutation of a serine (S65) to a threonine renders the GFP chromophore pH-sensitive, and each form of the chromophore may be examined separately by altering the pH of the solution. In dsFP483, mutation of the lysine (K70) to methionine results in a red shift in the absorption and emission maxima, causing this point mutant to strongly resemble the anionic state (see Table 3.1). This lysine lies directly underneath the excocyclic C=C in wild type dsFP483 (see Figure 3.2).

Raman spectroscopy is sensitive to the protonation state of the GFP-like chromophores, and the Raman spectra of pH sensitive GFP point mutants, such as S65T, has been described [5]. There are several pH-sensitive modes in the Raman of pH sensitive GFPs. One such mode is the stretch of the exocyclic C=C group that lies at 1640 $cm^{-1}$ for a neutral chromophore and at 1618 $cm^{-1}$ for an anion. Raman spectroscopy was performed on the wild type dsFP483 and its red shifted point mutant K70M. To determine the protonation state of the dsFP483 chromophore, and to gain insight into how the quantum yield for cyan light is optimized by the protein environment.

## 3.3 Materials and Methods

*Steady-State Raman Spectroscopy:* Steady-state Raman spectroscopy was performed on using an off resonance instrument that has been described previously [5]. Data for dsFP483 were collected with 752 nm excitation employing a 90° collection geometry. Power at the 2 mm by 2 mm fluorimeter cell that held 60 $\mu$L of sample was 670 mW. The dsFP483 protein at a concentration of 100 $\mu$M in 20 mM HEPES, 300 mM NaCl buffer (pH 7.9) was used. Spectra were acquired using 2 second accumulation times and 300 scans. After the protein spectrum had been acquired, a buffer spectrum containing no protein was obtained. The buffer spectrum was then subtracted from the

protein + buffer spectrum to give the Raman spectrum of the protein. Spectra were wavenumber calibrated using the Raman spectrum of cyclohexanone.

## 3.4 Results and Discussion

The recent crystal structure of dsFP483 (see Figure 3.2), is at a resolution of 2.1 angstroms, which leaves the protonation state of the modified tyrosine in question. Raman spectroscopy is sensitive to the protonation state of the GFP chromophore, and the Raman spectra of pH sensitive GFP mutants have been described. Specifically, the S65T point mutant of GFP renders the protein pH sensitive and large populations of either the anionic or neutral chromophore may be obtained by altering the pH.

*Raman spectrum of the pH sensitive GFP mutant S65T at high and low pH values:* The pH sensitive GFP mutant S65T was examined with Raman spectroscopy so the neutral and anionic forms of this chromophore could be compared to dsFP483. There are several pH-sensitive modes in the Raman spectrum of pH sensitive GFP mutants such as S65T. The Raman spectrum of the S65T GFP mutant at high and low pHs has been previously described [5] and is shown in Figures 3.4 and 3.5. The 1666 $cm^{-1}$ mode is due the amide I vibrations of the protein peptide backbone, and does not change with pH [5]. However, other high energy modes can be seen to alter in the Raman

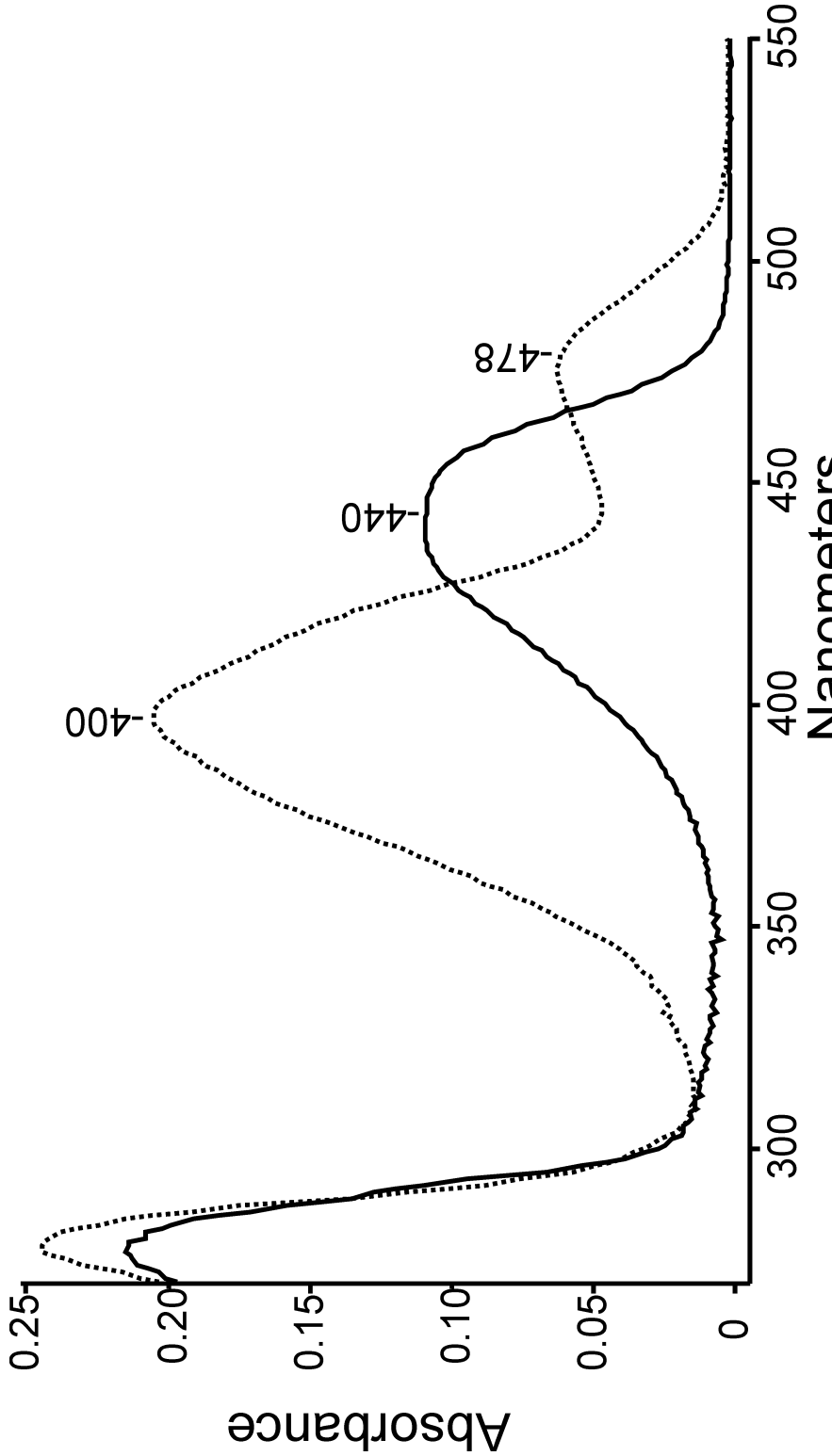


Figure 3.3: Steady-state absorbtion spectrum of dsFP483 (solid) and wild type GFP (dashed).

spectrum of GFP S65T when the pH of the solution is raised or lowered. The mode at 1619 $cm^{-1}$ in neutral GFP S65T shifts to 1640 $cm^{-1}$ when the pH is raised. This mode is assigned to the exocyclic C=C stretching vibration in GFP-like chromophores [17]. The 1600 $cm^{-1}$ mode seen in pH 5 GFP S65T is absent in the pH 8 spectrum. The 1600 $cm^{-1}$ mode is highly nonlocal and has contributions from the entire phenyl ring [5]. The intense 1540 $cm^{-1}$ mode seen in the pH 8 spectrum of GFP S65T has been assigned to the C=N stretch of the GFP chromophore. The 1540 $cm^{-1}$ mode shifts to 1558 $cm^{-1}$ in the GFP S65T pH 5 spectrum, although a shoulder can be seen in the pH 5 GFP S65T spectrum at 1544 $cm^{-1}$ that may be due to residual amounts of the anionic chromophore.

The lower energy modes of the pH sensitive S65T GFP mutant at 1496, 1446, 1250, 1168 $cm^{-1}$ are highly delocalized and have contributions from many of the bonds in the GFP chromophore. These modes do not alter with addition or removal of a proton to the phenolic end of the chromophore.

*Raman spectroscopy of wild type dsFP483 and its point mutant K70M:* The highest energy mode of the wild type dsFP483 is observed at 1666 $cm^{-1}$ and is due to amide I vibrations of the protein. The next mode in the dsFP483 Raman spectrum is quite broad and lies at 1633 $cm^{-1}$, in between that of the neutral and anion forms of the GFP S65T mutant (see Figures 3.4 and 3.5).

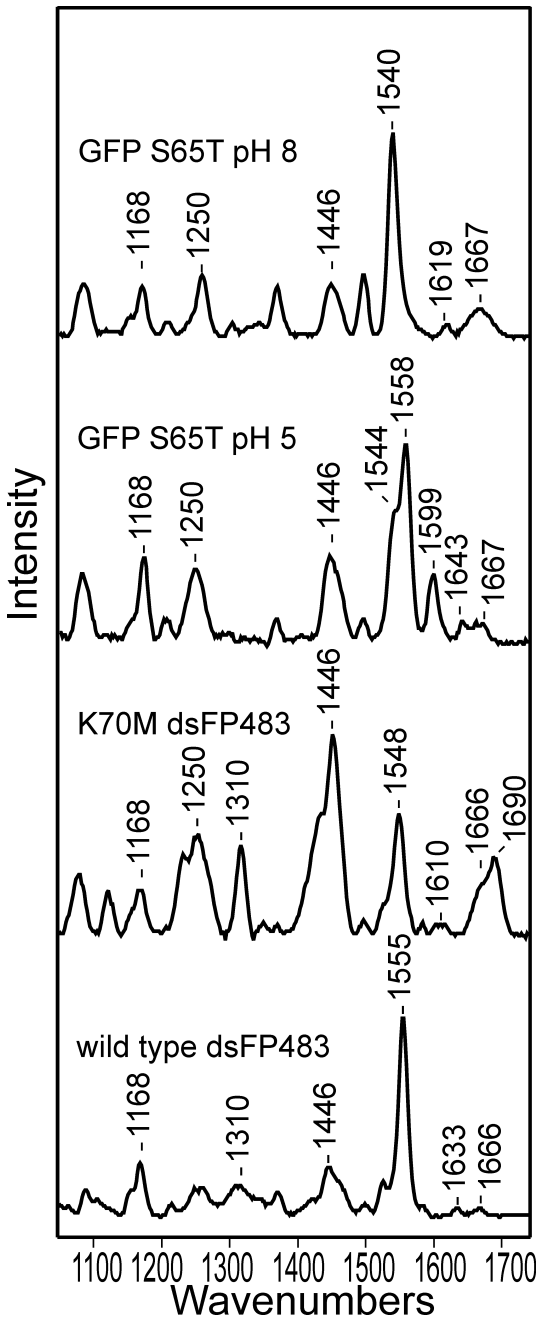


Figure 3.4: Off resonance Raman spectra of (A) GFP S65T, pH 8. (B) GFP S65T, pH 5.8. (C) K70M dsFP483. (D) Wild type dsFP483.

This vibrational information is consistent with the absorbtion and emission maxima (see Table 3.1 and Figure 3.3), which also have values in between those observed for anion and neutral GFP-like chromophores. The C=N stretch, which is at 1558 $cm^{-1}$ in the neutral GFP S65T spectrum, is at 1555 $cm^{-1}$ in wild type dsFP483. This mode changes to 1540 $cm^{-1}$ in the Raman spectrum of the anionic S65T GFP mutant. Therefore, the C=N stretch mode of wild type dsFP483 at 1555 $cm^{-1}$ is more in line with a neutral chromophore.

To explore the effect of the dsFP483 protein environment on its chromophore, site directed mutagenesis was employed. The dsFP483 mutant K70M possesses an electron absorbance peak red shifted to that of the wild type by about 10 nm (460 nm, see Table 3.1). The Raman spectrum of the dsFP483 K70M mutant contains the 1667 $cm^{-1}$ amide I band due to protein. In addition, a new mode is seen at 1690 $cm^{-1}$ in this dsFP483 mutant.

The exocyclic C=C stretch of the dsFP483 K70M mutant is broad and lies at 1610 $cm^{-1}$ (see Figure 3.5). The exocyclic C=C stretch is observed at 1618 $cm^{-1}$ in the Raman spectrum of anionic GFP S65T (see Figure 3.5). This C=C stretch mode, which is sensitive to protonation of the chromophore, indicates that the chromophore in the dsFP483 K70M mutant is in its anionic state (see Table 3.2).

The dsFP483 K70M mutant also has a slightly altered position for the

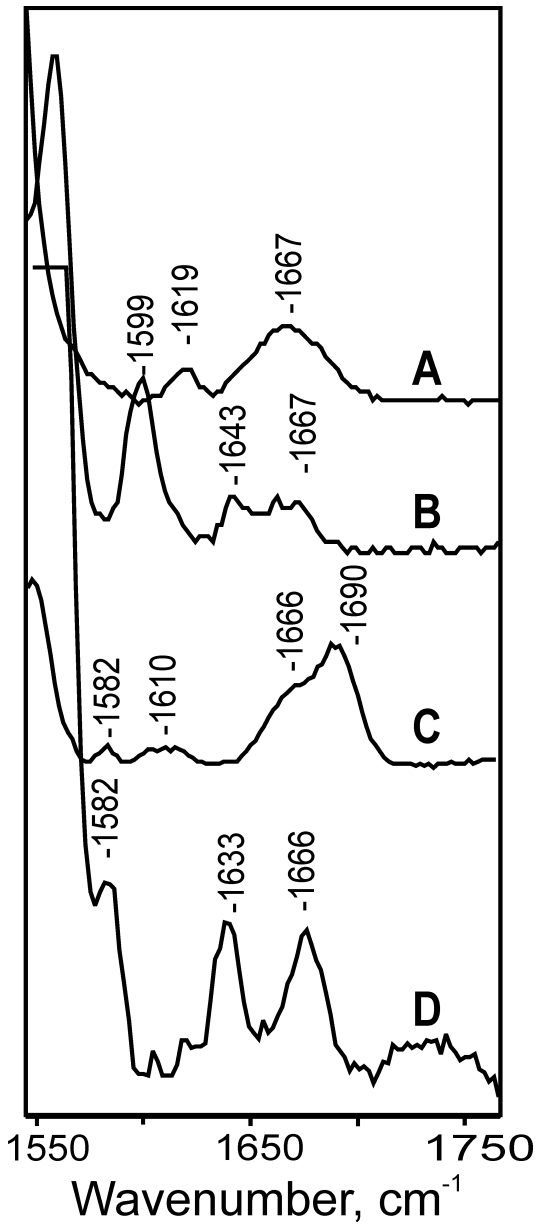


Figure 3.5: Off resonance Raman spectra of (A) GFP S65T, pH 8. (B) GFP S65T, pH 5.8. (C) K70M Cyan. (D) Wild type dsFP483.

Table 3.2: Raman modes that sensitive to the protonation state of the chromophore. Units in wavenumber ($cm^{-1}$).

| Assignment | GFP S65T pH 8 | GFP S65T pH 5 | dsFP483 wild type | dsFP483 K70M |
|---|---|---|---|---|
| C=C | 1618 | 1640 | 1633 | 1610 |
| C=N | 1540 | 1558 | 1555 | 1548 |

C=N stretching mode of the imidazolinone ring as compared to the wild type dsFP483 (see Figure 3.5). This mode is observed at 1548 $cm^{-1}$ in dsFP483 mutant and at 1555 $cm^{-1}$ in the wild type protein. In the GFP S65T anion this C=N mode is much further red shifted, from 1558 $cm^{-1}$ in the neutral to 1540 $cm^{-1}$ in the anion (see Table 3.2). The C=N stretch of the dsFP483 K70M mutant, therefore, is more consistent with an anionic chromophore than with a neutral one.

## 3.5 Summary

The Raman spectrum of dsFP483 is more consistent with a red-shifted neutral chromophore than a blue-shifted anion. The shift from 1643 $cm^{-1}$ (neutral GFP-S65T) to 1634 $cm^{-1}$ (dsFP483) may result from increased delocalization of electron density throughout the chromophores ring system, stabilized by the positive charge of the K70 side chain amino group positioned near the methylene bridge.

The point mutation K70M in dsFP483 once again demonstrates the important role of the protein environment in both shifted absorbtion and emission maxima and optimizing and enhancing the quantum yield of the desired light. The dsFP483 K70M mutant has photophysical proprieties and a Raman spectrum similar to those of an anionic, GFP-like chromophore (see Tables 3.1 and 3.2). Unlike the GFP case, the quantum yield for the K70M anionic chromophore is very low, suggesting that the dsFP483 protein environment is unable to suppress nonradiative decay reaction that occur in the excited state of the anion. This allows access to the range of colors obtained from the fluorescence of the neutral chromophore, the emission of which is blue shifted from the anionic form. Such properties are extremely valuable for FRET studies, where such a blue shifted range of emission is desirable for use as donors. The emission of the neutral chromophore overlaps well with the absorbance maximum of the anionic GFPs, which may serve as the acceptor.

In the GFP-like dsFP483, Raman spectroscopy of both the wild type and mutant proteins revealed the importance of the charged lysine (K70) lying directly beneath the chromophore. This position is occupied by either a lysine or arginine in the DsRed protein family [80]. Mutation to a methionine at this position in dsFP483 results in an anionic chromophore with a low quantum yield [41]. It would appear that the dsFP483 protein evolved to maximize

the fluorescence quantum yield from a neutral, not anionic, chromophore. The lysine at position 70 is key in shifting absorbtion and emission values of the chromophore as well as promoting a high quantum yield for neutral florescence.

# Chapter 4

# Ultrafast Infrared Studies of Isotopically Labeled Flavins Bound to the BLUF Domain of AppA

Parts of this work has been published in Stelling et al., 2007 [65] and Kondo et al., 2006 [30].

## 4.1 Abstract

The blue light using flavin (BLUF) domain is a photosensory protein that employs a noncovalently bound flavin as its chromophore. The BLUF domain of AppA (residues 5 - 125) from *Rhodobacter sphaeroides* was reconstituted with riboflavins containing either 2-$^{13}$C or 4, 10a-$^{13}$C labels. Steady state and ultrafast vibrational spectroscopies were performed on both unlabeled and

labeled samples, as well as on important mutants that alter the AppA BLUF photocycle. It was found that while several modes shift upon labeling of the flavin ring, a transient absorbtion at 1666 $cm^{-1}$, which has been shown by mutational studies to be an indicator of photoactive protein, does not. This mode may therefore be assigned to the AppA protein environment and is likely due to the tautomerization of the nearby glutamine (Q63) amide side chain.

## 4.2 Introduction

The BLUF class of photoreceptors is found in many bacteria and uses a flavin chromophore to sense and respond to lighting conditions. In *R. sphaeroides*, the full 400 amino acid protein AppA regulates gene expression in response to the environmental light and oxygen levels [44]. The BLUF domain in AppA consists of the first 125 residues in the protein. Illumination with blue light triggers photoconversion to a long-lived state of the protein that is unable to bind the transcriptional repressor PpsR. The released PpsR may then prevent the transcription of photosynthesis genes [44].

The signaling state of AppA is formed directly from the singlet excited state of the flavin on a nanosecond timescale [12]. This observation raises the question of how the ultrafast blue light signal is transmitted from the noncovalently bound flavin to the protein. While crystal structures of the

AppA BLUF domain in the dark exist [1], little structural information is available for the long-lived ($t_{1/2}$ = 30 min) red-shifted state of the protein. This light state features rapid quenching of the flavin excited state, and in the dark relaxes back to the resting state via a monoexponential process [33]. The formation of this signaling state is characterized by a 10 nm red shift in the electronic spectrum of the bound flavin chromophore [33] (see Figure 4.1). Other BLUF domains such as BlrB from *R. sphaeroides*, Tll0078 from *Thermosynechococcus elongatus*, and Slr1694 from *Synechocystis sp.* PCC6803, while all showing a similar 10 nm red shift upon entry into their lit states, exhibit different photophysical properties from those shown in the AppA case. Specifically, most BLUF domains have a higher Qy for formation of the signaling state (0.30 to 0.60) as well as a markedly reduced relaxation time back to the dark state of the protein ($t_{1/2}$ = 1.5 to 20 seconds).

Crystallography and modeling studies have been performed on BLUF domains from many species to elucidate the structure of the dark state and the light activated signaling state. The dark crystal structure of AppA shows a glutamine side chain in close proximity to the flavin N5/O4 atoms (see 4.2). The side chain carbonyl oxygen of glutamine 63 was found to be orientated towards the flavin C4 carbonyl and the N5, while the nitrogen is hydrogen bonded to the nearby tyrosine (Y21) in both the AppA and Slr1694 BLUF

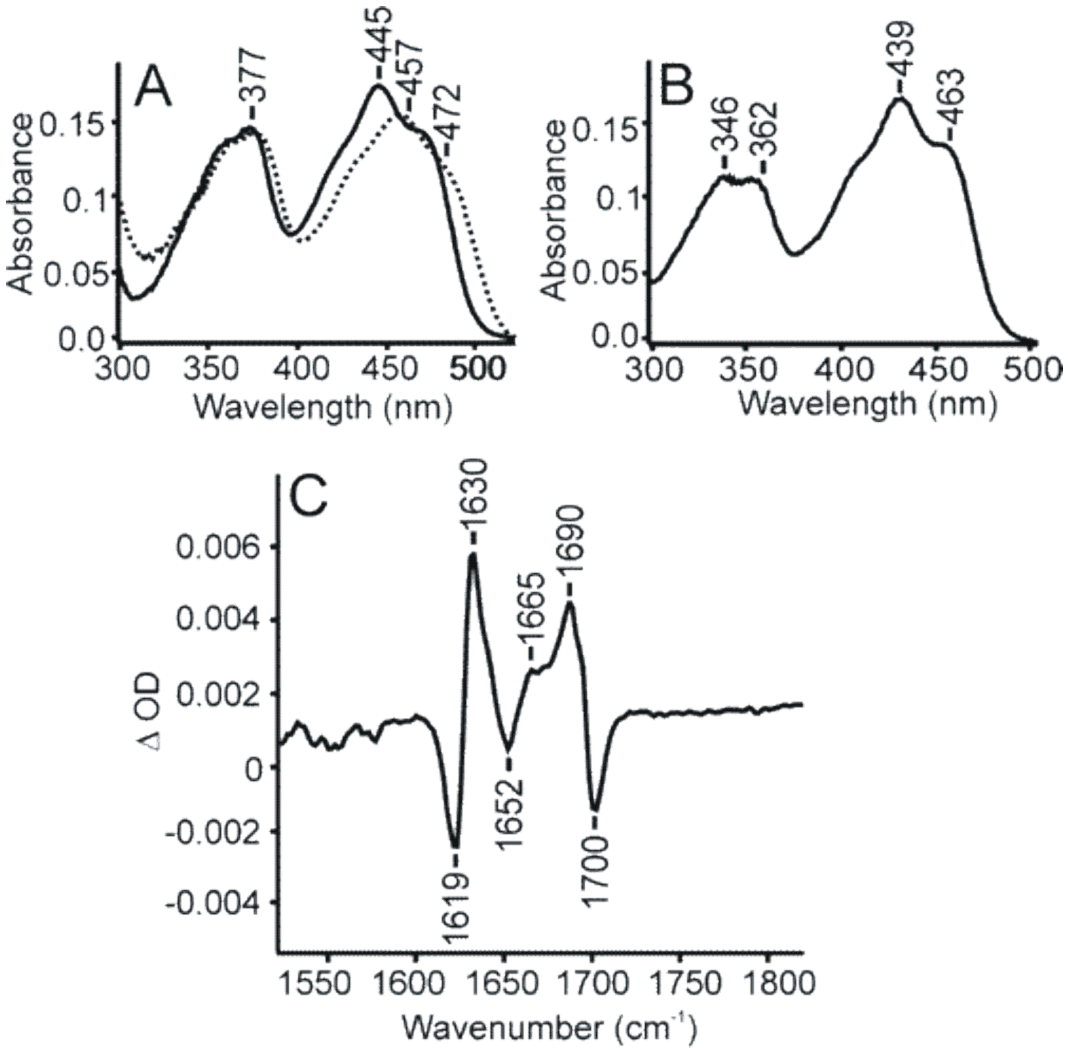


Figure 4.1: UV-visible absorption and FTIR difference spectra of wild type and mutant AppA. Steady-state absorption spectra for (A) wild-type AppA bound to FAD (dark, solid; irradiated, dashed) and (B) the photoinactive AppA Q63L bound to FAD. (C) The steady-state IR difference spectrum of wild type AppA bound to FAD (light minus dark) in pD 8 buffer. IR spectra were obtained using 2.5 mM AppA in a 50 $mu$m $CaF_2$ cell. The difference spectrum was obtained by subtracting the IR spectrum of AppA acquired before irradiation from that acquired after 3 minutes of irradiation with a 500 W XeHg lamp.

domains. This orientation was found to be reversed in the dark state crystal structures of BlrB (see 4.2) and T110078 (not shown), which both show the glutamine side chain carbonyl hydrogen bonding to the YOH, and the nitrogen interacting with the flavin atoms.

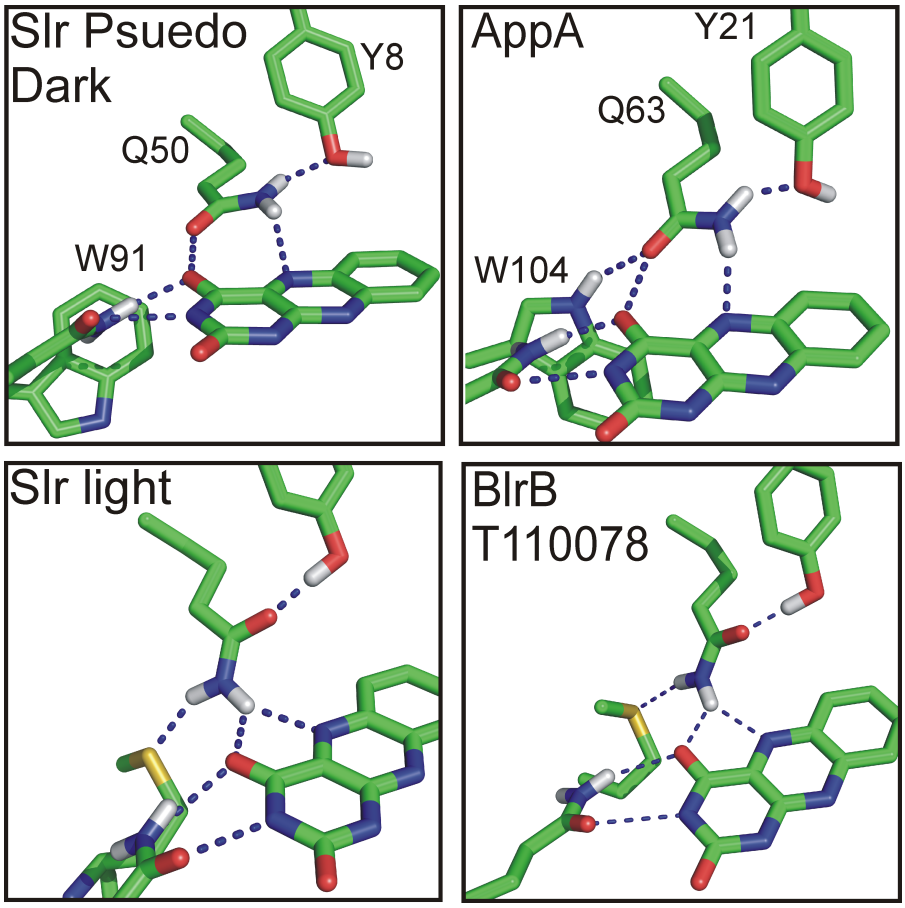


Figure 4.2: Crystal structures of the BLUF domains of AppA, BlrB, T110078, and Slr1694. From Jung et al., 2005 [25]; Yuan et al., 2006 [84]; Kita et al., 2005 [29]; and Anderson et al., 2005 [1].

The orientation of the glutamine side chain is thought to be important for

determining the photophysical prosperities of the BLUF domain, and its role in the initial photophysics of the BLUF system is under debate. One model for formation of the signaling state calls for a 180° flip of the glutamine side chain to alter the hydrogen bonding around the chromophore, see Figure 4.3 [1]. Initial electron transfer from the flavin to the nearby tyrosine followed by a flip of the glutamine would result in strengthened hydrogen bonds to the flavin C4=O and N5 [6]. Another model that would result in a similar hydrogen bonding environment involves the tautomeriztion, rather than rotation, of the glutamine (Q63) amide side chain [65, 59].

Modeling studies have been performed on BlrB, whose crystal structure shows the opposite orientation of the glutamine than AppA and Slr1694. The authors propose in their paper the possibility of a glutamine radical formed within the nanosecond lifetime of the photoexcited state of the dark flavin, formed after direct electron transfer to the tyrosine. Tautomerization of the glutamine radical occurs upon recombination of the flavin tyrosine radical pair. This tautomerization leads to a signaling state consisting of the imidic from of the glutamine with an altered hydrogen bonding pattern about the flavin C4=O and N5, without flipping of the glutamine side chain [59]. While this tautomerized residue would not immediately be in a form able to interact with the C4=O group of the flavin, low-temperature studies have isolated [11]

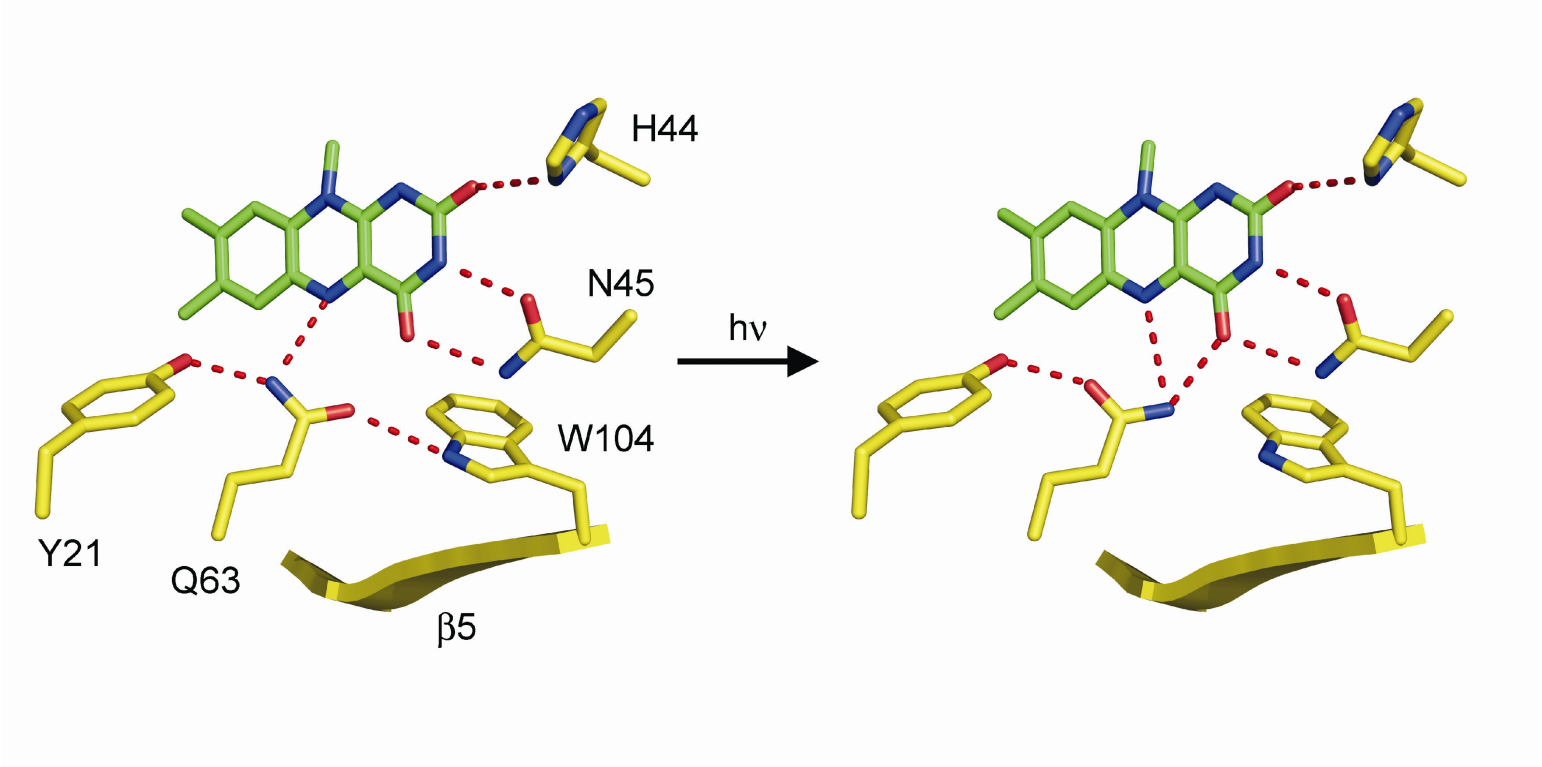


Figure 4.3: The flavin binding site and its protein environment of the AppA BLUF domain. Shown is a possible reaction leading to the light state of AppA where the glutamine 63 has been rotated 180 °. From Anderson et al., 2005 [1].

a 5 nm shifted intermediate in T110078 that may be due to a non-rearranged form of the protein environment. Such intermediates where excitation of a chromophore leads to both an ultrafast and slower response from the protein environment have been seen in the green fluorescent proteins as well [77].

Another key interaction shown in the BLUF crystal structures and studied by mutagenesis is a hydrogen bonding interaction between the glutamine 63 side chain and a tryptophan (104 in AppA). Other BLUF crystal structures show a methionine in this position (see 4.2). Mutation studies ([49, 48]) show that this position is crucial for determining the recovery time back to the dark state. Tyrosyl radicals have been implicated in the photocycles of other BLUF domains (Tll0078) [69], and have been observed in the infrared of other light activated proteins such as photosystem II [76, 4].

Steady-state vibrational studies revel a flavin carbonyl mode at 1706 $cm^{-1}$ that shifts to 1690 $cm^{-1}$ upon illumination in the UV [74] (see Figure 4.1). Infrared studies of the BLUF proteins Slr1694 [45] and Tll0078 [69] show similar features at high wavenumber corresponding to a change in the hydrogen bonding environment of the flavin C4=O. The features of the difference spectra of all the BLUF at wavenumbers lower than 1680 $cm^{-1}$ are dominated by changes to the protein, as shown by isotope studies in which the whole protein was $^{15}N$ or $^{13}C$ labeled [47]. The intensity of these protein modes vary greatly

between the different BLUF domains, although the positions are similar. Large difference modes at (+)1632, (-)1620 $cm^{-1}$ are seen in the AppA BLUF domain that have been attributed to protein. Pronounced modes at (-)1545, (+)1507 $cm^{-1}$ are seen in Slr1694 and weaker ones 1543, 1512 $cm^{-1}$ in Tll0078 that are attributable to protein as well [69].

Time-resolved IR studies have been performed on the BLUF domains as well. Recent papers explore the ultrafast behavior of the excited state flavin for the BLUF domains of both AppA and Slr [65, 6]. While most of the vibrational modes can be assigned to the flavin, the assignment of a transient absorption at 1666 to 1670 $cm^{-1}$ is under debate. A recent paper by Bonetti et al. assigns this mode to have major contributions from a neutral flavin radical species formed immediately upon excitation in the Slr1694 BLUF system [6]. Other studies performed on the AppA BLUF domain [65] suggest that this mode has contributions from a protein reside (or residues).

To aid in the understanding of the molecular mechanism of signal transfer from the flavin chromophore to the protein scaffolding and to determine contributions from flavin and protein in the vibrational modes, isotopes in specific positions around the flavin (2-$^{13}$C labeled riboflavin and 4, 10a-$^{13}$C labeled riboflavin) were synthesized. Steady-state and picosecond time resolved vibrational spectroscopies were used to investigate the formation and

structure of the AppA BLUF signaling state.

## 4.3 Materials and Methods

*Chemicals:* Isotopically labeled riboflavin compounds were graciously provided by Prof. Adelbert Bacher, Technische Universität München; and Dr. Boris Illarionov, Universität Hamburg.

*Sample Preparations:* The BLUF domain of AppA (residues 5 to 125) was purified as previously described [65].

The BLUF domain (residues 5-125) of AppA was amplified by PCR using the upstream primer AppaNdeIF: 5' GCG CAT ATG CTC GAG GCG GAC GTC ACG 3' and the downstream primer AppaBam- HIR 5'-CGC GGA TCC CTA CTG CCG GCT CTC GGC-3' (restriction sites in italics). The amplified PCR product was digested with NdeI and BamHI (Invitrogen) and ligated into the Nde1/BamHI restriction sites of the plasmid pET15b so that a His6-tag was encoded at the C terminus of the protein. Site directed mutagenesis was performed using Herculase (Stratagene). Primer sequences for W104F were 5'-CGC CGC TTT GCG GGA TTT CAC ATG CAG CTC TCC-3' (forward) and 5'-GGA GAG CTG CAT GTG AAA TCC CGC AAA GCG GCG- 3' (reverse); primer sequences for Q63L were 5'-GGC GTC TTC TTC CTC TGG CTC GAA GGC-3'(forward) and 5'-GCC TTC GAG CCA GAG GAA

GAC GCC-3' (reverse). All constructs were verified by DNA sequencing.

Wild-type and mutant AppA proteins were expressed and purified according to standard procedures [26, 47]. BL21DE3 E. coli cells transformed with plasmids containing the wild-type BLUF domain (residues 5 - 125), or the mutants Q63L and W104F, were grown in 1 L of LB medium (4 L flask) containing 0.5 mM ampicillin at 30 °C for 4 h until an OD600 was reached. Protein expression was then induced by addition of 0.8 mM IPTG followed by incubation at 18 °C overnight in the dark. Cells were harvested by centrifugation and resuspended in 30 mL of lysis buffer (50 mM sodium phosphate, 150 mM NaCl, pH 8.0) to which 15 $\mu$L of the protease inhibitor PMSF (50 mM stock solution in ethanol) had been added. After lysing the cells by sonication, cell debris was removed by centrifugation (33 K, 1.5 h) and the supernatant was allowed to incubate on ice in the dark with a molar excess of FAD of riboflavin (Sigma Aldrich) for 1 hour to ensure a homogeneous population of protein bound chromophore [34]. Subsequently, AppA was purified by Ni-NTA chromatography (Qiagen), using 30 to 40 mM imidazole buffer (50 mM sodium phosphate, 200 mM NaCl, pH 8) as the wash buffer and 250 mM imidazole in the same buffer to elute the protein from the column. Column fractions containing protein were combined and dialyzed overnight in the dark against 10 mM Tris-HCl pH 8 buffer containing

150 mM NaCl. Protein purity was assessed by SDS-PAGE electrophoresis and UV-vis spectroscopy (protein, $\epsilon_{270}$ = 35,800 $M^{-1}$ $cm^{-1}$; FAD$\epsilon_{446}$ = 8,500 $M^{-1}cm^{-1}$). Chromophore content was determined by the ratio of protein to FAD absorbance (4.2 for wild-type AppA with FAD bound [33]. Wild-type AppA and the mutants were concentrated to 1 mM, frozen in liquid $N_2$, and lyophilized overnight. Proteins were then reconstituted with deuterated buffer (10 mM Tris-HCl, 1 mM NaCl, pD 8), allowed to exchange for 5 hours in the dark at 4 °C, frozen in liquid $N_2$, and lyophilized overnight. The protein samples were subjected to at least 4 to 5 rounds of exchange into the deuterated buffer and were then stored at -20 °C.

*Binding of Riboflavin Isotopes:* Purified BLUF domain was allowed to incubate for an hour with a molar excess of either the 2-$^{13}$C labeled riboflavin or 4, 10a-$^{13}$C labeled riboflavin (Rf). Approximately 5 mg of Rf isotopes was solubilized in 50 uL DMSO. The solution was added to 15 mL of pD 8 buffer (1 mM NaCl, 20 mM $NaPO_4$) and allowed to incubate at 60 °C for at least 1.5 hours. The solubilized isotopes were cooled to 4 °C and then combined with 1000 to 500 $\mu$L of 1.5 mM AppA BLUF. The 15 mL solution of protein and isotopes were allowed to exchange in the dark at 4 °C for 1.5 hours. The protein was then reconcentrated to between 1.5 and 2 mM by centrifugation using Amicon filters with a MW cutoff of 3,000.

*Photoconversion:* Photoconversion experiments were performed with a 500 W Oriel XeHg lamp using a 405 nm band-pass filter as previously described [65]. Steady-state absorption spectra were recorded at 25 °C on a Varian Cary 300 UV-vis spectrometer.

*Steady-State Raman Spectroscopy:* Steady-state Raman spectroscopy was performed on this instrument as previously described. Data for AppA proteins were collected with 752 nm excitation obtained from a model 890 Ti:sapphire laser (Coherent, Santa Clara, CA), pumped by an Innova 308C argon ion laser (Coherent) and employing a 90° collection geometry. Power at the 2 mm by 2 mm fluorimeter cell that held 60 *mu*L of sample was 670 mW. AppA BLUF protein at a concentration of 1 to 2 mM in 20 mM $NaPO_4$, 1 mM NaCl buffer (pH/D = 8.0) was used. Spectra were acquired in the dark using 2 second accumulation times and 300 to 1200 scans. After the protein spectrum had been acquired, a buffer spectrum containing no protein was obtained. The buffer spectrum was then subtracted from the protein + buffer spectrum to give the Raman spectrum of the protein. Spectra were wavenumber calibrated using the Raman spectrum of cyclohexanone. All spectral analysis and calculation were performed with Win-IR software. Data were collected using WinSpec (Princeton Instruments, Trenton, NJ).

*Steady-State Infrared Spectroscopy:* Infrared spectra were collected on a

nitrogen-purged Nicolet 560 FTIR with a DTGS detector. 256 scans were recorded for each sample with as acquisition time of one second. AppA was exchanged into pD 8 $D_2O$ buffer containing 10 mM Tris-HCl and 1 mM NaCl and then concentrated using a centricon (Amicon, Millipore) with a 3,000 MW cutoff filter. Subsequently, 50 L of 2.5 mM protein were placed in a $CaF_2$ cell equipped with a 50 micron spacer. To generate the IR difference spectrum of light minus dark AppA, the protein sample was photoconverted in situ with 3 minutes of irradiation from the lamp described above, and the spectrum obtained before irradiation was subtracted from that obtained following photoconversion.

*Time-Resolved Infrared Spectroscopy:* Ultrafast time-resolved IR spectra were measured at the STFC Central Laser Facility. A description of the system and data collection methods has been published [66, 72]. The spot size and power of the pulse were adjusted so as to prevent photobleaching of the sample while retaining good signal-to-noise in the spectra (see below). Typical settings included a 200 $\mu$m spot size and energies invariably less than 2.5 $\mu$J per pulse. Protein samples were contained in cells with $CaF_2$ windows separated by spacers of 25 $\mu$m. Measurements typically consisted of spectra recorded at 3-5 randomly ordered time delays, with a 10 s collection period for each delay. Typically eight samples, each at around 1.5 to 2.5 mM, were

measured for each spectrum presented, and the results were averaged. For dark AppA measurements about 1 mM was placed in a low volume (2.6 mL) flow cell. Electronic absorption spectra were taken after each experiment to check for photobleaching of sample, as previously described [65].

## 4.4 Results

*Steady-state vibrational spectroscopy of wild type and mutant AppA BLUF domain bound to FAD:* The steady-state Raman spectrum of the dark and light states of the AppA BLUF domain is shown in Figure 4.4. The C4 carbonyl mode is at 1711 $cm^{-1}$ in water and at 1700 $cm^{-1}$ in $D_2O$. In the light state this mode shifts to about 1702 $cm^{-1}$ in water and 1692 $cm^{-1}$ in $D_2O$ in the light state, as previously reported [74]. The Raman spectrum of the photoactive mutant W104F and the photoinactive mutant Q63L are shown in Figure 4.5. The photoactive tryptophan mutant spectrum is virtually identical to the wild type spectrum. The photoinactive mutant Q63L shows a C4=O mode blue shifted to 1713 $cm^{-1}$, as previously reported [73]. This is consistent with the removal of hydrogen bonding interaction to the C4=O flavin bond by the introduction of the leucine [73].

*Time-resolved infrared spectroscopy of unbound FAD:* Time resolved infrared (TRIR) experiments were performed on free FAD in $D_2O$ buffer. Dif-

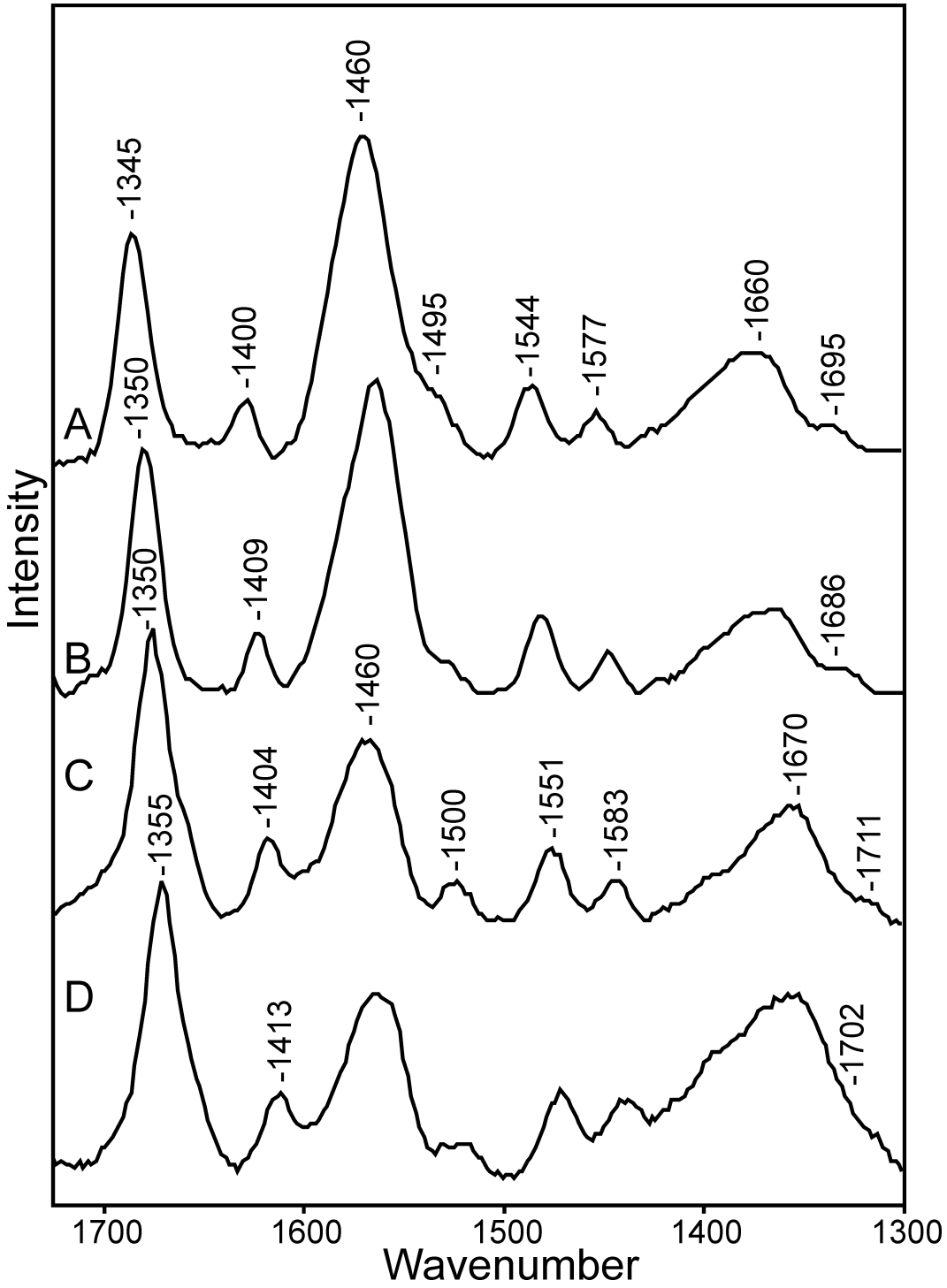


Figure 4.4: Steady-state Raman spectra of wild type AppA. A: Dark AppA in water buffer. B: Light AppA in water buffer. C: Dark AppA in $D_2O$ buffer. D: Light AppA in $D_2O$ buffer. Concentrations from 1 to 1.5 mM.

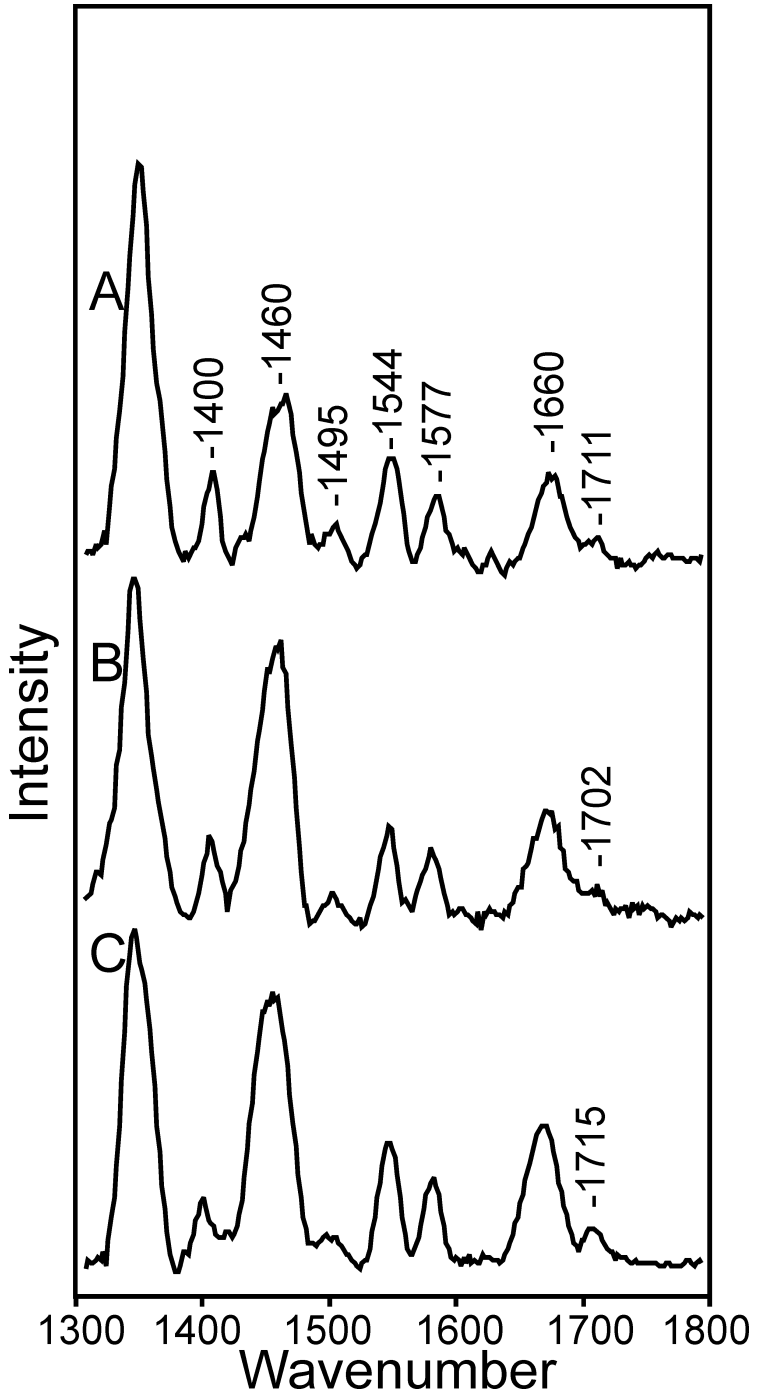


Figure 4.5: Steady-state Raman spectra of AppA mutants. A: Dark AppA W104F in water buffer. B: Light AppA W104F in water buffer. C: AppA Q63L in water buffer. Concentrations from 1 to 1.5 mM.

ference spectra are obtained by subtracting the ground state of a molecule from its excited state. Therefore, in time-resolved IR spectra, modes with negative intensity (indicated by a (-) in front of the mode) are due to the loss of that mode in the ground state. These ground state modes are often referred to as bleaches. Modes arising from excited states have positive intensity (indicated by a (+) in front of the mode) in the TRIR, and are also referred to as transient absorptions, or transients.

The time-resolved infrared spectrum of FAD in $D_2O$ is shown in Figure 4.6. The bleach at 1650 $cm^{-1}$ is due to loss of the ground state C2=O carbonyl mode of FAD, while the bleach at 1628 $cm^{-1}$ is from loss of the C4a-N5 mode. The bleach at 1578 $cm^{-1}$ is the result of the loss of the C4a-N5 ground state mode, while the intense bleach at 1650 $cm^{-1}$ is primarily from the C10a-N1 mode [30]. FAD is rapidly quenched by an energy transfer reaction in the exited state with its adenosine side chain, resulting in the fast decay of the excited state ($t_{1/2}$ = 50 picoseconds) [30].

*Time-resolved infrared spectroscopy of the AppA BLUF domain and mutants:* Time-resolved infrared studies were performed on the light and dark states of the AppA BLUF domain bound to FAD. Several AppA mutants were also examined.

The dark AppA TRIR spectrum in $D_2O$ buffer is shown in Figure 4.7 and

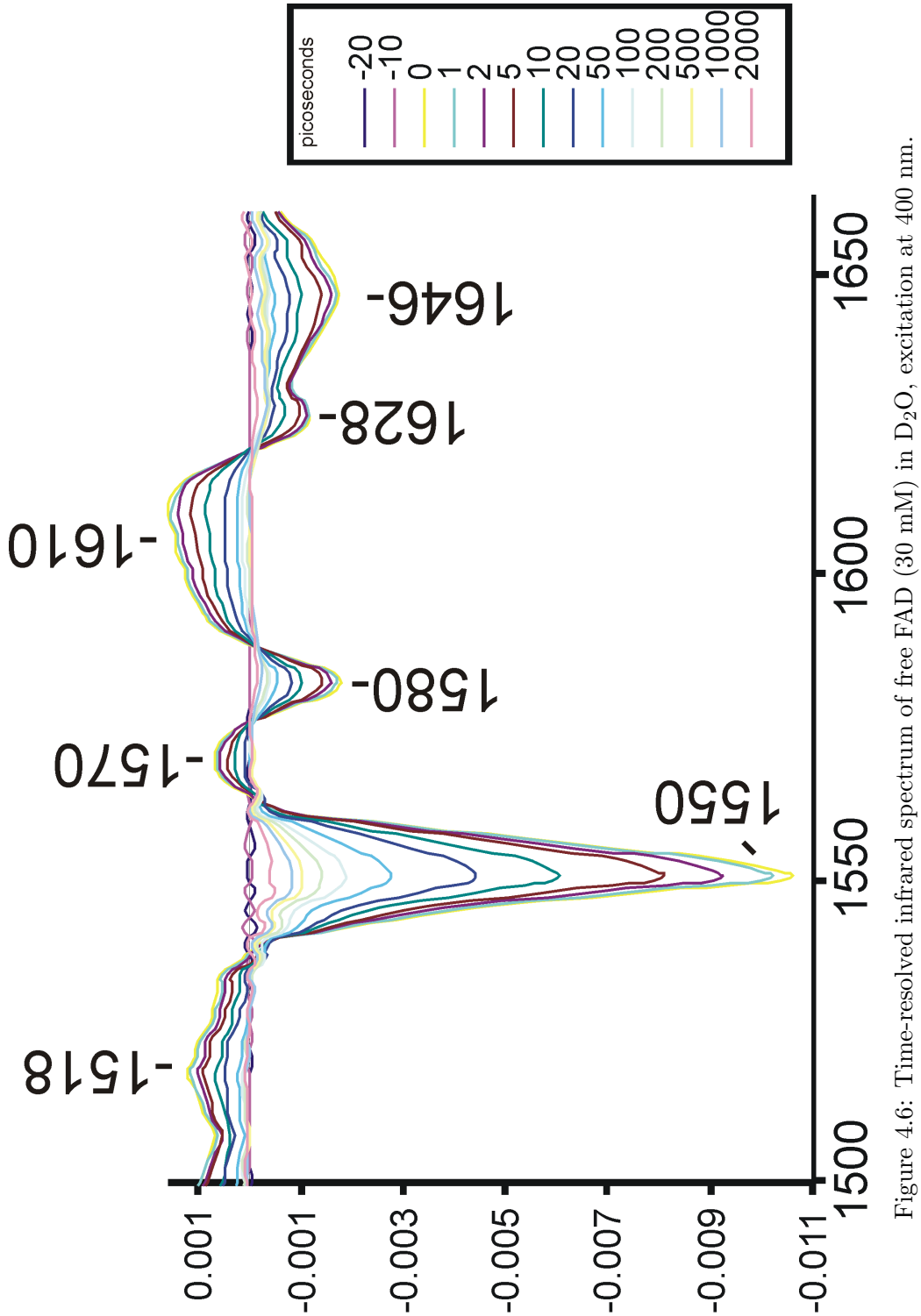


Figure 4.6: Time-resolved infrared spectrum of free FAD (30 mM) in $D_2O$, excitation at 400 nm.

is dominated by the ground state bleaches of the FAD C4=O group mode at 1696 $cm^{-1}$ and the C2=O group mode at 1650 $cm^{-1}$. A positive mode at 1666 $cm^{-1}$ is observed in the dark AppA TRIR spectrum that is not present in free FAD. The transient absorption at 1630 $cm^{-1}$ is also not present in free FAD, nor is a bleach mode at 1617 $cm^{-1}$. The transient absorption mode at 1602 $cm^{-1}$ is observed in free FAD and has been assigned to the excited states of the flavin carbonyls [30]. The bleach at 1578 $cm^{-1}$ is observed in free FAD, and is assigned to loss of the ground state of the delocalized flavin C4a=N5, C10a=N1 mode [7].

The decay time of FAD bound to AppA, about 2000 picoseconds, is much slower than observed in free FAD. Presumably the FAD bound to AppA cannot be quenched by its adenosine side chain, resulting in a slower decay of the excited state.

The TRIR spectrum of light AppA is shown in Figure 4.8. The light state is very similar to the dark state of the protein, however, consistent with the steady-state infrared studies, the C4=O flavin mode is red shifted to 1692 $cm^{-1}$. Additionally, an intense bleach at 1686 $cm^{-1}$ is seen in the light AppA TRIR spectrum which is not present in either the free FAD or the dark AppA spectra. The red shift of this carbonyl mode is consistent with a change in the the hydrogen bond number to the C4=O of the flavin when AppA enters its

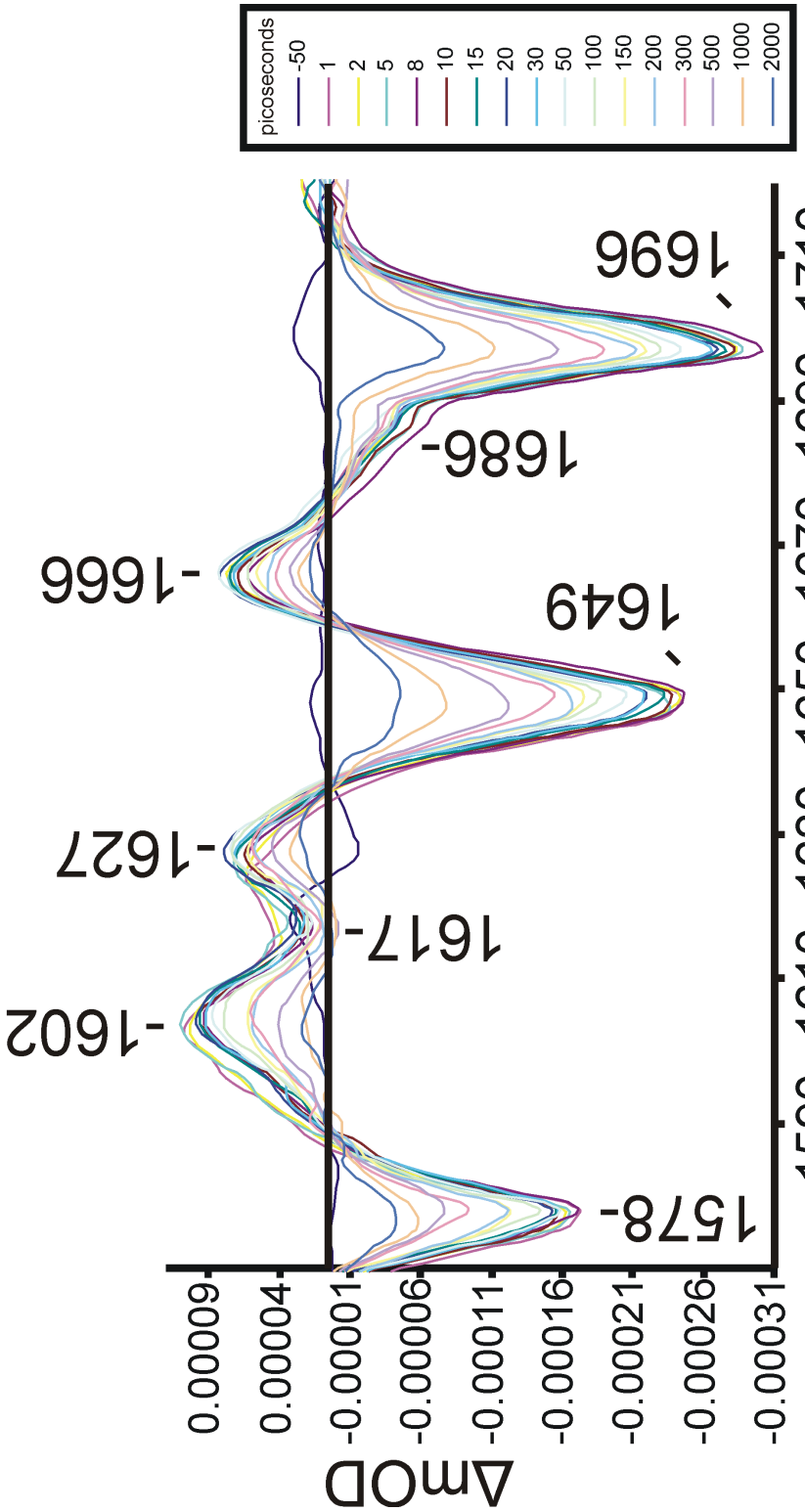


Figure 4.7: Time resolved infrared spectrum of 1 mM dark AppA bound to FAD in $D_2O$ (pD = 8.0), excitation at 400 nm.

light state.

The 1666 $cm^{-1}$ mode, which is reasonably intense in the dark AppA spectrum, appears to be absent in the light AppA spectrum. However, a very weak transient at 1666 $cm^{-1}$ is present in the light AppA TRIR. The 1666 $cm^{-1}$ mode is suppressed by the intense ground state bleach at 1686 $cm^{-1}$ that is present only in the light AppA spectrum. Additionally, the light AppA excited state decays in 1000 picoseconds, which is half the time observed for the decay of the dark state of AppA.

The TRIR spectra of two photoinactive mutants, Y21F and Q63L, are shown in Figure 4.9. The most striking difference between these mutants and the wild type AppA is that each mutant lacks a 1666 $cm^{-1}$ transient absorption. Additionally, the Y21F mutant lacks the features at 1630 $cm^{-1}$ and 1620 $cm^{-1}$, modes which are also not present in the free FAD TRIR. A photoactive mutant of AppA, W104F, was also examined. Mutation of the tryptophan at 104 in AppA results in altered recovery times and quantum efficiencies. The 1666 $cm^{-1}$ transient absorption is present in the light and dark states of the photoactive W104F mutant [65]. In fact, the TRIR spectra of the light and dark W104F mutant is virtually identical to the wild type protein. This mutant, however, had much more rapid decay times, with both light and dark decay times reduced to half that of the wild type protein.

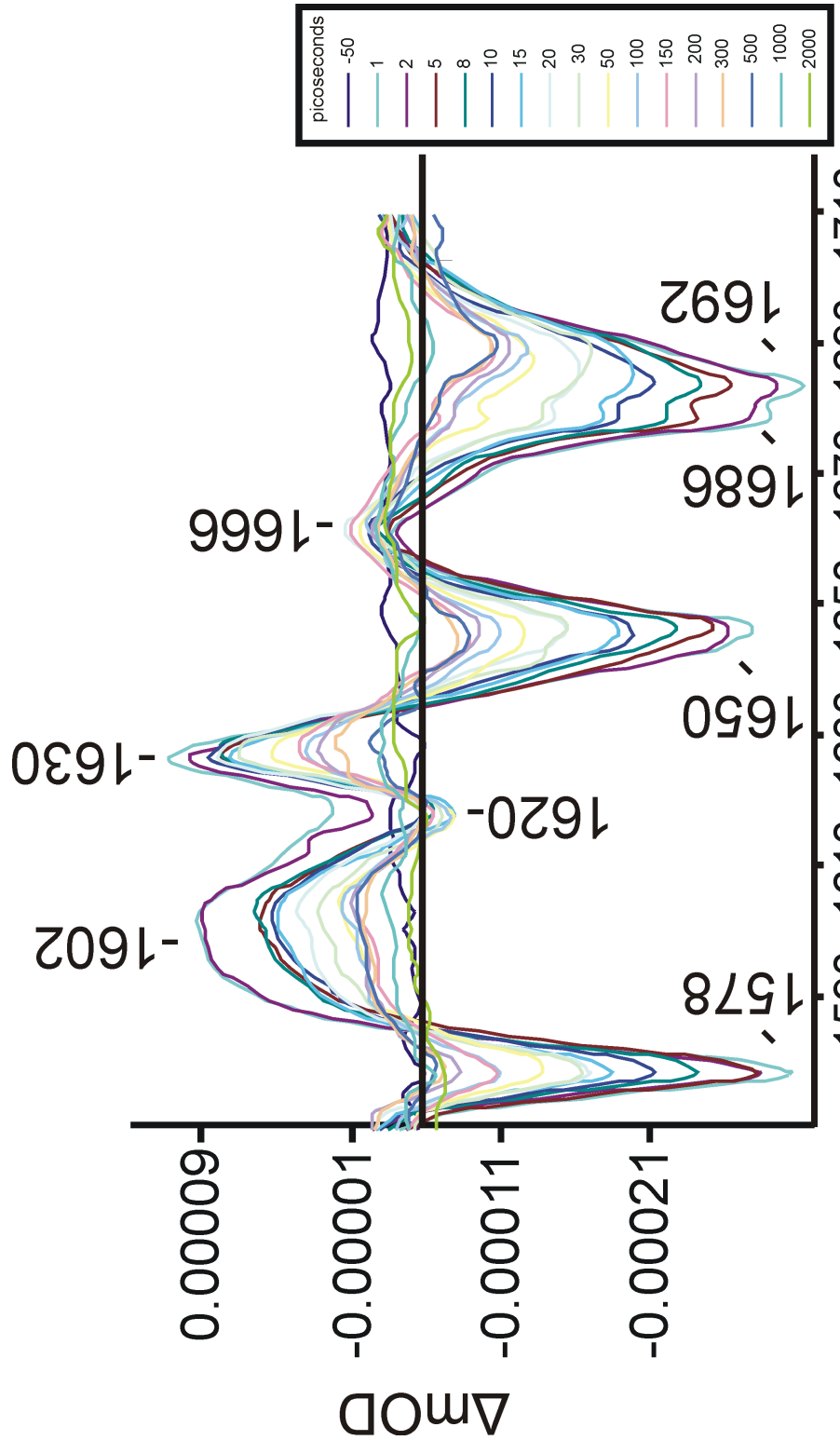


Figure 4.8: Time-resolved infrared spectrum of 1 mM light AppA bound to FAD in $D_2O$ (pD = 8.0), excitation at 400 nm.

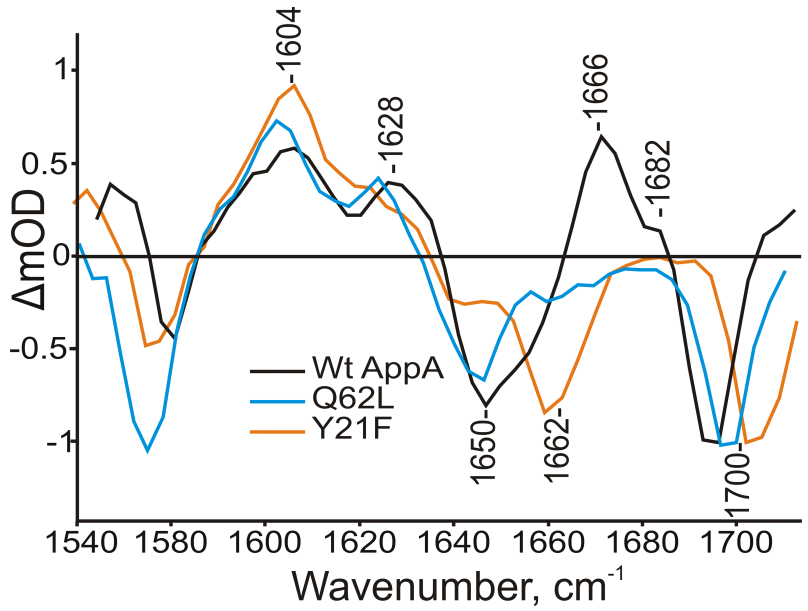


Figure 4.9: TRIR of wtAppA 3 picoseconds after excitation in the dark state overlaid with the Y21F and Q63L mutants. All proteins in pD 8 buffer at concentrations from 1.5 to 2 mM.

While most of the vibrations present in the AppA TRIR spectra are due to FAD, the modes at 1666, 1630, and 1620 $cm^{-1}$ are not present the free FAD and also disappear in the photoinactive mutants of AppA. These modes could be due to changes in the AppA protein environment that occur upon excitation of the flavin, and therefore the assignment of these modes may aid in the elucidation of the mechanism by which the blue light signal is transmitted in AppA. To aid in the assignment of these modes and to determine the contribution of the flavin to the TRIR spectrum of AppA, isotopically labeled riboflavins were synthesized and bound to wild type AppA.

*Steady-state vibrational spectroscopy of unbound riboflavin isotopes:* While the AppA BLUF domain binds all flavins present in the cell (FAD, FMN and riboflavin), most studies of this domain use protein reconstituted with FAD. The adenosine dinucleotide side chain of FAD dramatically increases the solubility of the isoalloxazine ring in water (see Figure 4.10). Studies have shown, however, that the side chain of the bound flavin does not participate in the photochemistry of the BLUF domain [46]. Isotopically labeled riboflavins, see Figure 4.10, were used instead of FAD, as this flavin derivative is easier to synthesize. However, loss of the adenosine side chain renders riboflavin less soluble in water.

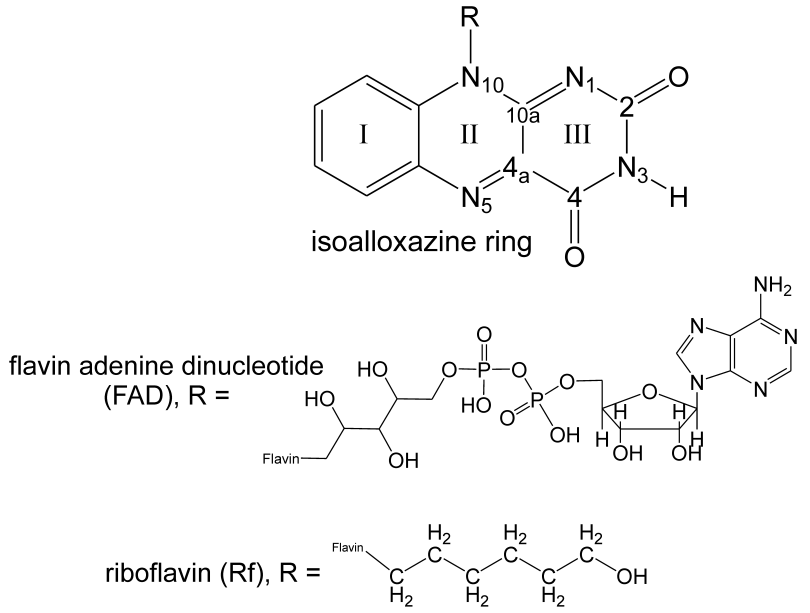


Figure 4.10: Side chains of FAD and riboflavin.

The steady-state Raman spectra of the unlabeled riboflavin (Rf), $^{13}$C-C2 labeled Rf (C2) and $^{13}$C-C4, C10a labeled Rf (C4) in $H_2O$ are shown in Figure 4.11 and Table 4.1. The mode at 1712 cm$^{-1}$ shifts to 1700 cm$^{-1}$ in the $^{13}$C-C2 labeled riboflavin and to 1680 cm$^{-1}$ in the $^{13}$C-C4, C10a, indicating that this mode has major contributions from the C4=O flavin group and minor contributions from the flavin C2=O.

The next mode lies at 1647 cm$^{-1}$ in unlabeled riboflavin, and is shifted to 1632 cm$^{-1}$ mode in the $^{13}$C-C2 isotope, while $^{13}$C-C4, C10a labeling leaves the mode unshifted, indicating this mode has major contributions from the C2=O stretch. Subtraction of the labeled riboflavin from the unlabeled reveals that the 1645 cm$^{-1}$ mode has shifted to 1640 cm$^{-1}$ in the $^{13}$C-C4, C10a isotope and to 1626 cm$^{-1}$ in the $^{13}$C-C2 spectrum (see inset in Figure 4.11), again indicating that the major contributor to this vibrational mode is the C2=O group of the flavin. This is in line with lumiflavin calculations done by Bowman and Spiro [7].

The Raman spectrum of riboflavin and the isotopes in $D_2O$ is shown in Figure 4.12. The N-H of the flavin (see Figure 4.10) is deuterated when riboflavin is in $D_2O$. The N-H wag is a contributor to many of the flavin high energy modes [30], and so many of these modes are shifted from the frequencies observed in $H_2O$. The 1700 cm$^{-1}$ mode in the the unlabeled spectrum shifts to

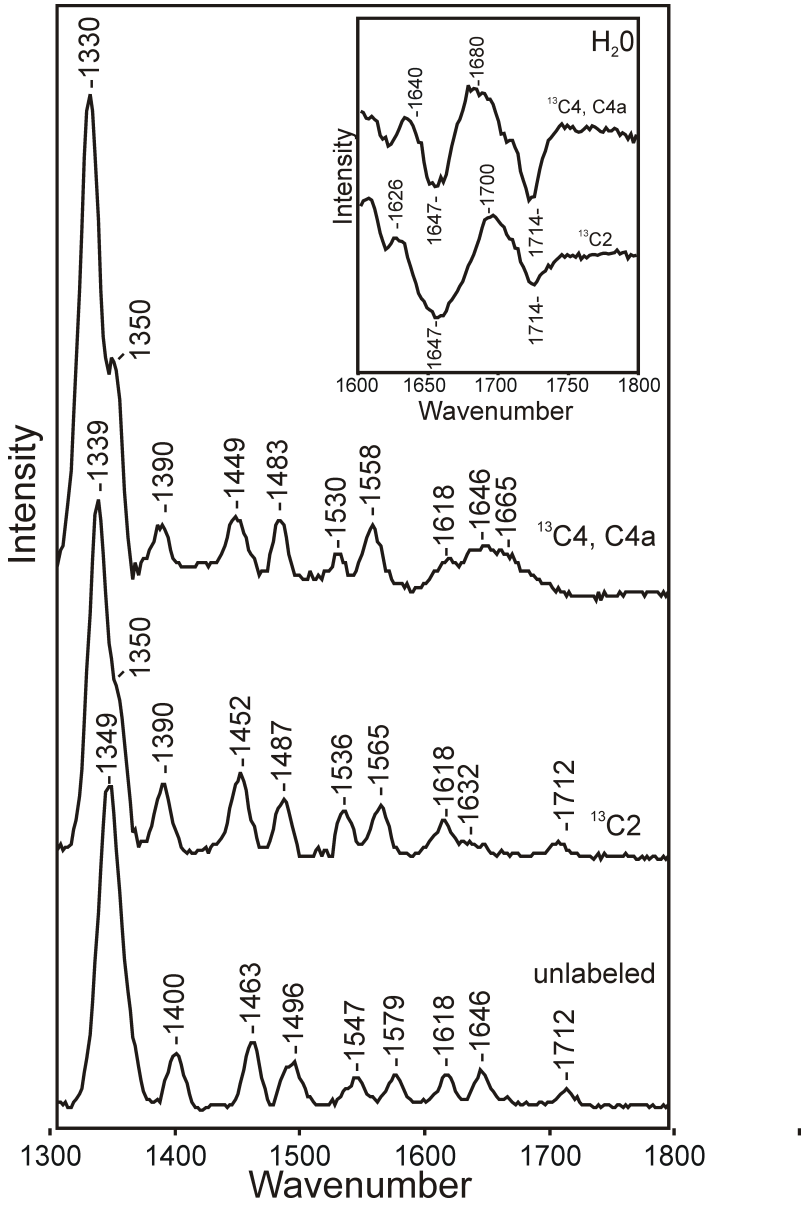


Figure 4.11: Raman spectra of unlabeled Rf (bottom), $^{13}$C-C2 labeled Rf (middle) and C4$^{13}$C-C4, C10a labeled Rf (top) in $H_2O$ (pH = 8.0), concentrations between 0.5 to 1 mM. Inset: subtraction spectra of isotopically labeled riboflavins. Top, $^{13}$C4, C10a minus unlabeled; bottom, $^{13}$C2 labeled minus unlabeled.

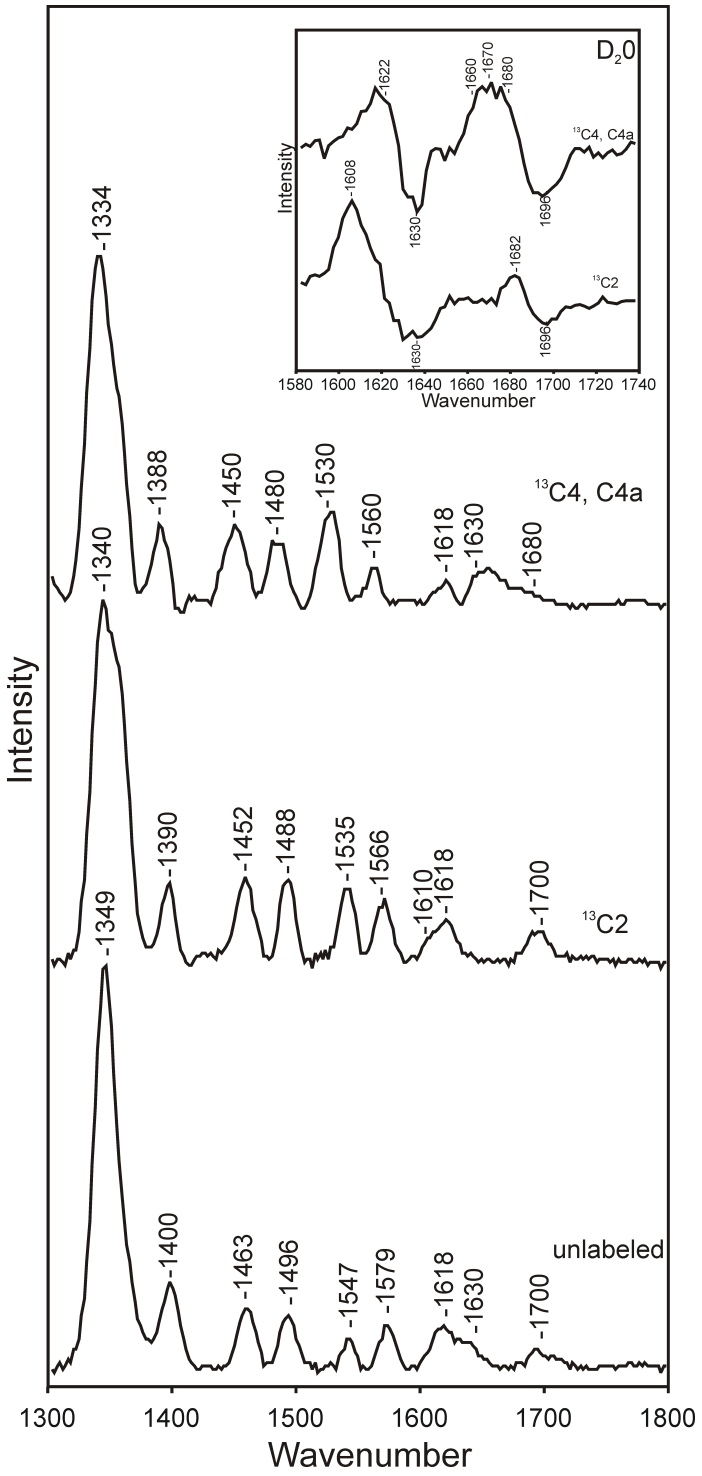


Figure 4.12: Raman spectra of unlabeled Rf (bottom), $^{13}$C-C2 labeled Rf (middle) and C4$^{13}$C-C4, C10a labeled Rf (top) in $D_2O$ (pD = 8.0), concentrations between 0.5 to 1 mM. Inset: subtraction spectra of isotopically labeled riboflavins. Top, $^{13}$C4, C10a minus unlabeled; bottom, $^{13}$C2 labeled minus unlabeled.

1680 $cm^{-1}$ in the $^{13}$C-C4, C10a spectrum, further confirming the assignment of this mode to the C4=O of the flavin. The mode at 1547 $cm^{-1}$ in $H_2O$, which has major contributions from the C2=O group, shifts to 1630 $cm^{-1}$ in $D_2O$. The observed shift is due to deuteration of the $N_3$-H in the flavin. Therefore, the mode observed at 1630 $cm^{-1}$ contains contributions from the $N_3$-H group. mode seen in unlabeled riboflavin shifts in both isotopes as well, but the new frequencies are covered by the 1618 $cm^{-1}$ mode that does not shift and is due to a nonlocal vibration of the ring III of the flavin (see Figure 4.10) [7].

The steady-state infrared spectra of the unbound isotopes in acetonitrile is similar to the Raman (see 4.13). Once again labeling at the C4 shifts the 1730 $cm^{-1}$ carbonyl mode down to 1686 $cm^{-1}$, and labeling at the C2 produces a shift from 1640 $cm^{-1}$ down to 1630 $cm^{-1}$. As the $^{13}$C-C4, C10a riboflavin isotope has two $^{13}$C labels, other modes shift in its infrared spectrum. The 1580 $cm^{-1}$ and 1540 $cm^{-1}$ modes are both shifted down 10 $cm^{-1}$ in the $^{13}$C-C4, C10a labeled isotope.

*TRIR of Riboflavin Isotopes:* Show in Figure 4.14 are the time-resolved infrared spectra (TRIR) of unlabeled Rf, $^{13}$C-C2 labeled Rf and $^{13}$C-C4, C10a labeled Rf (also see Table 4.2). The bleach at 1701 $cm^{-1}$ has been assigned to the loss of the C4=O upon excitation. This mode is shifted to 1666 $cm^{-1}$ in the $^{13}$C-C4, C10a labeled riboflavin. The carbonyl mode of C2=O has been

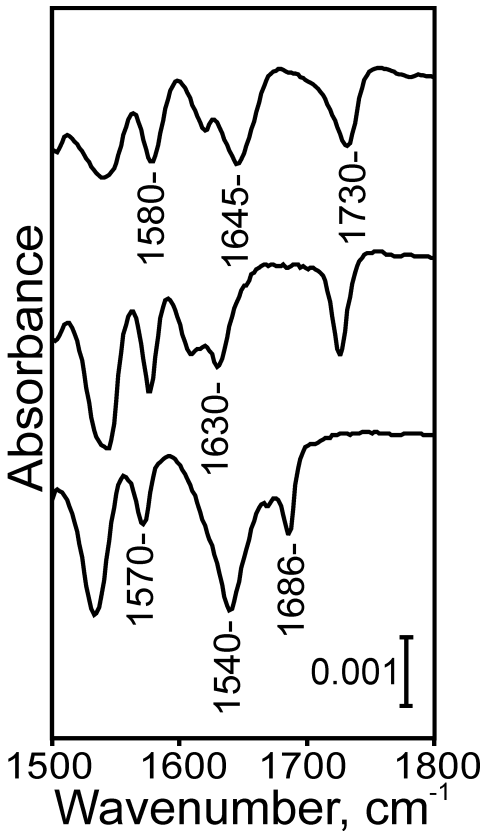


Figure 4.13: Steady-state infrared spectra of unlabeled Rf (top), $^{13}$C-C2 labeled Rf (middle) and C4$^{13}$C-C4, C10a labeled Rf (bottom) in deuterated acetonitrile, concentrations at 130 mM.

Table 4.1: Table of unlabeled and labeled riboflavin modes in the $H_2O$ Raman spectrum. Assignments from Bowman and Spiro, 1981 [7]

| Unlabeled | $^{13}$C-C2 | $^{13}$C-C4, C10a | Assignment |
|---|---|---|---|
| 1723 | 1694 | 1680 | C4=O |
| 1640 | 1626 | 1635 | C2=O*, C10a=N |
| 1618 | 1618 | 1618 | C4=O*, C2=O, C10a=N1* |
| 1577 | 1565 | 1560 | C4a=N5, C10a=N1 |
| 1540(br) | 1520(br) | 1536(br) | C4a=N5, C10a=N1 |
| 1497 | 1488 | 1482 | ring III deformation |
| 1460 | 1453 | 1450 | C4a=N5, C10a=N1 |
| 1405 | 1405 | 1405 | ring III deformation |
| 1350 | 1350 | 1366 (sh), 1345 | N5-C5a |

assigned to the 1650 $cm^{-1}$ bleach [7]. The $^{13}$C-C2 isotope has a bleach at 1600 $cm^{-1}$. The 1579 $cm^{-1}$ bleach in Rf is shifted slightly upon C2=O labeling to 1574 $cm^{-1}$ and to 1571 $cm^{-1}$ upon C4=O labeling. Similar behavior is seen for the intense 1543 $cm^{-1}$ bleach which shifts slightly with C2=O labeling (1543 $cm^{-1}$ and more with $^{13}$C-C4, C10a labeling (1538 $cm^{-1}$). An additional bleach is seen in the $^{13}$C-C4, C10a labeled riboflavin at 1490 $cm^{-1}$ which is neither the unlabeled or the $^{13}$C-C2 labeled spectra.

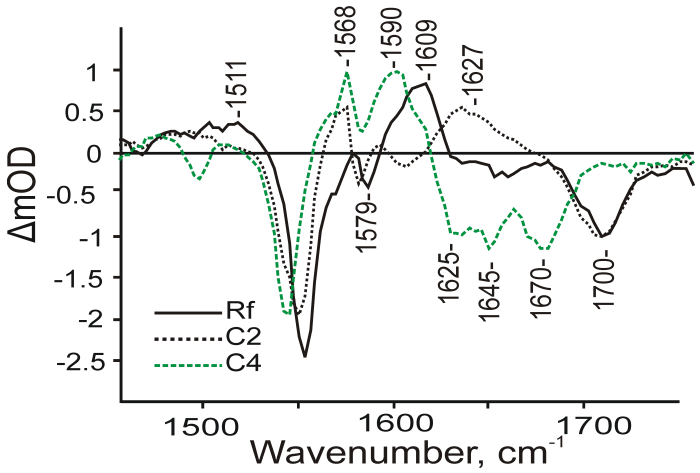


Figure 4.14: TRIR spectra 3 picoseconds after excitation of unlabeled, $^{13}$C-C2 labeled, and C4, C10a labeled riboflavin in pD 8 buffer. Concentrations at 1 mM.

The C2=O labeled flavin has an intense transient absorbtion at 1630 $cm^{-1}$ which may be suppressed in the unlabeled riboflavin due to the bleach at 1650 $cm^{-1}$. Another transient absorbtion is at 1610 $cm^{-1}$ in the unlabeled Rf spectrum, and at 1588 $cm^{-1}$ in the $^{13}$C-C4, C10a labeled spectrum. The 1630 $cm^{-1}$ bleach in the $^{13}$C-C2 labeled spectrum is likely due to the excited state

of the C4=O, while the small transient absorbtion at 1585 $cm^{-1}$ results from the excited state of the C2=O. Thus, the transient absorbtion at 1610 $cm^{-1}$ in the unlabeled Rf is due mostly to the C2=O mode. The 1574 $cm^{-1}$ transient absorbtion in the unlabeled Rf is also shifted slightly with labeling to 1568 $cm^{-1}$ in the $^{13}$C-C2 and 1562 $cm^{-1}$ in the $^{13}$C-C4, C10a labeled riboflavin. A broad, weak transient absorbtion from 1514 to 1468 $cm^{-1}$ is seen in both unlabeled and $^{13}$C-C2 labeled riboflavin. $^{13}$C-C4, C10a labeling produces more resolved transients at 1503 $cm^{-1}$ and at 1473 $cm^{-1}$.

*Steady-State Vibrational Studies of the BLUF Domain Bound to Labeled Flavins:* Steady-state Raman and infrared experiments were performed on the wild type BLUF domain bound to both unlabeled riboflavin (Rf) and to riboflavin isotopes.

The light minus dark spectrum of bound, unlabeled Rf is in good agreement with the earlier findings of Unno et al. [74] [73], who assigned the difference mode at (-)1701/(+)1690 $cm^{-1}$ (see 4.15) to a strengthening in the hydrogen bonding environment of the flavin C4=O carbonyl upon entry into the signaling state. The assignment of this difference mode to the C4=O flavin is further confirmed by $^{13}$C-C4, C10a labeling, which shifts this mode down to (-)1687 $cm^{-1}$ and (+)1673 $cm^{-1}$ (see 4.15).

The spectrum of AppA bound to unlabeled Rf also shows difference modes

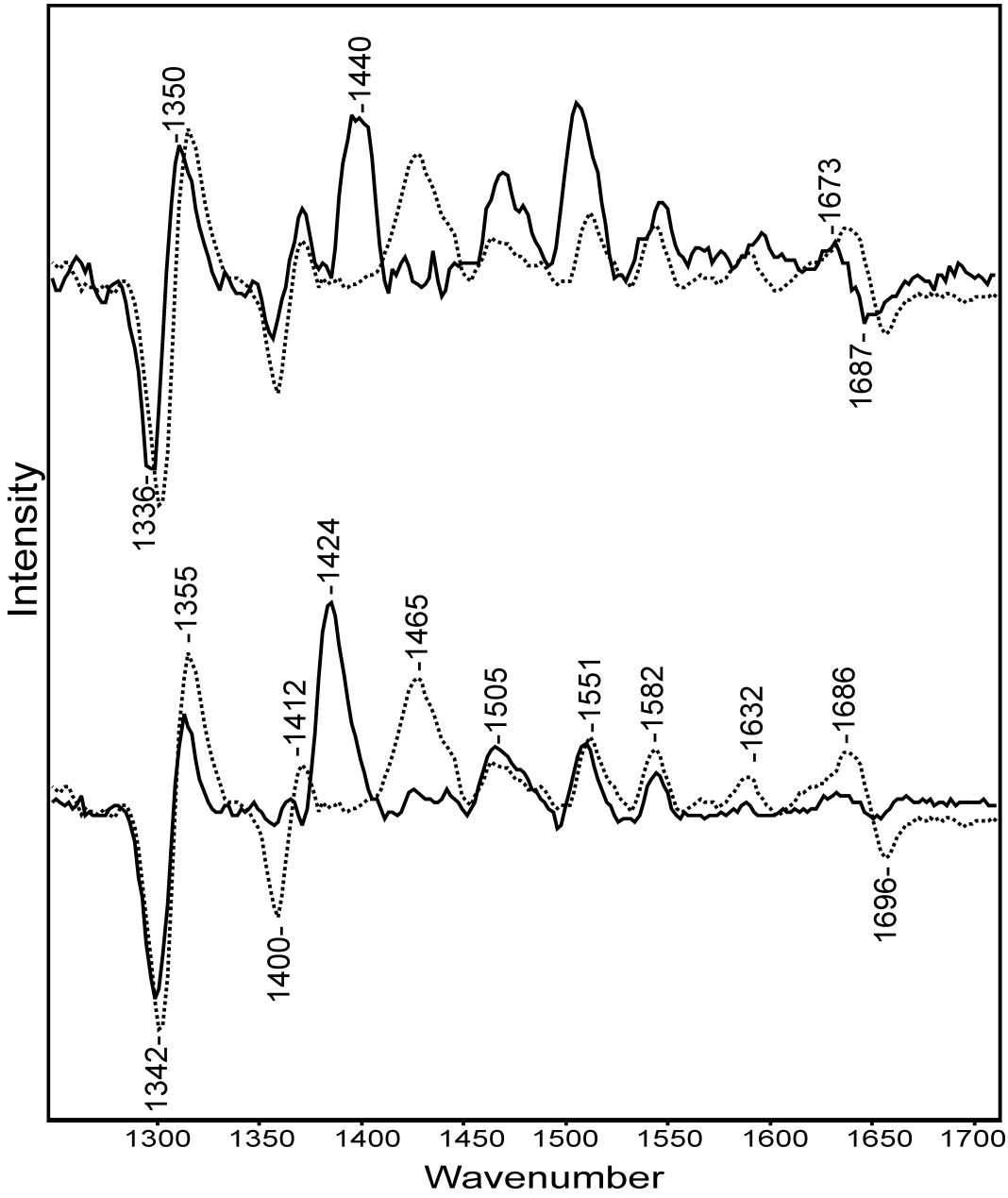


Figure 4.15: Steady-state Raman difference spectra (light - dark) of wild type AppA (pD 8) bound to Rf (dashed), the $^{13}$C-C4, C10a labeled isotope (top, solid) and the $^{13}$C-C2 isotope (bottom, solid). Concentrations from 1 to 1.5 mM.

at (+)1411/(-)1400 $cm^{-1}$ and (+)1345/(-)1342 $cm^{-1}$. The 1410 $cm^{-1}$ mode has been assigned by Unno et al [74] to ring I and II CN and CC stretching. Labeling of the C4 and C10a positions shifts the difference mode at 1350 $cm^{-1}$ to (+)1345/(-)1332 $cm^{-1}$, indicating that changes occur to these atoms upon entry into the signaling state. The 1340 $cm^{-1}$ mode been assigned to the N5-C5a bond by Bowman and Spiro [7]. The 1355 $cm^{-1}$ mode has been seen in reduced flavins and is due to the N1-H, N5-H bend [86].

Like the Raman, steady-state IR studies of the light minus dark spectrum of Appa bound to FAD have shown the C4=O flavin mode lies at (+)1701 to (-)1690 $cm^{-1}$ [47]. The steady-state difference IR of the BLUF domain bound to unlabeled riboflavin, 2-$^{13}$C labeled riboflavin and 4, 10a-$^{13}$C is shown in 4.16.

As in the Raman spectrum, the C4=O modes are shifted to (-)1682/(+)1674 $cm^{-1}$ in the IR $^{13}$C-C4, C10a labeled riboflavin. The (+)1632/(-)1620 $cm^{-1}$ modes, which are thought have contributions from the protein backbone [47], do not shift in either of the labeled spectra.

The$^{13}$C-C2 ladled riboflavin IR is quite similar to the unlabeled IR. The C4=O modes lie at (-)1701 / (+)1690 $cm^{-1}$) in each spectra. A mode in the $^{13}$C-C2 labeled spectrum at (+)1684 $cm^{-1}$) is not present in the unlabeled spectrum, and likely contributes to the (+)1690 $cm^{-1}$) mode in the unlabeled

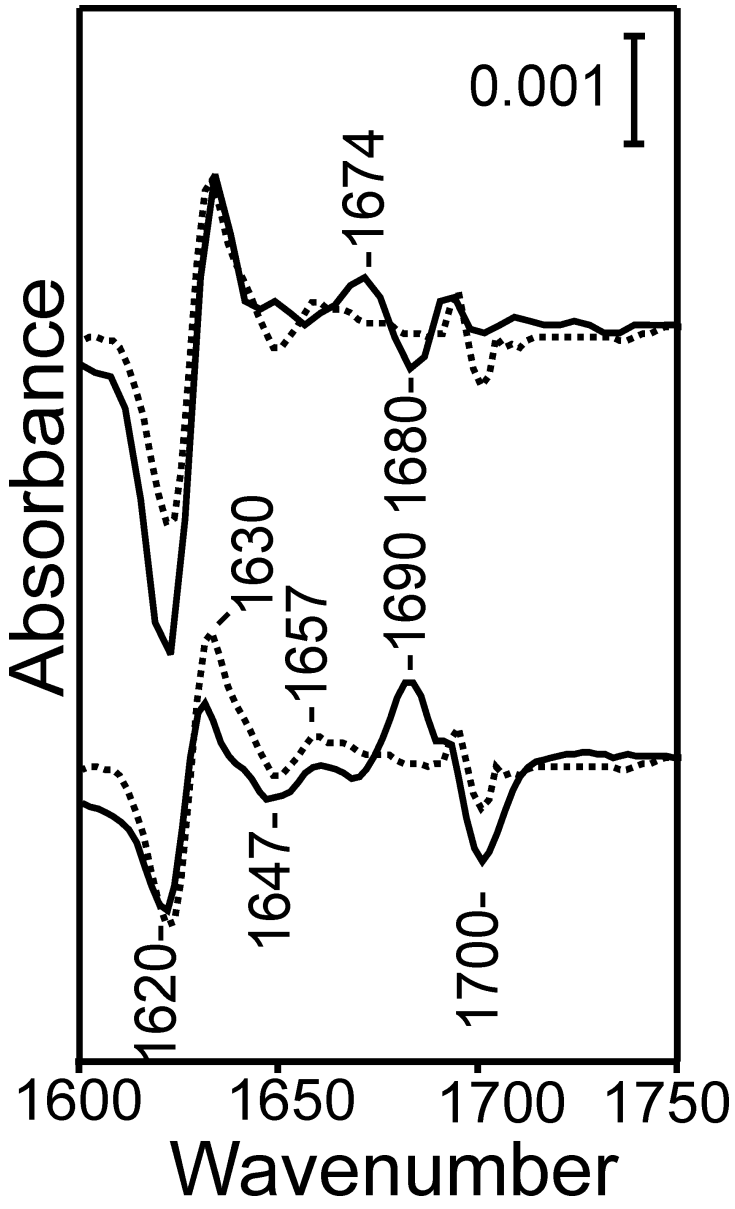


Figure 4.16: Steady-state IR difference spectra (light - dark) of wild type AppA (pD 8) bound to unlabeled Rf (dashed), the $^{13}$C-C4, C10a isotope (top), and to the $^{13}$C-C2 labeled isotope (bottom). Concentrations at 1.8 to 2.5 mM.

spectrum. This mode may be due to changes in the C2=O mode in the flavin upon entry into the light adapted state.

*TRIR of Isotopes bound to BLUF Domain of AppA:* The BLUF domain of wtAppA was reconstituted with both $^{13}$C-C2 and $^{13}$C-C4, C10a labeled Rf. Both the dark, photoactive state and the irradiated state of the protein were examined with time revolved infrared spectroscopy. Time-resolved data

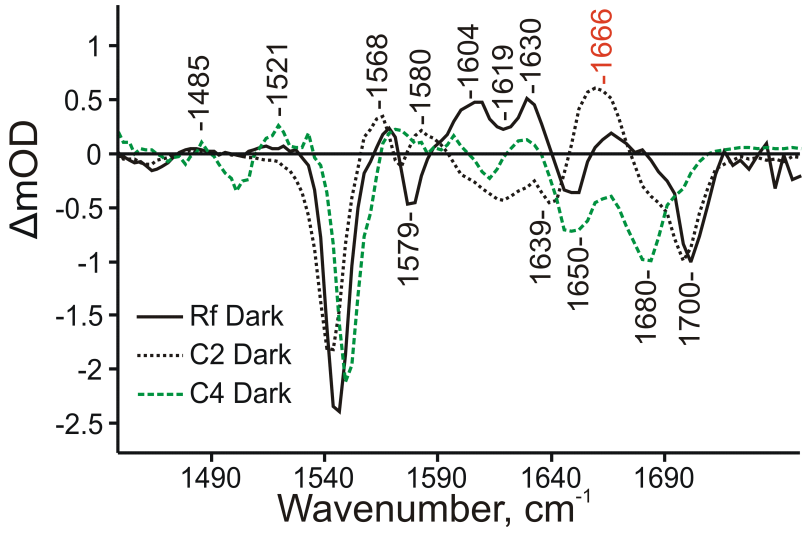


Figure 4.17: TRIR of dark wtAppA (pD 8) 2 picoseconds after excitation bound to unlabeled riboflavin, $^{13}$C-C2 labeled riboflavin, and $^{13}$C-C4, C10a riboflavin. Concentrations from 1.5 to 2 mM.

for the dark adapted, isotopically bound BLUF domain are shown in 4.17. The$^{13}$C-C2 labeled spectrum is similar to the unlabeled spectrum at high wavenumbers, while C4$^{13}$C-C4, C10a labeling, as in the steady-state spectra, shifts the carbonyl mode to 1680 cm$^{-1}$. There is a small transient absorbtion

in the $^{13}$C-C4, C10a labeled spectrum from 1652 to 1662 cm$^{-1}$ that appears to be suppressed by the intense bleaches surrounding the feature.

The C2 carbonyl mode is found at 1650 cm$^{-1}$ in the dark unlabeled spectrum. This mode is shifted to 1639 cm$^{-1}$ upon labeling to revel a strong, broad transient from 1652 to 1668 cm$^{-1}$. This transient absorbtion is at 1666 cm$^{-1}$ in the unlabeled spectrum, and does not appear to shift with flavin labeling. The intense 1650 cm$^{-1}$ bleach suppresses this transient in both the unlabeled and the $^{13}$C-C4, C10a labeled spectra.

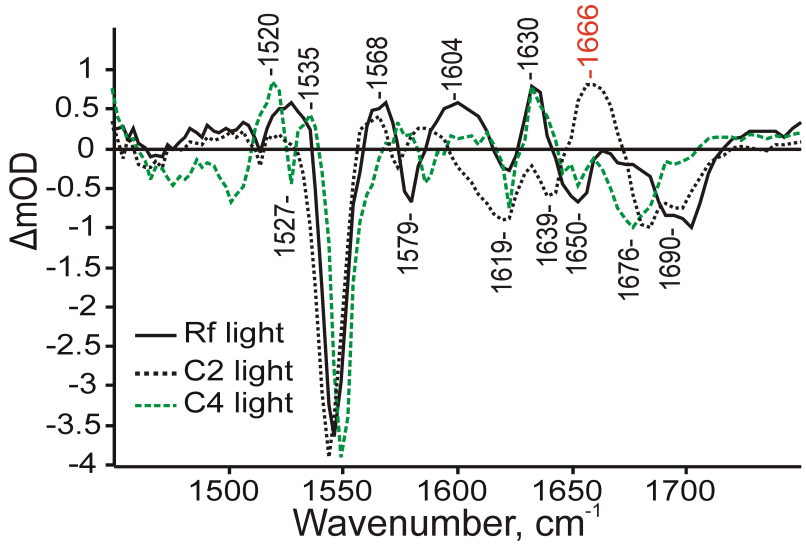


Figure 4.18: TRIR 3 picoseconds after excitation of wtAppa (pD 8) in the red-shifted state bound to unlabeled riboflavin, $^{13}$C-C2 labeled riboflavin, and $^{13}$C-C4, C10a labeled riboflavin. Concentrations from 1.5 to 2 mM.

Upon entering the light state (4.18), a shift in the C4=O frequency from 1701 cm$^{-1}$ to 1690 cm$^{-1}$ is seen for both the unlabeled and $^{13}$C-C2 labeled

species. The $^{13}$C-C4, C10a labeling shifts this bleach to 1673 cm$^{-1}$.

The 1666 cm$^{-1}$ transient absorbtion is suppressed by the shifted C4=O carbonyl bleach in the light adapted, unlabeled spectrum. In the $^{13}$C-C2 labeled spectrum, there is a broad, strong transient absorbtion from 1666 to 1652 cm$^{-1}$ in both states. In the $^{13}$C-C4, C10a labeled spectrum this region is occupied in both states by the by the strong bleach from the isotope shifted C4=O.

AppA bound to unlabeled Rf shows an increase in absorbtion in the broad modes at 1521 to 1535 cm$^{-1}$ upon entering the light state. These modes are obscured in both states of the protein by a strong bleach at 1546 cm$^{-1}$. Shifting of the 1545 cm$^{-1}$ mode to 1552 cm$^{-1}$ in $^{13}$C-C4, C10a labeled revels weak transients at 1532 and 1521 cm$^{-1}$.

## 4.5 Discussion

*Dark and light states of isotopically labeled Appa:* The steady-state Raman and IR spectra show changes in flavin modes and well as protein modes. The difference modes found in both spectra at 1701, and 1696 cm$^{-1}$ may be assigned to changes in hydrogen bonding to the C4=O of the flavin. Rotation of the glutamine (Q63) side chain to an orientation where the amide may donate a hydrogen bond is thought by many to be responsible for this spectral change [1]

Table 4.2: Table of TRIR modes for the light and dark states of AppA bound to Rf and the $^{13}$C-C2 (C2) and $^{13}$C-C4, C10a (C4) isotopes. Also listed are modes of Rf and the isotopes free in pD 8 buffer.

| Free | | | Dark | | | Light | | | Assignment |
|---|---|---|---|---|---|---|---|---|---|
| Rf | C2 | C4 | Rf | C2 | C4 | Rf | C2 | C4 | |
| (-)1701 | (-)1701 | (-)1670 | (-)1701 | (-)1701 | (-)1680 | (-)1690 | (-)1690 | (-)1670 | Flavin C4=O |
| - | (+)1625 | - | (+)1666 | (+)1666 | (+)1666 | (+)1666 | (+)1666 | (+)1666 | protein, Q63 |
| (-)1650 | - | (-)1650 | (-)1650 | (-)1640 | (-)1650 | (-)1650 | (-)1650 | (-)1650 | Flavin C2=O |
| - | - | - | (+)1630 | (+)1630 | (+)1630 | (+)1630 | (+)1630 | (+)1630 | protein |
| - | - | - | (-)1620 | (-)1620 - 1610 | (-)1620 | (-)1620 | (-)1620 - 1610 | (-)1620 | protein |
| (+)1610 | (+)1590 | (+)1600 | (+)1605 | (+)1580 | (+)1590 | (+)1600 | (+)1590 | (+)1600 | C2=O/C4=O TA |
| (-)1580 | (-)1574 | (-)1574 | (-)1580 | (-)1574 | (-)1585 | (-)1580 | (-)1574 | (-)1585 | vCN, vCC(ring I, 8b) |
| (+)1571 | (+)1568 | (+)1560 | (+)1570 | (+)1565 | (+)1570 | (+)1568 | (+)1565 | (+)1574 | TA |
| (-)1543 | (-)1543 | (-)1538 | (-)1546 | (-)1543 | (-)1548 | (-)1546 | (-)1543 | (-)1548 | vC=C(ring I, 8a) |
| (+)1511 | (+)1490 | (+)1500 | (+)1521 | - | (+)1532 | (+)1527 | (+)1516 | (+)1521 | |

[73], however a similar environment may also be achieved by tautomerization of the glutamine [65].

The slight shift upon labeling to the difference mode at (+)1345/(-)1342 $cm^{-1}$ indicates that this mode has contributions from the C10a atom. Changes to the hydrogen bonding environment of the N5 would account for this difference. A stronger hydrogen bond to the N5 from the proximal glutamine would make the flavin more electronically more similar to the reduced form in the signaling state, and alter the photophysical prosperities of the chromophore in the light state environment.

Aside from the red shift of the C4=O bleach, there is little difference in shape between the light and the dark TRIR spectra. While the 1666 $cm^{-1}$ seems reduced in intensity in the light state of AppA, this may be due to suppression by the red-shifted carbonyl mode. Labeling at the C2 of the flavin reveals a TA in both states from 1655 to 1666 $cm^{-1}$.

In fact, the most dramatic difference between the two states are the decay times, with the lighted state quenched more rapidly ($t_{1/2}$ = 50 ps) than the dark ($t_{1/2}$ = 2 ns) [65]. This suggests that the two states are very similar in structure. It is proposed that there are changes in hydrogen bonding about the chromophore when the BLUF domain enters the light state. Glutamine 63 is essential for a photocycle, and is positioned near the N5 of the chromophore.

A tyrosine and a tryptophan has been implicated in the photocycle as well. Mutation of the tyrosine 21 to phenylalanine results in photoinactive protein. The Q63L mutant lacks a photocycle and its TRIR spectrum shows no 1670 - 1655 $cm^{-1}$ transient absorbtion [65]. The TRIR of Y21F lacks both this transient absorbtion and modes at (-)1620 to 1610/(+)1630 $cm^{-1}$ (see 4.9). None of these modes appear to shift with flavin labeling, and so may be assigned to protein modes.

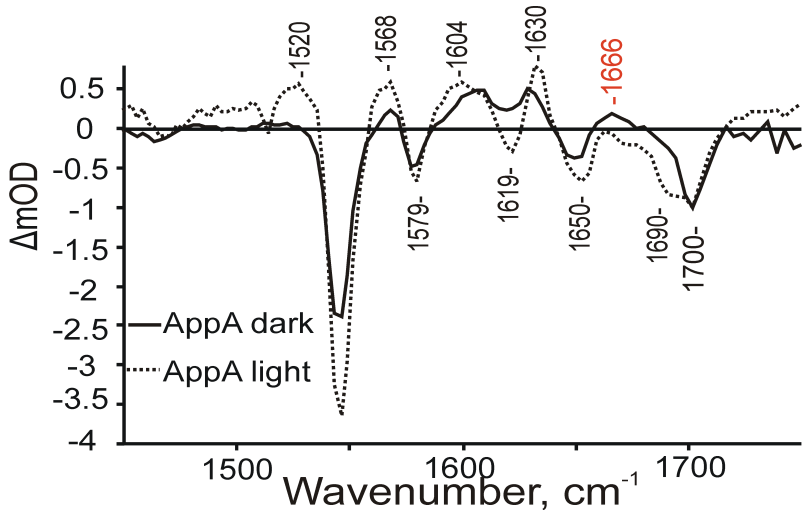


Figure 4.19: Overlay of the dark and light states of wtAppA (pD 8), 3 picoseconds after excitation.

In contrast, mutation of the tryptophan 104 to phenylalanine does not inactivate the photocycle but instead increases the quantum yield for light state formation and decreases the time for relaxation back to the dark state [48], behavior that is seen in other BLUF domains such as Slr1694 and Tll0078

that have a methionine in this position (see 4.2. Since the tryptophan mutant retains a photocycle, this residue is unlikely to be involved in any redox chemistry. Additionally, the TRIR of W104F is very similar to the wild type protein for both its states [65].

The positions of the (-)1620/(+)1630 $cm^{-1}$ modes do not significantly alter with illumination in the wild type TRIR. There are intensity differences between the dark and light states for these modes, and they appear in the baseline of the dark adapted protein. The modes appear in the steady-state IR difference spectrum as well, and shift when the protein is uniformly $^{13}C$-labeled. Mutation of the glutamine (Q63) to leucine abolishes the 1666 $cm^{-1}$ TA but retains the (-)1620/(+)1630 $cm^{-1}$ features. Mutation of Y21 to phenylalanine results in loss of both the 1666 transient and the (-)1620/(+)1630 $cm^{-1}$ absorbances (see 4.2).

Flavins exhibiting electochemistry show shifts in the C4a-C10a bond region (modes at 1580, 1540 and 1520 $cm^{-1}$) [31]. Radicals of tyrosine are expected to have strong absorbances at 1515, 1524 and 1610 $cm^{-1}$ [4] as well. While the broad, weak transient absorptions below 1550 $cm^{-1}$ become more intense in the illuminated AppA spectrum, flavins have modes in this region as well, making interpretation difficult. The 1610 $cm^{-1}$ mode, however, does appear in the TRIR spectrum, and may be due to loss of the neutral tyrosine [6].

The higher energy transient at 1666 $cm^{-1}$ is in the amide region. A glutamine near the flavin N5 is required for photoactive protein. The 1666 $cm^{-1}$ transient absorbtion may be due to changes to the amide side chain of the glutamine, and may overlap with absorbance from a flavin neutral radical, which is also in this frequency range [43].

## 4.6 Summary

*A model for light state formation in the AppA BLUF domain:* The mechanism for transmission of the ultrafast signal to a signal on the timescale of a biological response is currently under debate. The role of a conserved glutamine proximal to the flavin N5 is under scrutiny. While most scenarios call for electron transfer to a nearby tyrosine, the route for recombination of the radical pair may occur via several paths. The two current models exist for conversion to and the structure of the signaling state of the protein. One calls for the direct formation of a tyrosine-flavin radical pair [6] upon excitation of the flavin, followed by rotation by 180 degrees of the glutamine. The other involves the initial formation of a tyrosine-flavin radical pair followed by tautomerization and isomerization of the glutamine [59].

One theory for the for the altered hydrogen bonding to the C4=O in the light state of AppA involves the rotation of glutamine 63 [1]. Crystal structures

leave the orientation of this residue ambiguous. The AppA glutamine 63 amide nitrogen appears, however, to hydrogen bond to the tyrosine oxygen lone pairs in the dark state structure. The tyrosine hydroxy proton is known to be solvent accessible in the dark state from NMR data. This proton is not exchangeable in the light state [15]. Proton abstraction from the glutamine nitrogen by the excited state flavin N5 may cause the amide side chain to tautomerize. This would result in the formation of a neutral flavin radical and would place an electron on the oxygen of the glutamine side chain. This glutamine radical would have a longer C-O bond and may sterically interfere with the C4=O.

In the dark state crystal structure this length is 2.7 Å. This gap would be expected to shrink upon flavin excitation as the C4=O oxygen gains electron density [43]. The steric interference may provide motivation for reorientation of this reside so it may now abstract a proton from the tyrosine. The tyrosine radical may then recombine with the neutral flavin radical to form the light adapted AppA state. This state may be rapidly quenched by the reorientated Q and tyrosine [59], but spectroscopically strongly resembles the dark protein. This model is similar to that proposed by Sadeghian et al., however it is worth noting that the BlrB crystal structure used in their modeling studies has the glutamine side chain in the opposite orientation than that shown in the AppA crystal structure. It is likely that tautomerization is important for forming a

short lived signaling state, as seen in BlrB (2 seconds), where all that is needed to recover to the dark state is the back tautomerization. Tautomerization followed by rotation may been seen for the AppA/Slr1694 orientation of the glutamine, as this would rewire the proton exchange network to the tyrosine such that the oxygen of the glutamine participates in the enhanced quenching of the flavin in its light state. The lifetime of the AppA light state (15 minutes) would be further enhanced by a hydrogen bond to the W104. This position is occupied by a methionine in the Slr1694 light crystal structure, and the recovery for this protein to the dark is shortened as well (20 seconds).

Recent TRIR studies of the BLUF domain Slr1694 from *Synechocystis sp.* implicate a flavin anion radical in the photocycle, and assign the 1666 $cm^{-1}$ TA to the neutral semiquinone C4=O [6]. Were the 1666 $cm^{-1}$ mode due to flavin radical C4=O absorbance, it would be expected to shift upon C4=O labeling, as shown in steady-state and time resolved studies of the free isotopes. A TA at 1666 $cm^{-1}$ is still seen in the dark TRIR of both isotopes employed in this study, implying that this absorption in the BLUF domain of AppA is from protein. This mode is in the correct frequency range for amide/imidate interconversion [36] as well as several flavin modes involving atoms not labeled in this study. Additionally, a 1636 $cm^{-1}$ bleach is observed in the TRIR of this domain. This bleach is attributed to a flavin anion [6], however, it is not

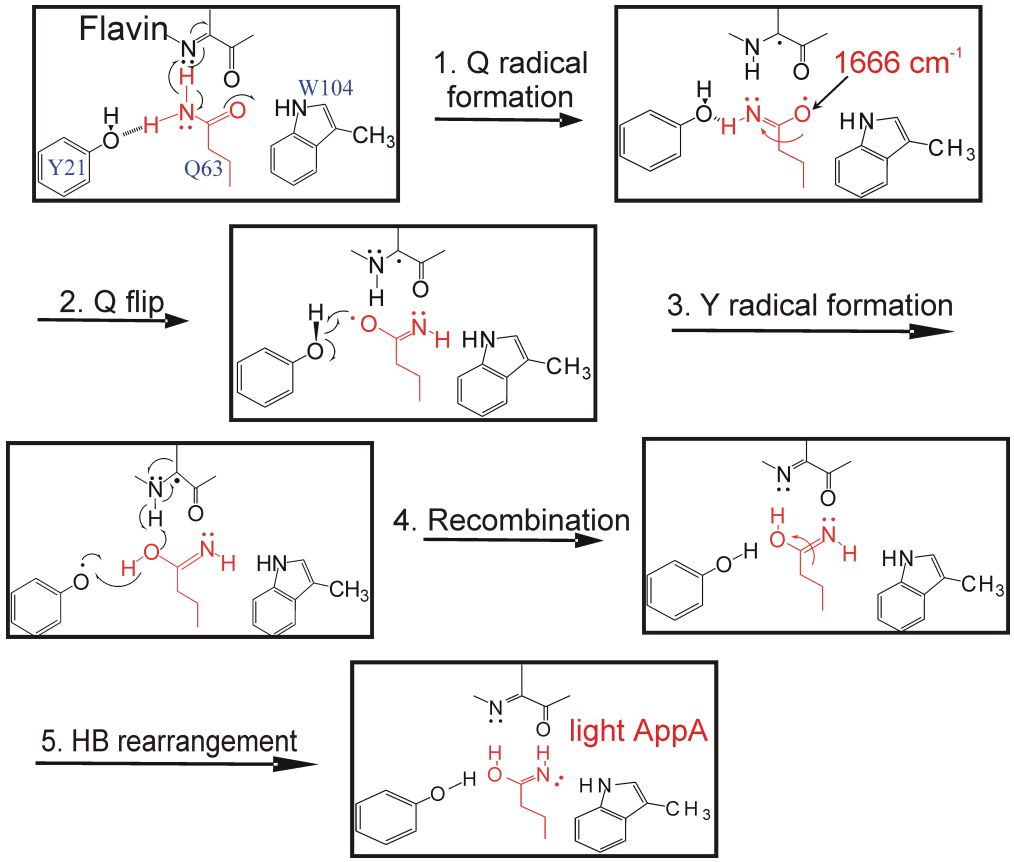


Figure 4.20: Possible conversion route to the rapidly quenched light state of AppA.

seen in the AppA spectrum.

Bonetti et al. [6] also claim the 1617 $cm^{-1}$ transient absorbtion is a redox active tyrosine residue. In the unlabeled spectra a bleach is seen. In the labeled spectra, the 1604 $cm^{-1}$ transient absorbtion from the flavin carbonyl modes is downshifted to approximately 1580 $cm^{-1}$ and reveals a very broad bleach mode from 1608 to 1620 $cm^{-1}$. This bleach is again seen in both states of AppA but it is intensified in the light state. An enhanced rate of electron transfer to this residue in the lit state would account for this increase.

Tryptophan 104 is not required for the photocycle, however, mutation in this position shortens the recovery time to the dark state as well as increasing the quantum yield for formation of the light adapted state [49]. The tryptophan forms a hydrogen bond to the glutamine 63 side chain carbonyl in the dark state [1]. Mutations resulting in the loss of this hydrogen bond would decrease the barrier for rotation of the glutamine. Loss of the tethering effect of the tryptophan would increase ease of glutamine side chain rotation and thus the yield of light state formation. An alternate, non-productive pathway for electron transfer to the tryptophan could exist in the dark state.

While the tryptophan is not essential for the AppA photocycle, it does appear to tune the photophysical properties of the domain. The crystal structure [84] of Slr1694 show this W in two conformations. One conformation

involves the inside the protein (W-in, see 4.2), as in the case of AppA. In the other, the tryptophan is solvent-exposed and a methionine has occupied its place (W-out). Both conformations are seen in the dark, while the W-out is populated upon light exposure. Mutation of either reside to an alanine shortens the recovery time to the signaling state [84]. The tryptophan in AppA does not become solvent exposed in its light state [71]. The 104 position, therefore, tunes the recovery rate back to the dark state of the protein.

The photophysical prosperities of the bound flavin are manipulated though noncovalent interactions with the AppA protein environment. The extremely long lived signaling state observed in AppA is atypical for the BLUF containing proteins, and this protein may have evolved a longer recovery time to allow the slower processes of DNA regulation to occur. Other BLUFs regulate more rapid cellular processes like phosphorylation and cAMP levels, and correspondingly have much quicker recovery times from their light adapted forms. It is clear from crystal structures that the initial, dark orientation of the glutamine 63 is key for determining the recovery kinetics. This reside thus responds to flavin excitation on an ultrafast timescale by forming a tautomerized radical that then rotates to allow slow (2000 ps) proton transfer to the tyrosine. In the light state of AppA, the glutamine side chain is flipped and fast proton transfer (1000 ps) to the tyrosine may occur.

Time-resolved infrared spectroscopy was employed to examine the ultrafast behavior of the light and dark states of the BLUF domain of AppA. While many modes in the excited state spectrum of the BLUF domain are due to the bound flavin chromophore, several do not shift with when the flavin is isotopically labeled. Specifically, the 1666, 1630, and 1620 $cm^{-1}$ modes arise from an ultrafast response of the BLUF protein environment to the flavin excited state. The Y21F and Q63L mutants of the AppA BLUF domain are photoinactive, and these residues are close to the bound flavin. The 1666 mode was not observed in the TRIR spectrum of either of these photoinactive mutants. The 1630 and 1620 modes were observed in the Q63L mutant, while the Y21F mutant lacked all three (1666, 1630, and 1620 $cm^{-1}$). These modes are therefore assigned to changes in these residues upon photoexcitation of the flavin chromophore.

# Bibliography

[1] V. Anderson, S. Dragnea, S. Masuda, J. Ybe, K. Moffat, and B. C. Structure of a novel photoreceptor, the bluf domain of appa from rhodobacter sphaeroides. *Biochemistry*, 44(22):7998–8005, 2005.

[2] M. Andresen, M. C. Wahl, A. C. Stiel, F. Graster, L. V. Schfer, S. Trowitzsch, G. Weber, C. Eggeling, H. Grubmller, S. W. Hell, and S. Jakobs. Structure and mechanism of the reversible photoswitch of a fluorescent protein. *Proceedings of the National Academy of Sciences of the United States of America*, 102(37):13070–74, 2005.

[3] R. Balu, H. Zhang, E. Zukowski, J.-Y. Chen, A. G. Markelz, and S. K. Gregurick. Terahertz spectroscopy of bacteriorhodopsin and rhodopsin: Similarities and differences. *Biophysical Journal*, 94(8):3217–3226, 2008.

[4] B. Barry and O. Einarsdottir. Insights into the structure and function of redox-active tyrosines from model compounds. *Journal of Physical Chemistry B*, 109:6972–81, 2005.

[5] A. Bell, X. He, R. Wachter, and P. Tonge. Probing the ground state structure of the green fluorescent protein chromophore using raman spectroscopy. *Biochemistry*, 39(15):4432–31, 2000.

[6] C. Bonetti, T. Mathes, I. van Stokkum, K. Mullen, M. Groot, R. Grondelle, P. Hegemann, and J. Kennis. Hydrogen bond switching among flavin and amino acid side chains in the bluf photoreceptor observed by ultrafast infrared spectroscopy. *Biophys. J.*, 2008.

[7] W. D. Bowman and T. G. Spiro. Normal mode analysis of lumiflavin and interpretation of resonance raman spectra of flavoproteins. *Biochemistry*, 20(11):3313–18, 1981.

[8] C. A. Brautigam, B. S. Smith, Z. Ma, M. Palnitkar, D. R. Tomchick, M. Machius, and J. Deisenhofer. Structure of the photolyase-like domain

of cryptochrome 1 from arabidopsis thaliana. *Proceedings of the National Academy of Sciences of the United States of America*, 101(3):12142–47, 2004.

[9] S. Crosson, S. Rajagopal, and K. Moffat. The lov domain family: Photoresponsive signaling modules coupled to diverse output domains. *Biochemistry*, 42(1):2–10, 2003.

[10] T. Domratcheva, B. L. Grigorenko, I. Schlichting, and A. Nemukhin. Molecular models predict light-induced glutamine tautomerization in bluf photoreceptors. *Biophysical Journal*, 94(10):3872–3879, 2008.

[11] Y. Fukushima, K. Okajima, Y. Shibata, M. Ikeuchi, and S. Itoh. Primary intermediate in the photocycle of a blue-light sensory bluf fad-protein, tll0078, of thermosynechococcus elongatus bp-1. *Biochemistry*, 44(13):5149–58, 2005.

[12] M. Gauden, S. Yeremenko, W. Laan, I. vanStokkum, J. Ihalainen, R. vanGrondelle, K. Hellingwerf, and J. Kennis. Photocycle of the flavin-binding photoreceptor appa, a bacterial transcriptional antirepressor of photosynthesis genes. *Biochemistry*, 44(10):3653–62, 2005.

[13] E. Getzoff, K. Gutwin, and U. Genick. Anticipatory active-site motions and chromophore distortion prime photoreceptor pyp for light activation. *Nature Structural Molecular Biology*, 10(8):663–668, 2003.

[14] B. Grigorenko, A. Savitsky, I. Topol, S. Burt, and A. Nemukhin. trans and cis chromophore structures in the kindling fluorescent protein asfp595. *Chemical Physics Letters*, 424(1-3):184 – 188, 2006.

[15] J. Grinstead, M. Avila-Perez, K. Hellingwerf, R. Boelens, and R. Kaptein. Light-induced flipping of a conserved glutamine sidechain and its orientation in the appa bluf domain. *Journal of the American Chemical Society*, 126:15066–15067, 2006.

[16] J. S. Grinstead, S. T. Hsu, W. Laan, A. M. Bonvin, K. J. Hellingwerf, R. Boelens, and R. Kaptein. The solution structure of the appa bluf domain: Insight into the mechanism of light-induced signaling. *ChemBioChem*, 7(1):187–193, 2006.

[17] X. He, A. Bell, and P. Tonge. Isotopic labeling and normal-mode analysis of a model green fluorescent protein chromophore. *Journal of Physical Chemistry B*, 106(23):6056–66, 2002.

[18] X. He, A. Bell, and P. Tonge. Ground state isomerization of a model green fluorescent protein chromophore. *FEBS Letters*, 549(1-3):35–38, 2003.

[19] X. He, A. F. Bell, and P. J. Tonge. Synthesis and spectroscopic studies of model red fluorescent protein chromophores. *Organic Letters*, 4(9):1523–1526, 2002.

[20] N. Hoang, E. Schleicher, S. Kacprzak, J. Bouly, M. Picot, W. Wu, A. Berndt, E. Wolf, R. Bittl, and M. Ahmad. Human and drosophila cryptochromes are light activated by flavin photoreduction in living cells. *PLoS Biology*, 6(7):160, 2008.

[21] D. Hoersch, H. Otto, M. A. Cusanovich, and M. P. Heyn. Distinguishing chromophore structures of photocycle intermediates of the photoreceptor pyp by transient fluorescence and energy transfer. *Journal of Physical Chemistry B*, 112(30):9118–25, 2008.

[22] M. Hofmann, C. Eggeling, S. Jakobs, and S. W. Hell. Breaking the diffraction barrier in fluorescence microscopy at low light intensities by using reversibly photoswitchable proteins. *Proceedings of the National Academy of Sciences of the United States of America*, 104(49):17565–69, 2005.

[23] A. B. Houtsmuller and W. Vermeulen. Macromolecular dynamics in living cell nuclei revealed by fluorescence redistribution after photobleaching. *Histochemistry and Cell Biology*, 115(1):13–21, 2001.

[24] S. Hu, K. M. Smith, and T. G. Spiro. Assignment of protoheme resonance raman spectrum by heme labeling in myoglobin. *Journal of the American Chemical Society*, 118(50):12638–46, 1996.

[25] A. Jung, T. Domratcheva, M. Tarutina, Q. Wu, W. H. Ko, R. L. Shoeman, M. Gomelsky, K. H. Gardner, and I. Schlichting. Structure of a bacterial bluf photoreceptor: Insights into blue light-mediated signal transduction. *Proc. Natl. Acad. Sci. U.S.A*, 102(35):12350–5., 2005.

[26] A. Jung, J. Reinstein, T. Domratcheva, R. L. Shoeman, and I. Schlichting. Crystal structures of the appa bluf domain photoreceptor provide insights into blue light-mediated signal transduction. *Journal of Molecular Biology*, 362(4):717–732, 2006.

[27] Y. T. Kao, C. Tan, S. H. Song, N. Ozturk, J. Li, L. Wang, A. Sancar, and D. Zhong. Ultrafast dynamics and anionic active states of the

flavin cofactor in cryptochrome and photolyase. *Journal of the American Chemical Society*, 130(24):7695–7701, 2008.

[28] J. Kennis and M. Groot. Ultrafast spectroscopy of biological photoreceptors. *Current Opinion in Structural Biology*, 17(5):623–630, 2007.

[29] A. Kita, K. Okajima, Y. Morimoto, M. Ikeuchi, and K. Miki. Structure of a cyanobacterial bluf protein, tll0078, containing a novel fad-binding blue light sensor domain. *Journal of Molecular Biology*, 349(1):1–9, 2005.

[30] M. Kondo, J. Nappa, K. Ronayne, A. Stelling, P. Tonge, and S. Meech. Ultrafast vibrational spectroscopy of the flavin chromophore. *Journal of Physical Chemistry B*, 110(14):20107–110, 2006.

[31] T. Kottke, A. Batschauer, M. Ahmad, and J. Heberle. Blue-light-induced changes in arabidopsis cryptochrome 1 probed by ftir difference spectroscopy. *Biochemistry*, 45:2472–9, 2006.

[32] T. Kottke, P. Hegemann, B. Dick, and J. Heberle. The photochemistry of the light-, oxygen-, and voltage-sensitive domains in the algal blue light receptor phot. *Biopolymers*, 82(4):373–378, 2006.

[33] W. Laan, T. Bednarz, J. Heberle, and K. Hellingwerf. Chromophore composition of a heterologously expressed bluf-domain. *Photochem. Photobiol. Sci.*, 3:1011–6, 2004.

[34] W. Laan, M. Gauden, S. Yeremenko, R. vanGrondelle, J. Kennis, and K. Hellingwerf. On the mechanism of activation of the bluf domain of appa. *Biochemistry*, 45(1):51–60, 2006.

[35] E. W. Lamont, F. O. James, D. B. Boivin, and N. Cermakian. Circadian rhythms in sleep medicine: From circadian clock gene expression to pathologies. *Sleep Medicine*, 8(6):547–556, 2007.

[36] J. Ledbetter. Infrared spectra of n-aryl imines of o-hydroxybenzaldehyde between 2000 and 1500 cm-1. *J. Phys. Chem.*, 81:54–59, 1977.

[37] Q. Li and H. Yang. Cryptochrome signaling in plants. *Photochemistry and Photobiology*, 83(1):94–101, 2007.

[38] C. Lin and T. Todo. The cryptochromes. *Genome Biology*, 6(5):220, 2005.

[39] H. Luecke, B. Schobert, J. Cartailler, H. Richter, A. Rosengarth, R. Needleman, and J. K. Lanyi. Coupling photoisomerization of retinal to directional transport in bacteriorhodopsin. *Journal of Molecular Biology*, 300(5):1237–1255, 2000.

[40] S. Maddalo and M. Zimmer. The role of the protein matrix in green fluorescent protein fluorescence. *Photochemistry and Photobiology*, 82(2):3767–372, 2006.

[41] G. Malo, M. Wang, D. Wu, A. Stelling, P. Tonge, and R. Wachter. Crystal structure and raman studies of dsfp483, a cyan fluorescent protein from discosoma striata. *Journal of Molecular Biology*, 378(4):871 – 886, 2008.

[42] O. Markova, M. Mukhtarov, E. Real, and Y. Jacob. Genetically encoded chloride indicator with improved sensitivity. *Journal of Neuroscience Methods*, 170(1):67–76, 2008.

[43] C. Martin, M. L. Tsao, C. Hadad, and M. Platz. The reaction of triplet flavin with indole. a study of the cascade of reactive intermediates using density functional theory and time resolved infrared spectroscopy. *Journal of the American Chemical Society*, 124(24):7226–34, 2002.

[44] S. Masuda and C. Bauer. Appa is a blue light photoreceptor that antirepresses photosynthesis gene expression in rhodobacter sphaeroides. *Cell*, 10:5:613–623, 2002.

[45] S. Masuda, K. Hasegawa, A. Ishii, and T.-a. Ono. Light-induced structural changes in a putative blue-light receptor with a novel fad binding fold sensor of blue-light using fad (bluf); slr1694 of synechocystis sp. pcc6803. *Biochemistry*, 43(18):5304–13, 2004.

[46] S. Masuda, K. Hasegawa, and T. Ono. Adenosine diphosphate moiety does not participate in structural changes for the signaling state in the sensor of blue-light using fad domain of appa. *FEBS Letters*, 579 (20):4329–4332, 2005.

[47] S. Masuda, K. Hasegawa, and T. Ono. Light-induced structural changes of apoprotein and chromophore in the sensor of blue light using fad (bluf) domain of appa for a signaling state. *Biochemistry*, 44(4):1215–24, 2005.

[48] S. Masuda, K. Hasegawa, and T. Ono. Tryptophan at position 104 is involved in transforming light signal into changes of beta-sheet structure

for the signaling state in the bluf domain of appa. *Plant Cell Physiol.*, 46(12):1894–01, 2005.

[49] S. Masuda, Y. Tomida, H. Ohta, and K. Takamiya. The critical role of a hydrogen bond between gln63 and trp104 in the blue-light sensing bluf domain that controls appa activity. *Journal of Molecular Biology*, 368:1223–30, 2007.

[50] T. McAnaney, W. Zeng, C. Doe, N. Bhanji, S. Wakelin, D. Pearson, P. Abbyad, X. Shi, S. Boxer, and C. Bagshaw. Protonation, photobleaching, and photoactivation of yellow fluorescent protein (yfp 10c): A unifying mechanism. *Biochemistry*, 44(14):5510–24, 2005.

[51] A. Miyawaki. Visualization of the spatial and temporal dynamics of intracellular signaling. *Developmental Cell*, 4(3):295–305, 2003.

[52] H. Nagai, Y. Fukushima, K. Okajima, M. Ikeuchi, and H. Mino. Formation of interacting spins on flavosemiquinone and tyrosine radical in photoreaction of a blue light sensor bluf protein tepixd. *Biochemistry*, 2008.

[53] M. Nakasako, K. Zikihara, D. Matsuoka, H. Katsura, and S. Tokutomi. Structural basis of the lov1 dimerization of arabidopsis phototropins 1 and 2. *Journal of Molecular Biology*, 381(3):718–733, 2008.

[54] R. Nifosi and T. Tozzini. Cis-trans photoisomerization of the chromophore in the green fluorescent protein variant e2gfp: A molecular dynamics study. *Chemical Physics*, 323(2-3):358–368, 2006.

[55] A. Pakhomov and V. Martynov. Gfp family: Structural insights into spectral tuning. *Chemistry and Biology*, 15(8):755–764, 2008.

[56] C. Partch and S. A. Photochemistry and photobiology of cryptochrome blue-light photopigments: The search for a photocycle. *Photochemistry and Photobiology*, 81(6):1291–1304, 2005.

[57] S. Remington. Fluorescent proteins: maturation, photochemistry and photophysics. *Current Opinion in Structural Biology*, 16(6):714–721, 2006.

[58] N. C. Rockwell, Y. S. Su, and J. C. Lagarias. Phytochrome structure and signaling mechanisms. *Annu. Rev. Plant Biol.*, 57:837–858, 2006.

[59] K. Sadeghian, M. Bocola, and M. Schtz. A conclusive mechanism of the photoinduced reaction cascade in blue light using flavin photoreceptors. *J. Am. Chem. Soc*, Web Release Date: August 23, 2008.

[60] L. Schafer, G. Groenhof, A. Klingen, M. Ullmann, M. Boggio-Pasqua, M. Robb, and H. Grubmller. Photoswitching of the fluorescent protein asfp595: Mechanism, proton pathways, and absorption spectra. *Angewandte Chemie*, 46(4):530–536, 2007.

[61] S. Schroder-Lang, M. Schwarzel, R. Seifert, T. Strunker, S. Kateriya, J. Looser, M. Watanabe, U. B. Kaupp, P. Hegemann, and G. Nagel. Fast manipulation of cellular camp level by light in vivo. *Nature Methods*, 4(1):39–42, 2007.

[62] N. C. Shaner, G. H. Patterson, and M. W. Davidson. Advances in fluorescent protein technology. *Journal of Cell Science*, 120(24):4247–4260, 2007.

[63] X. Shi, J. Basran, H. E. Seward, W. Childs, C. R. Bagshaw, and S. G. Boxer. Anomalous negative fluorescence anisotropy in yellow fluorescent protein (yfp 10c):  quantitative analysis of fret in yfp dimers. *Biochemistry*, 46(50):14403–17, 2007.

[64] O. Shimomura. The discovery of aequorin and green fluorescent protein. *Journal of Microscopy*, 217(1):3–15, 2005.

[65] A. Stelling, K. Ronayne, J. Nappa, P. Tonge, and S. Meech. Ultrafast structural dynamics in bluf domains: Transient infrared spectroscopy of appa and its mutants. *J. Am. Chem. Soc.*, 129:15556–64, 2007.

[66] D. Stoner-Ma, A. Jaye, P. Matousek, M. Towrie, S. Meech, and P. Tonge. Observation of excited-state proton transfer in green fluorescent protein using ultrafast vibrational spectroscopy. *Journal of the American Chemical Society*, 127(9):2864–5, 2005.

[67] D. Stoner-Ma, E. Melief, J. Nappa, K. Ronayne, P. Tonge, and S. Meech. Proton relay reaction in green fluorescent protein (gfp): Polarization-resolved ultrafast vibrational spectroscopy of isotopically edited gfp. *Journal of Physical Chemistry B*, 110(43):22009–18, 2006.

[68] H. Suzuki, K. Okajima, M. Ikeuchi, and T. Noguchi. Lov-like flavin-cys adduct formation by introducing a cys residue in the bluf domain

of tepixd. *Journal of the American Chemical Society*, 130(39):12884–85, 2008.

[69] R. Takahashi, K. Okajima, H. Suzuki, H. Nakamura, M. Ikeuchi, and T. Noguchi. Ftir study on the hydrogen bond structure of a key tyrosine residue in the flavin-binding blue light sensor tepixd from thermosynechococcus elongatus. *Biochemistry*, 46:6459–67, 2007.

[70] C. Takanishi and E. Bykova. Gfp-based fret analysis in live cells. *Brain Research*, 1091(1):132–139, 2006.

[71] K. C. Toh, I. H. M. van Stokkum, J. Hendriks, M. T. A. Alexandre, J. C. Arents, M. A. Perez, R. van Grondelle, K. J. Hellingwerf, and J. T. M. Kennis. On the signaling mechanism and the absence of photoreversibility in the appa bluf domain. *Biophysics Journal*, 95(1):312–321, 2008.

[72] M. Towrie, D. C. Grills, J. Dyer, J. A. Weinstein, P. Matousek, R. Barton, P. D. Bailey, N. Subramaniam, W. M. Kwok, C. S. Ma, D. Phillips, A. W. Parker, and M. W. George. Development of a broadband picosecond infrared spectrometer and its incorporation into an existing ultrafast time-resolved resonance raman, uv/visible, and fluorescence spectroscopic apparatus. *Applied Spectroscopy*, 57(4):367–80, 2003.

[73] M. Unno, S. Masuda, T. Ono, and S. Yamauchi. Orientation of a key glutamine residue in the bluf domain from appa revealed by mutagenesis, spectroscopy, and quantum chemical calculations. *Journal of the American Chemical Society*, 128(17):5638–39, 2006.

[74] M. Unno, R. Sano, S. Masuda, T. Ono, and Y. S. Light-induced structural changes in the active site of the bluf domain in appa by raman spectroscopy. *Journal of Physical Chemistry B*, 109(25):12620–6, 2005.

[75] M. vanderHorst and K. Hellingwerf. Photoreceptor proteins, "star actors of modern times": A review of the functional dynamics in the structure of representative members of six different photoreceptor families. *Accounts of Chemical Research*, 37(1):13–20, 2004.

[76] I. Vassiliev, A. Offenbacher, and B. Barry. Redox-active tyrosine residues in pentapeptides. *Journal of Physical Chemistry B*, 109:23077–85, 2005.

[77] R. Wachter. The family of gfp-like proteins: Structure, function, photophysics and biosensor applications. introduction and perspective. *Photochemistry and Photobiology*, 82(2):339–344, 2006.

[78] R. Wachter, M. Elsliger, K. Kallio, G. Hanson, and S. Remington. Structural basis of spectral shifts in the yellow-emission variants of green fluorescent protein. *Structure*, 6(10):1267–1277, 1998.

[79] J. R. Wagner, J. S. Brunzelle, K. T. Forest, and R. D. Vierstra. A light-sensing knot revealed by the structure of the chromophore-binding domain of phytochrome. *Nature*, 438(7066):325–331, 2005.

[80] M. A. Wall, M. Socolich, and R. Ranganathan. The structural basis for red fluorescence in the tetrameric gfp homolog dsred. *Nature Structural Molecular Biology*, 7(12):1072–8368, 200.

[81] G. Wille, M. Ritter, R. Friedemann, W. Mantele, and G. Hubner. Redox-triggered ftir difference spectra of fad in aqueous solution and bound to flavoproteins. *Biochemistry*, 42(50):14814–14821, 2003.

[82] X. Yang, J. Kuk, and K. Moffat. Crystal structure of pseudomonas aeruginosa bacteriophytochrome: Photoconversion and signal transduction. *Proceedings of the National Academy of Sciences*, 105(38):14715–20, 2008.

[83] M. K. Yasushi I. Structure and photoreaction of photoactive yellow protein, a structural prototype of the pas domain superfamily. *Photochemistry and Photobiology*, 83(1):40–49, 2007.

[84] H. Yuan, S. Anderson, S. Masuda, V. Dragnea, K. Moffat, and C. Bauer. Crystal structures of the synechocystis photoreceptor slr1694 reveal distinct structural states related to signaling. *Biochemistry*, 45(42):12687–94, 2006.

[85] L. Zhang, H. N. Patel, J. W. Lappe, and R. M. Wachter. Reaction progress of chromophore biogenesis in green fluorescent protein. *Journal of the American Chemical Society*, 128(14):4766–4772, 2006.

[86] Y. Zheng, P. Carey, and B. Palfey. Raman spectrum of fully reduced flavin. *Journal of Raman Spectroscopy*, 35:521–4, 2004.

# Appendix A

# Appendix

## A.1 Characterization of the $^{15}$N Lumiflavin Isotope

The $^{15}$N lumiflavin isotope was synthesized according to the scheme shown in A.3. Solid-state FTIR of the labeled lumiflavin showed a small shift in the mode at 1584 cm$^{-1}$ down to 1576 cm$^{-1}$. This small shift is consistent with previous assignments of this mode to the N5=C4a and N1=C10a groups in the flavin molecule.

The Raman spectra of wild type AppA bound to lumiflavin and the $^{15}$N lumiflavin isotope are shown in Figure A.2. Attempts to irradiate the protein when bound to lumiflavins resulted in precipitation of the protein and a rise in the absorbance at 280 nm. Thus, only the dark state of AppA is shown in Figure A.2. The 1584 cm$^{-1}$, with major contributions from the N5=C4a and N1=C10a groups, shifts to 1576 cm$^{-1}$, in line with the FTIR data.

*Steady-State Raman Spectroscopy:* Steady-state Raman spectroscopy was performed on this instrument as previously described. Data for wild type AppA bound to lumiflavin (Sigma) and $^{15}$N5-labeled lumiflavin were collected

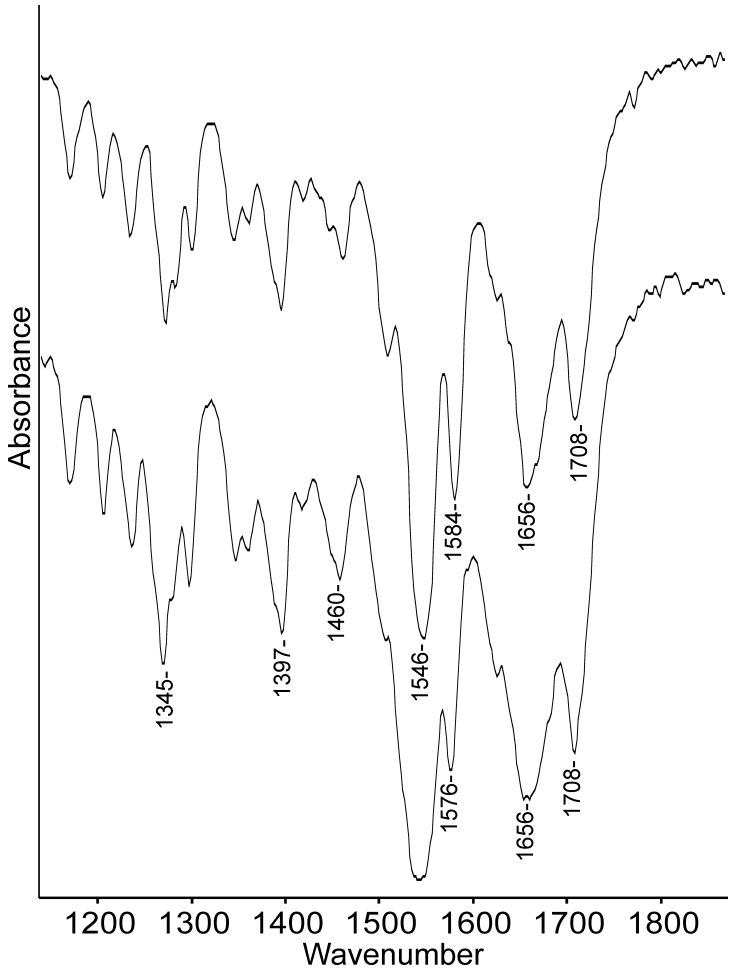


Figure A.1: Steady-state infrared spectra of lumiflavin (Sigma) and the $^{15}$N5-labeled lumiflavin isotope (KBr pellet).

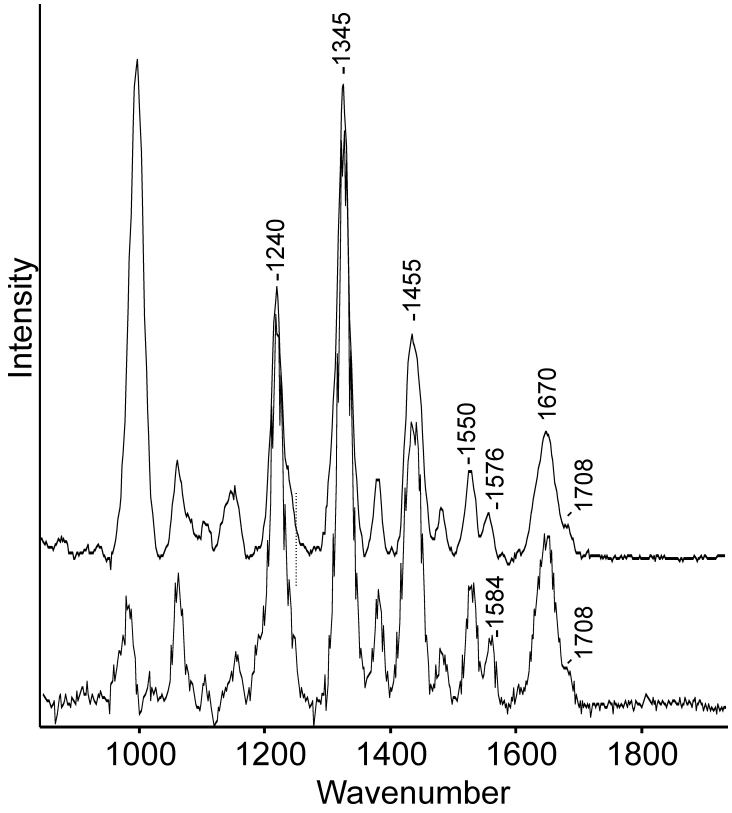


Figure A.2: Top: Steady-state Raman spectra of the $^{15}$N5-labeled lumiflavin isotope bound to wild type AppA (0.3 mM). Bottom: Raman spectrum of wild type AppA bound to lumiflavin (0.1 mM). Proteins in 10 mM sodium chloride, 20 mM sodium phosphate buffer, pH 8.

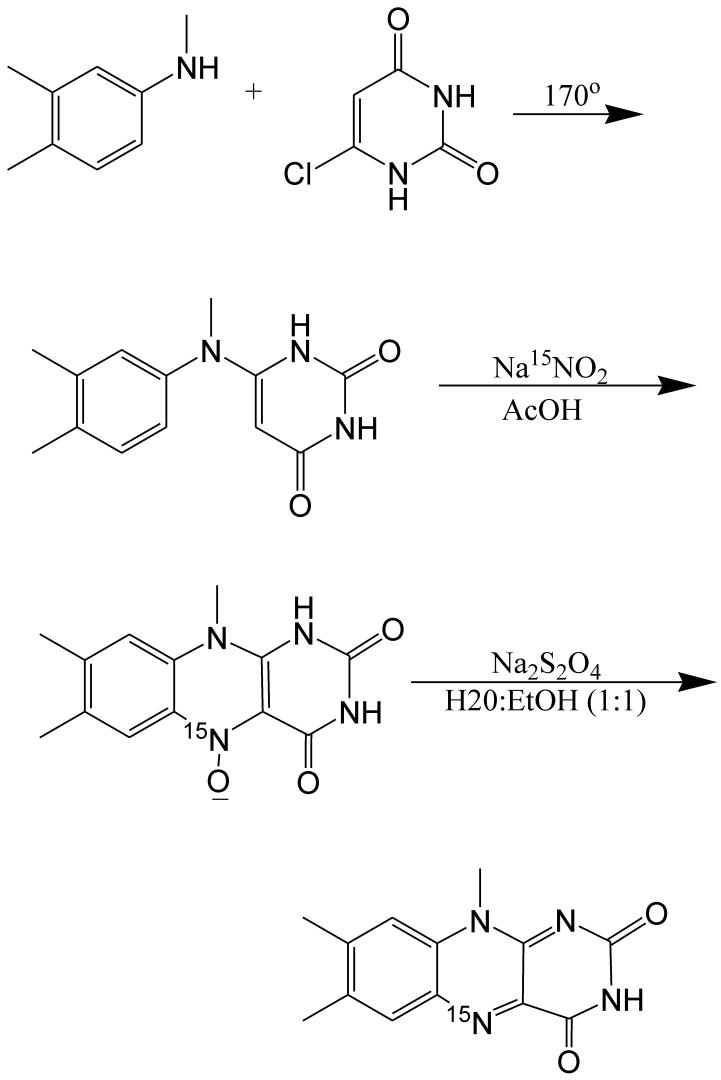


Figure A.3: Scheme for the synthesis of $^{15}$N5-labeled lumiflavin.

with 752 nm excitation obtained from a model 890 Ti:sapphire laser (Coherent, Santa Clara, CA), pumped by an Innova 308C argon ion laser (Coherent) and employing a 90° collection geometry. Power at the 2 mm by 2 mm fluorimeter cell that held 60 *mu*L of sample was 670 mW. AppA concentrations ranged from 1 to 2 mM and were in 20 mM $NaPO_4$, 1 mM NaCl buffer (pH = 8.0). Spectra were acquired in the dark using 2 second accumulation times and 300 scans. After the protein spectrum had been acquired, a buffer spectrum containing no protein was obtained. The buffer spectrum was then subtracted from the protein + buffer spectrum to give the Raman spectrum of the protein. Spectra were wavenumber calibrated using the Raman spectrum of cyclohexanone. All spectral analysis and calculation were performed with Win-IR software. Data were collected using WinSpec (Princeton Instruments, Trenton, NJ).

*Steady-State Infrared Spectroscopy:* Infrared spectra were collected on a Mattson Galaxy 3000 FTIR spectrophotometer with a DTGS detector. 16 scans were recorded for each sample. Spectra were obtained of solid state samples pressed into KBr disks.

## A.2 Raman Spectroscopy of Hemin and Myoglobin

Hemin is a widely employed chromophore, and is frequently used in nitrogen sensing protein such as H-NOX to detect $NO_2$. The Raman spectra of myoglobin in $H_2O$ buffer, a hemin-containing protein that can be readily purchased, and unbound hemin in acetonitrile are shown in Figure A.4.

Myoglobin has modes at 1650, 1615, 1564, 1542, 1515, 1447 and 1374 $cm^{-1}$ in its off resonance Raman spectrum. The mode at 1650 $cm^{-1}$ is the amide I stretch from the protein, and is not seen in the hemin spectrum. The 1615 $cm^{-1}$ mode has contributions from the C=C bonds in the hemin chromophore. This modes is a 1620 $cm^{-1}$ in unbound hemin, and is quite broad. These assignments are in agreement with previous resonance Raman studies on myoglobin bound to labeled hemin [24]. The lower frequency modes are highly nonlocal and have contributions from many atoms in the hemin [24].

*Steady-State Raman Spectroscopy:* Steady-state Raman spectroscopy was performed on this instrument as previously described. Data for myoglobin were collected with 752 nm excitation obtained from a model 890 Ti:sapphire laser (Coherent, Santa Clara, CA), pumped by an Innova 308C argon ion laser (Coherent) and employing a 90° collection geometry. Power at the 2 mm by

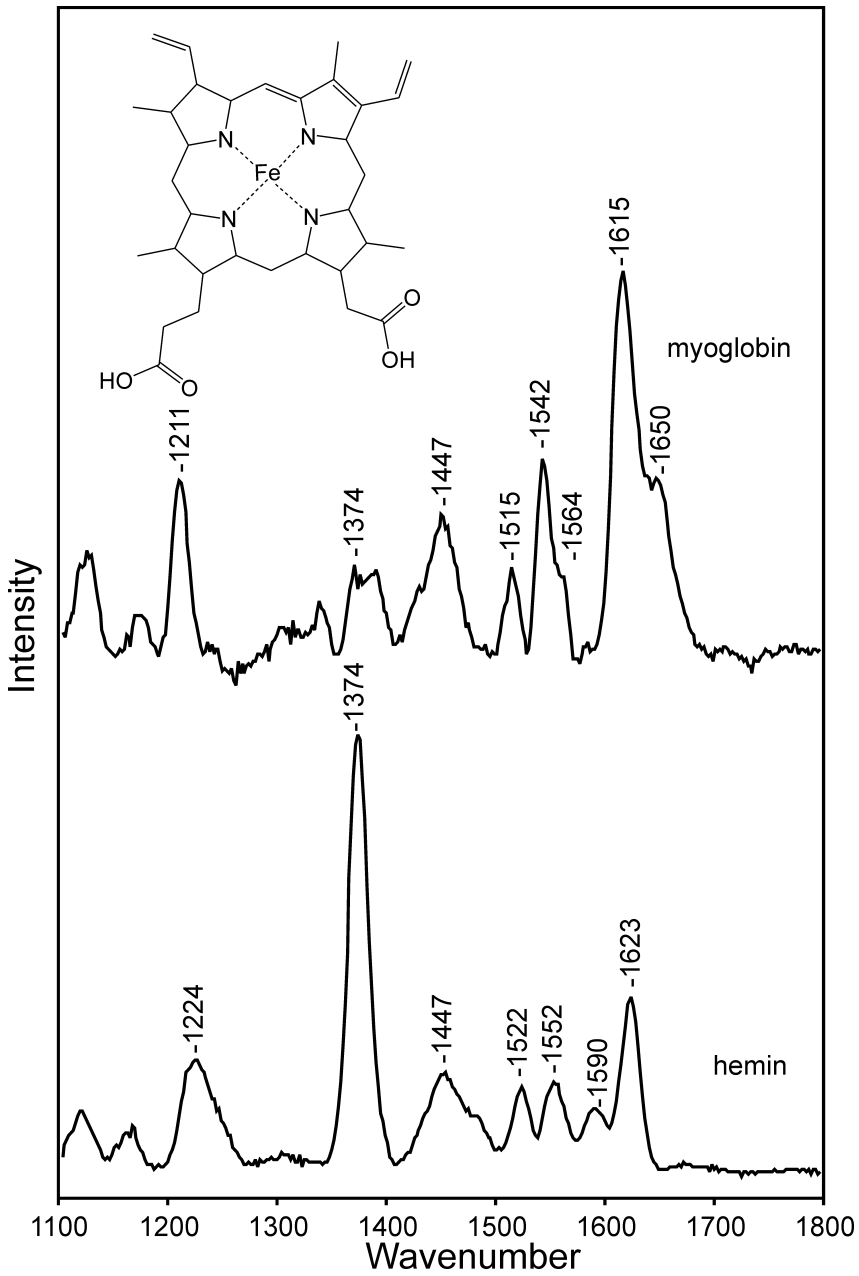


Figure A.4: Top: Raman spectra of myoglobin (Sigma, 200 $\mu$M) in 10 mM sodium chloride, 20 mM sodium phosphate buffer, pH 7.5. Myoglobin samples were prepared fresh before every experiment, as the protein would degrade overnight. Bottom: hemin (Sigma) in acetonitrile.

2 mm fluorimeter cell that held 60 $mu$L of sample was 670 mW. Myoglobin concentrations ranged from 200 to 400 $\mu$M and were in 50 mM $NaPO_4$, 100 mM NaCl buffer (pH = 8.0) and were made fresh the day of the experiment. Hemin measurements were performed using a saturated solution in acetonitrile. Spectra were acquired in the dark using 2 second accumulation times and 300 scans for the protein and hemin. After the protein spectrum had been acquired, a buffer spectrum containing no protein was obtained. The buffer spectrum was then subtracted from the protein + buffer spectrum to give the Raman spectrum of the protein. Spectra were wavenumber calibrated using the Raman spectrum of cyclohexanone. All spectral analysis and calculation were performed with Win-IR software. Data were collected using WinSpec (Princeton Instruments, Trenton, NJ).

## A.3 Time Resolved Infrared Spectroscopy of Glucose Oxidase

Glucose oxidase is a flavoprotein that performs one electron redox reactions. Its noncovalently bound FAD cofactor can be prepared in either the neutral (pH 6) or anionic (pH 9) semiquinone forms when under anaerobic conditions. Each of these flavin states is thought to be important to signal

transduction in flavin containing photosensing proteins, such as the BLUFs and the cryptochromes. Glucose oxidase may be readily purchased, and therefore this enzyme was chosen for isolation of FAD in the anionic semiquinone state. The excited-state of oxidized flavin in the glucose oxidase environment was then examined with time-resolved infrared spectroscopy.

The bleach at 1702 $cm^{-1}$ is due to the loss of the ground state C4=O flavin mode upon excitation. The transient mode at 1676 $cm^{-1}$ could be due to the excited state of the C4=O flavin group, although a greater shift is expected [81]. The next bleach lies at 1665 $cm^{-1}$, with a transient at 1655 $cm^{-1}$. While these might have contributions from the flavin carbonyl groups, the ground state FTIR spectrum of glucose oxidase does not contain these modes, and they may have contributions from the protein as well. The major contributor to the bleach at 1640 $cm^{-1}$ is the C2=O flavin group [81], and the transient mode for the excited state of this group is broad, from 1614 to 1697 $cm^{-1}$. A transient mode is observed at 1634 $cm^{-1}$, and a bleach at 1626 $cm^{-1}$. These modes are in the right frequency range to contain contributions for the C=N groups in the flavin. Another possible assignment for the 1634/1626 $cm^{-1}$ modes is the formation of a reduced flavin species, whose C4=O group shifts to 1634 $cm^{-1}$ upon reduction [81]. The modes at 1580 $cm^{-1}$ and 1550 $cm^{-1}$ have contributions from the flavin C=N modes [81]. The small transients

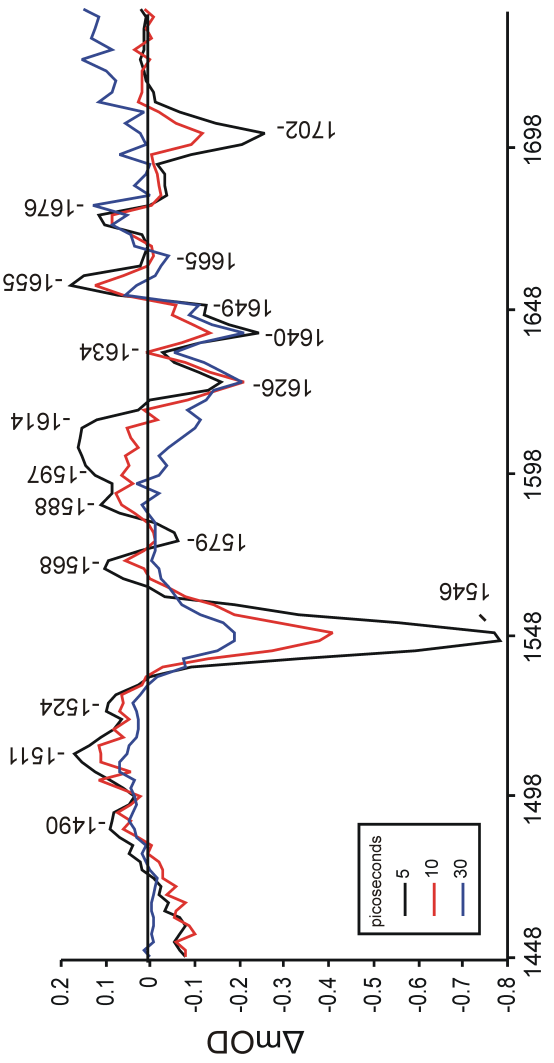


Figure A.5: Time-resolved infrared spectrum of 1.5 mM glucose oxidase (Sigma) in 1 mM sodium chloride, 20 mM sodium phosphate buffer (pD 8), after excitation at 400 nm.

centered at around 1520 to 1490 $cm^{-1}$ are in the correct frequency range for the N1-H, N5-H groups of reduced flavin [81].

*Time-Resolved Infrared Spectroscopy:* Ultrafast time-resolved IR spectra were measured at the STFC Central Laser Facility. A description of the system and data collection methods has been published [66, 72]. The spot size and power of the pulse were adjusted so as to prevent photobleaching of the sample while retaining good signal-to-noise in the spectra (see below). Typical settings included a 200 $\mu$m spot size and energies invariably less than 2.5 $\mu$J per pulse. Glucose oxidase samples were contained in cells with $CaF_2$ windows separated by spacers of 25 $\mu$. Measurements typically consisted of spectra recorded at 3-5 randomly ordered time delays, with a 10 s collection period for each delay. Electronic absorption spectra were taken after each experiment to check for photobleaching of the sample, as previously described [65].